

TESTING ELECTROMAGNETIC ENERGY PENETRATION AND ABSORPTION
UNDER RESERVOIR CONDITIONS: THE INFLUENCE OF PIEZOELECTRICITY

A Dissertation

by

MATTHEW K. MORTE

Submitted to the Office of Graduate and Professional Studies of
Texas A&M University
in partial fulfillment of the requirements for the degree of

DOCTOR OF PHILOSOPHY

Chair of Committee,	Berna Hascakir
Committee Members,	Hiroko Kitajima
	Hadi Nasrabadi
	Sam Noynaert
Head of Department,	Jeff Spath

December 2019

Major Subject: Petroleum Engineering

Copyright 2019 Matthew K. Morte

ABSTRACT

The potential of microwave technology in the context of enhanced oil recovery is a concept whose technical feasibility has been expounded by numerous pilot tests. However, poor penetration depth and limited understanding of dependencies of complex permittivity on the dynamic downhole environment have proven prohibitive in terms of economic viability. Addressing the concerns of relatively poor stimulated reservoir volume as a function of low penetration depths as well as illuminating dependencies of complex permittivity in the reservoir enables the industry to take steps towards economic implementation.

Manipulation of absorption and penetration dynamics of the wave is achieved in this study by means of triggering the direct piezoelectric effect. Dynamic polarization of the quartz crystals in sandstone reservoirs manifests itself as a function of a differential stress imposed upon the rock. Acoustic waves are propagated into the reservoir rock where the mechanical wave nature vibrates the particles in the medium; so an additive stress on the rock is created. The direct piezoelectric effect dictates that the quartz crystals, which are a piezoelectric element, will be polarized in the presence of the mechanical stress. Therefore, simultaneously introducing an acoustic wave and microwave to the reservoir takes advantage of inherent piezoelectricity realized by the quartz crystals, increasing the penetration depth of the microwave.

Complex permittivity is the parameter which governs the absorption and penetration dynamics in the reservoir and is accordingly integral to any prospective microwave

treatment. Reservoir heterogeneity requires that complex permittivity be calculated both as a function of time and space as reservoir properties change during production. Dependencies of this parameter in a reservoir environment are not well understood or adequately described in literature with current estimation techniques being overly simplistic. Mixing rules employed are derived on the basis of mutual exclusivity and volumetric proportionality and are not capable of predicting the behavior in the complex downhole environment. A new estimation model is created by use of a multivariable regression of a statistically significant number of experiments. The regressed model innately captures all interactions in the reservoir and provides for a more realistic interpretation of wave propagation. All dependencies of complex permittivity are isolated and explicitly quantified with the result being a more accurate technique for predicting the complex permittivity in the reservoir.

Minimal profit margins of microwave heating inhibit what is otherwise a technically viable and productive technique with vast potential. Triggering the direct piezoelectric effect in sandstone reservoirs is one way to stimulate greater volume, thereby enhancing the transmissibility of a larger volume of fluid. Also, optimization of microwave processes is performed by numerical simulation. Complex permittivity governs the microwave absorption in the reservoir and is of primary importance to any estimation model. A regressed model as a function of a multitude of measurements on unconsolidated cores provides for an accurate and effective predictor of complex permittivity as a function of reservoir properties.

DEDICATION

I dedicate this dissertation to my parents who have provided me with endless support throughout the entirety of my life.

CONTRIBUTORS AND FUNDING SOURCES

Contributors

All research in this study was supported by my dissertation committee consisting of my committee chair and advisor, Dr. Berna Hascakir, followed by the other members of my committee Dr. Hadi Nasrabadi, Dr. Samuel Noynaert, and Dr. Hiroko Kitajima. Their input and encouragement was vital to the success of this study.

Data collection for Part 4 of this study was performed with the help of Hasan Alhafidh, an undergraduate worker in the Department of Petroleum Engineering. All other experiments as well as all of the data analysis was performed independently by the student.

Funding Sources

The research in this study was conducted due to support from the Texas A&M Petroleum Engineering Department and more specifically, the Heavy Oil, Oil shales, Oil sands, and Carbonate Analysis and Recovery Methods (HOCAM) research group.

NOMENCLATURE

EM	Electromagnetic
MW	Microwave
RF	Radio Frequency
VNA	Vector Network Analyzer
\bar{D}	Electric Flux Density Vector
\bar{B}	Magnetic Flux Density Vector
\bar{E}	Electric Field Intensity Vector
\bar{J}	Electric Current Density Vector
P	Charge Density
ϵ_0	Electric Permittivity of Free Space
μ_0	Electric Permeability of Free Space
ϵ'	Real Component of Complex Permittivity, Dielectric Constant
ϵ''	Imaginary Component of Complex Permittivity, Loss Index
$\tan(\delta)$	Loss Tangent
α	Attenuation Constant, m^{-1}
d_p	Penetration Depth, m
P_d	Absorbed Power
f	Frequency, Hz
Φ	Porosity
L-LN	Natural Logarithmic Lichtenecker Method
LR	Lichtenecker-Rother Method

CRIM	Complex Refractive Index Method
ε'_{rm}	Measured Real Relative Permittivity of the Rock Matrix
v_{rm}	Volume Fraction of the Rock Matrix
ε'_p	Measured Real Relative Permittivity of the Pore Space
v_p	Volume Fraction of the Pore Space
ε'_t	Mixture's Real Relative Permittivity
S_w	Volume of Water Multiplied by Complex Permittivity of Water
S_o	Volume of Oil Multiplied by the Complex Permittivity of Oil
V_q	Volume of Quartz, fraction
V_L	Volume of Limestone, fraction
V_{Kao}	Volume of Kaolinite Clay, fraction
V_{Bent}	Volume of Bentonite Clay, fraction
p	Pressure, psig
f	Frequency, Hz
T	Temperature, °F

TABLE OF CONTENTS

	Page
ABSTRACT	ii
DEDICATION	iv
CONTRIBUTORS AND FUNDING SOURCES.....	v
NOMENCLATURE.....	vi
TABLE OF CONTENTS	viii
LIST OF FIGURES.....	x
LIST OF TABLES	xiii
1. INTRODUCTION.....	1
References	23
2. PART 1: PENETRATION DEPTH OF MICROWAVES UNDER THE INFLUENCE OF STATIC MECHANICAL STRESS: THE DIRECT PIEZOELECTRIC EFFECT	28
Abstract	28
Introduction	29
Experimental Procedure	33
Experimental Results and Discussion	40
Conclusions	47
References	48
3. PART 2: INCREASING THE PENETRATION DEPTH OF MICROWAVE RADIATION USING ACOUSTIC STRESS TO TRIGGER PIEZOELECTRICITY ..	52
Abstract	52
Introduction	53
Experimental Procedure	57
Experimental Results and Discussion	64
Conclusions	73
References	76

4. PART 3: CHARACTERIZATION OF COMPLEX PERMITTIVITY FOR CONSOLIDATED CORE SAMPLES BY UTILIZATION OF MIXING RULES	79
Abstract	79
Introduction	80
Experimental Procedure	85
Experimental Results and Discussion	90
Conclusions	100
References	104
5. PART 4: MULTIVARIABLE REGRESSION OF COMPLEX PERMITTIVITY AS A FUNCTION OF RESERVOIR PROPERTIES	108
Abstract	108
Introduction	109
Experimental Procedure	114
Experimental Results and Discussion	119
Conclusions	135
References	138
6. CONCLUSIONS	141

LIST OF FIGURES

	Page
Figure 1.1 - Illustration of the concept with additive penetration being achieved by the presence of the mechanical stress from the acoustic wave	14
Figure 2.1 - Both the vector network analyzer and dielectric probe kit utilized to measure the complex permittivity of the sample	34
Figure 2.2 - Real and imaginary components of relative permittivity as a function of frequency for the quartz control crystal	36
Figure 2.3 - Penetration depth of unstressed and stressed quartz crystal	37
Figure 2.4 - Penetration depth of unstressed and stressed Sample 1 core saturated with oils (A) C1, (B) C2, and (C) C3.....	41
Figure 2.5 - Penetration depth of unstressed and stressed Sample 2 core saturated with oils (A) C1, (B) C2, and (C) C3.....	43
Figure 2.6 - Penetration depth of unstressed and stressed Sample 3 core saturated with oils (A) C1, (B) C2, and (C) C3.....	44
Figure 2.7 - Penetration depth of unstressed and stressed water-saturated cores for lithological cores (A) Sample 1, (B) Sample 2, and (C) Sample 3.....	46
Figure 3.1 - The experimental equipment used to generate and introduce the acoustic signal into the core volume while simultaneously imposing the pressure state	60
Figure 3.2 - Experimental setup for the simultaneous introduction of the microwave and acoustic wave	61
Figure 3.3 - Picture of the oil-saturated consolidated cores utilized in the experiments for all three different lithologies	62
Figure 3.4 - Penetration depth of oil-saturated sample 1 (quartz rich sandstone) cores with the unstressed and imposed stress states.....	65
Figure 3.5 - Penetration depth of oil-saturated sample 2 (quartz rich sandstone) cores with the unstressed and imposed stress states.....	67
Figure 3.6 - Magnitude of increased reservoir volume as a function of percent increase in penetration depth	68

Figure 3.7 - Penetration depth of oil-saturated sample 3 (carbonate rich) cores with the unstressed and imposed stress states.....	69
Figure 3.8 - Penetration depth of all water-saturated cores with the unstressed and imposed stress states	71
Figure 4.1 - Illustration of the binary (rock matrix and pore space) nature of the reservoir	83
Figure 4.2 - Experimentally measured dielectric properties of the constituent components of bulk oil and rock matrix	90
Figure 4.3 - Mixing rule relationships for the frequency-dependent real relative permittivity for sample 1 cores with all four saturating fluids	94
Figure 4.4 - Mixing rule relationships for the frequency-dependent real relative permittivity for sample 2 cores with all four saturating fluids	95
Figure 4.5 - Mixing rule relationships for the frequency-dependent real relative permittivity for sample 3 cores with all four saturating fluids	96
Figure 4.6 - Loss tangent of all experimentally measured cores comparatively to the estimated mixing rule utilizing the CRIM	98
Figure 5.1 - Picture of the before and after of the mixing of the unconsolidated core material including the rock mineralogy and the fluids	116
Figure 5.2 - Pictorial description of all three planes of the core-holders utilized to maintain structural integrity.....	118
Figure 5.3 - Isolated dependency of complex permittivity on variable water saturation of the reservoir rock	121
Figure 5.4 - Isolated dependency of complex permittivity on variable quartz volume of the reservoir rock.....	122
Figure 5.5 - Isolated dependency of complex permittivity on variable kaolinite clay volume of the reservoir rock.....	124
Figure 5.6 - Isolated dependency of complex permittivity on variable bentonite clay volume of the reservoir rock.....	126
Figure 5.7 - Isolated dependency of complex permittivity on variable temperature of the reservoir rock	127

Figure 5.8 - Isolated dependency of complex permittivity on variable pressure of the reservoir rock	128
Figure 5.9 – Magnitude of microwave penetration depth increase between the stressed and unstressed state as a function of variable quartz content	129
Figure 5.10 – Predicted and Measured Components of Complex Permittivity for the Unconsolidated Core Samples Test 1 and Test 2	132
Figure 5.11 – Predicted and Measured Components of Complex Permittivity for the Consolidated Core Sample 1	133
Figure 5.12 – Predicted and Measured Components of Complex Permittivity for the Unconsolidated Core Samples Test 3	134

LIST OF TABLES

	Page
Table 2.1 - Properties of core samples including quartz content	38
Table 2.2 - Properties of all reservoir fluid samples including complex permittivity	40
Table 4.1 - Experimental and calculated real relative permittivity for all four models pertaining to the C1 saturated core samples	91
Table 4.2 - Experimental and calculated real relative permittivity for all four models pertaining to the C2 saturated core samples	92
Table 4.3 - Experimental and calculated real relative permittivity for all four models pertaining to the C3 saturated core samples	92
Table 4.4 - Experimental and calculated real relative permittivity for all four models pertaining to the water-saturated core samples.....	93
Table 4.5 - Experimental and calculated loss index for all four models pertaining to the C1 saturated core samples.....	99
Table 4.6 - Experimental and calculated loss index for all four models pertaining to the C2 saturated core samples.....	99
Table 4.7 - Experimental and calculated loss index for all four models pertaining to the C3 saturated core samples.....	99
Table 4.8 - Experimental and calculated loss index for all four models pertaining to the water-saturated core samples	99
Table 5.1 - Comparative investigation into the isolated dependency of the dielectric constant (ϵ') on pore volume	123

1. INTRODUCTION

Continued increase in demand of petroleum requires identification of an economically viable means of exploiting the expansive worldwide distributions of heavy oil and bitumen resources (Meyer et al. 2007; Sorrell et al. 2010). Petroleum is a very versatile product that has permeated the entirety of society, rising to prominence as an integral resource used for energy, chemicals, and plastics. The functionality of petroleum and the world's dependence on hydrocarbons requires efficient extraction of the resource. However, preferential production of easily accessible conventional resources has resulted in a rising volumetric proportion of unconventional reserves such as heavy oil and bitumen (Bera and Babadagli 2015; Owen et al. 2010). They are defined as unconventional on the basis of fluid properties, specifically viscosity, which make economic exploitation very difficult. Prohibitively high viscosity experienced by these resources manifests itself through a complete lack of transmissibility through the pore space. Without fluid flow, the petroleum in the reservoir has no value to the industry, therefore, the manipulation of the fluid properties to be more conducive to transmission of the fluid is vital. Manufacturing a more desirable flow potential in the reservoir is contingent upon influencing the fluid characteristics. Predominately, this is accomplished by exploiting the exponential nature of the relationship between heat and viscosity.

For thermal enhanced oil recovery techniques, the driving force of additive production is the decrease in viscosity associated with the increase in temperature. Therefore, additive energy is required to the system to manipulate flow potential

(Alvarado and Manrique 2010; Kokal and Al-Kaabi 2010). Steam injection is principally implemented as a means of imparting heat energy to lower the viscosity but is associated with inherent inefficiency (Fanchi 1990; Mukhametshina and Martynova 2013; Sarathi and Olsen 1992). The nature of steam as a heat transporting fluid limits the efficacy of the process (Carrizales et al. 2008). The exchange of heat occurs at the interface of the fluids which requires the steam to contact the oil. This directionality necessary for effective steam treatment has implications in the reservoir as the fluid nature of steam dictates propagation through the path of least resistance (Hasanvand and Golparvar 2014). The steam is transmitted through the pore space and owing to innate heterogeneity in the vertical and horizontal permeability, the steam is often lost to the system. Accordingly, thin reservoirs present a challenge for economic implementation of steam processes as there is a higher likelihood that the steam will be lost to the overburden (Fanchi 1990). The target zone is small and ensuring that the steam remains in the threshold of the boundaries of the target zone is extremely difficult. The inability to control the direction of propagation of the steam directly correlates to poor thermal efficiency as any steam that bypasses the target zone is equivalent to loss of additive energy (Hascakir et al. 2009).

Deep reservoirs also present a challenge for steam processes as the quality of the steam decreases with depth. Increased depth corresponds to increased pressure and therefore the capacity to exchange heat decreases (Sahni et al. 2000). Idealized conditions for the steam are more difficult to maintain owing to the intrinsic relationship between temperature and pressure. A byproduct of the poor steam quality is a corresponding inability to realize the benefit of latent heat; so, heat exchange in the reservoir is

minimized. Temperature rise in the reservoir when introducing steam hinges upon the exchange of energy from a heat-transporting fluid. Steam is not capable of generating heat in the reservoir but instead essentially serves as a conduit, carrying heat energy into the reservoir. By definition, exchange between two entities requires contact to impart the carried heat energy from the source. Interfacial heating is accomplished only through direct contact where the mechanism of energy input is convection. Reservoirs that suffer from poor communication between the injector and producer are accordingly poor candidates for steam injection. Ensuring contact between the steam and the aqueous oil phase is exceedingly difficult if a pathway from the injector well to the producer is not established. Likewise, reservoir heterogeneity causing considerable degree of deviance between the vertical and horizontal permeability creates the potential to preferentially flow steam in the vertical plane instead of into the reservoir. Contact with expansive volumes of the reservoir is difficult to realize in the presence of significant heterogeneity resulting in steam bypassing the target zone (Chhetri and Islam 2008; Mutyala et al. 2010). Heating the reservoir by inundation with EM waves is a technology that has gained traction owing to the great potential in addressing the inadequacies of steam.

Electromagnetic waves are a known phenomenon that have been extensively studied for their unique fundamental properties that offer great applications to the petroleum industry. Superior control in the reservoir with improved heating characteristics are realized as a function of the waveform introduced with EM heating. The mechanism of heat generation allows for propagation through a material instead of to the interface, offering advantage over the convective heating of steam (Jha and Chakma 1999; Mutyala

et al. 2010). Instantaneous heating of the entirety of the material makes volumetric heating realized as a function of EM wave introduction more desirable than the surface heating of a steam counterpart (Chhetri and Islam 2008; Hasanvand and Golparvar 2014; Kasevich et al. 1994). Also, improved control within the confines of the target zone is experienced stemming from the wave nature of the technology. Propagation of the wave is not dependent upon the path of least resistance as the wave travels similarly through all materials. Directionality achieved by the wave allows for better targeting of specific locations of the reservoir while simultaneously minimizing energy loss to the surrounding overburden. Application of EM technology for the purpose of heating the reservoir accordingly has the potential to be very efficient and effective (Fanchi 1990; Mukhametshina and Martynova 2013).

Electromagnetic energy travels in the form of a wave with both a magnetic and electric field which oscillate orthogonal to one another (Faraday 1832; Maxwell 1865). The wave nature has no mass associated so the governing physics are energy conversion instead of energy transfer. The absorption of the incident microwaves generate heat in the reservoir governed by dipole rotation (Mutyala et al. 2010; Sahni et al. 2000). Propagation of EM energy through porous media is governed by Maxwell's equations which are depicted below where D is the electric flux density vector, B is the magnetic flux density vector, E is the electric field intensity vector, J is the electric current density vector, ρ is the charge density, ϵ_0 is the electric permittivity of free space, and μ_0 is the electric permeability of free space (Maxwell 1865).

$$\nabla \cdot \vec{D} = \frac{\rho}{\epsilon_0} \quad \text{Eq 1.1}$$

$$\nabla \cdot \vec{B} = 0 \quad \text{Eq 1.2}$$

$$\nabla \times \vec{E} = -\frac{\partial \vec{B}}{\partial t} \quad \text{Eq 1.3}$$

$$\nabla \times \vec{B} = \mu_0 \left(\vec{J} + \epsilon_0 \frac{\partial \vec{E}}{\partial t} \right) \quad \text{Eq 1.4}$$

Gauss' Law is described in Eq 1.1 and mathematically states that the net electric flux through any closed surface is equal to the net electric charge enclosed in that surface (Gauss 1813). The implication of Eq 1.1 is that with a known electric field at all points in space, the distribution of electric charge can be calculated. Regional charge can be deduced through an integration of the electric field to find the flux through the closed surface. Gauss' Law is applied to magnetism in Eq 1.2 and states what is intuitively known to be true, that magnetic field lines are closed loops (Gauss 1867). There cannot exist a magnetic monopole. The building block or basic entity of magnetism is the magnetic dipole rather than a magnetic charge. The law states that for every volume element in space, there exists the same number of magnetic field lines entering and leaving the closed surface. A real-life example would be the South and North Pole. Neither can exist without the other. The main difference between the two Gaussian laws is that electric fields are able to build up electric charge in a volume in contrast to the magnetic field.

The third law which comprises Maxwell's equations is that of Faraday's seen in Eq 1.3 which describes the fact that a time-dependent magnetic field produces an electric field (Faraday 1839). Finally, Eq. 1.4 is the Ampere-Maxwell law and states that a time-

dependent electric field produces a magnetic field (Maxwell 1865). Both of the above mentioned equations state that there is an electromotive force, defined as work done on a unit charge, accompanying any conductive loop with a time-dependent magnetic or electric flux. They are coupled in nature and, once formed, are self-propagating where the presence of one produces the other. Therefore, they do not require a medium to propagate through and are a massless form of energy capable of transmitting in a vacuum. A feedback loop is essentially generated where, in stepwise fashion, the generated electric or magnetic field generates its counterpart. Electromagnetic waves are unique in their ability to propagate in a vacuum which is founded in the interaction between the electric and magnetic fields. The combination of the last two equations results in a theoretical infinite propagation but wave attenuation occurs due to interactions with the material. In the case of the petroleum reservoir, both the skeletal frame, or rock matrix, and fluid in the pore space impede the passage of the wave. The material provides a resistance to flow which is accompanied by energy dissipation relative to the wave. Positively charged particles in the material are accelerated in the same linear orientation of the field when there is contact with the material. However, due to the impedance of the material, the polarization vector lags the electric field creating power dissipation. Attenuation, or energy loss relative to the wave, occurs as a result of the phase difference between the incident electric field vector and the induced polarization vector.

Heat generation as a result of the introduction of EM waves is directly dependent on the frequency of the wave. Utilization of low-frequency waves below 300 kHz is denoted electrical resistive heating where the fundamental mechanism of heat transfer is

by means of a resistive element in an imposed current (Joule 1850). The formation itself serves as the resistive element and the current is maintained by the presence of liquid water as the conductor where ohmic losses account for the heat generation (McGee and Vermeulen 2007; Oliveira et al. 2009). The benefit in terms of heat generation is only seen while the current is maintained through the resistive element. Therefore, the implementation of low-frequency heating is predicated on a conductive path remaining at all times in the reservoir. The conductive path is established by the presence of liquid water in the pore space; so the temperature must be maintained below the boiling point (Wattenbarger and McDougal 1988). The imposed threshold of temperature corresponds to lesser intensity of wave and accordingly less heat generation. However, the lower frequency also experiences a greater penetration depth relative to the higher frequency heating.

The potential realized with the introduction of low-frequency EM waves has been reported in numerous field trials (Davison 1995; Pizarro and Trevisan 1990; Rice et al. 1992). Encouraging results were seen with a statistically significant increase in production due to the rapid heat introduction. However, the heating rates were not able to be maintained as a function of phase change from liquid water to steam. Preventing the flashing of steam is integral to the success of these projects and maintaining idealized temperatures proved very difficult. Numeric solutions further demonstrate the technical viability of the concept with simulated recovery increases of over 60% (Hiebert et al. 1986; Islam and Wadadar 1991; Oliveira et al. 2009; Pizarro and Trevisan 1990; Sahni et al. 2000). Production increase evidenced both in numeric simulation as well as field testing

further illustrate EM waves as an attractive technique, however, the restrictive condition of the temperature threshold limits the viability in the low-frequency range.

Opposed to the low-frequency counterpart, high-frequency waves do not require the presence of liquid water to experience heat generation. The ability to avoid the fundamental mechanism of the resistive element allows for temperature increases well above that of the boiling point of water. High-frequency heating addresses some of the shortcomings of the low-frequency wave alluded to earlier as dielectric heating is the mechanism that dominates. The origin of the heat generation when high-frequency waves are employed is the ability of the electric field to polarize the material charges and the corresponding inability of the polarization to keep phase with the rapidly oscillating field. The polarization is directly dependent on the displacement of electrons from the nuclei. The disturbed state creates induced dipoles as the charged particles deviate from equilibrium as a function of the applied field. As the wave propagates through the material, particles in the material attempt to align themselves with the corresponding positive or negative half cycle of the oscillation (Davletbaev et al. 2011; Rehman and Meribout 2012; Sresty et al. 1986; Wacker et al. ; Wilson 2012). The dipole rotation of the oriented particles accordingly results in frictional heat generation. Heat transfer to the porous medium results in viscosity reduction of the fluids and an enhanced capability of transmission of the oil for production. As energy from the wave is absorbed by the material the wave will decrease both in size and amplitude as it travels.

The vast potential of MW implementation into the reservoir garnered interest for the ability to achieve large temperature gain with no restriction of liquid water. However,

nuances and dependencies needed to be properly understood before any capital investment of the magnitude required for a field-scale could be achieved (Bjorndalen and Islam 2004; Bjorndalen et al. 2003). Lab-scale studies were performed to allow for upscaling to the field and to test the technical components of the process to determine if the energy balance was advantageous. Studies demonstrated the ability to heat the fluids in the reservoir through energy conversion from the wave; however, the overall success of the project hinges on the efficiency of the system. Economics dictates that more energy equivalent be produced than is directed into the wellbore for stimulation. Heating of the reservoir is useless if the system is too energy intensive and introduced energy is never recuperated. Profitability of the concept is sustained when more energy in the form of barrels of oil is produced than is expended in the form of generation and propagation of the microwave. Success of the near-wellbore heating with microwave frequencies was achieved with very high efficiency (Kovaleva et al. 2004). Microwave heating can be considered energy conversion instead of energy transfer and this equates to an advantageous energy balance. So, the MW heating process has the potential to be economic with more energy produced than is required for stimulation.

Having corroborated the local efficiency of the system in terms of input energy, a comparative analysis of electrical resistive heating was necessary. Resistive heating is achieved in the lower frequency range where the mechanism of heating revolves around the Joule effect. Resistive heating requires conductance through a resistive element to maintain heat generation. In the reservoir, the only true conductive element is the connate water so the presence of water is essential for continuous propagation of the EM wave

(Gunal and Islam 2000). Therefore limitations are introduced where the temperature threshold of liquid water is present. To warrant the higher capital expenditure with a microwave treatment, greater production must be achieved at an enhanced rate.

Comparative analysis illustrated a more pronounced impact on the oil phase was achieved with microwave heating relative to the electrical heating counterpart. Also, faster production relative to electrical heating was experienced with greater local efficiency (Alomair et al. 2012). Furthermore, higher EM frequencies provide faster heating rates and overcome problems associated with discontinuity in the medium. The microwave frequency range is much less sensitive to reservoir heterogeneity and propagation can be sustained without the presence of liquid water. Microwaves can heat the reservoir even to temperatures above the flashing point of steam (Bientinesi et al. 2013).

Other factors were also considered including the initial saturation conditions and inundation time. Water saturation in the reservoir is the absorber of microwave energy and so greater water content generates greater temperature rise. Accordingly, higher initial water saturation and water-wet reservoir rocks result in higher overall oil recovery. Finally, both the heating time and the power were seen to increase the overall recovery which led to the conclusion that heating should be continuous (Hascakir et al. 2009). Concerns over the penetration depth of the higher frequency waves were posed owing to the inverse relationship between frequency and penetration. Higher frequency is associated with greater energy content and increased heat but at the cost of wave propagation. However, studies found that heating of the entire pay zone is not necessary for moderately heavy oil (less than 1000 cP) due to convection (Jha and Chakma 1999).

With the lab studies providing results indicative of great promise, various field tests were conducted to establish the viability of heat generation in the reservoir using EM waves. High-frequency waves were employed to demonstrate the additive heat gained at N. Midway Field in California where an increase of 100 K was measured 3 meters from the wellbore over the course of 20 hours (Kasevich et al. 1994). Similar frequency was used in the tar sands of Utah at Asphalt Ridge where temperatures exceeded 473 K and 35% recovery was achieved (Sresty et al. 1986). Canadian heavy oil was also tested in the Lloydminster area with a peak stimulation ratio of 3.75 (Davison 1995). These field tests expound the technical feasibility to recover bitumen and heavy oil using EM waves. However, the system exhibits relatively poor penetration depth associated with high attenuation of the incident wave which makes this technology marginal in terms of economic return (Carrizales et al. 2008; Das 2008; Koolman et al. 2008). Lower stimulated reservoir volumes associated with the utilization of microwaves inhibits the economic viability of microwaves as a heating mechanism.

Therefore, optimization of the process was required to further investigate the process in terms of investment over a period of many years. Pilot tests are incapable of accounting for delayed benefit as a function of time as they cannot be conducted over a significant time domain. Simulation studies have the unique advantage of modeling fluid flow and representing large changes in time in a much more manageable manner. Accordingly, numerical simulations have also been implemented to further investigate the feasibility of EM heating in the reservoir (Hascakir et al. 2008). Fanchi conducted sensitivity tests which displayed the dependency of the simulation on parameters of

electrical permittivity and water saturation (Fanchi 1990). He also reported that EM power attenuates exponentially in a homogenous, and dielectric medium. The attenuation is a function of the frequency employed so the range in frequencies was also tested. Sahni et al. investigated EM waves as a preheating tool in both the low-frequency resistive heating and the high-frequency dipolar heating ranges (Sahni et al. 2000). It was found that the presence of the EM waves significantly accelerated production while attaining a higher cumulative recovery. Resistive heating in the lower frequency range requires the presence of water to maintain a current through the reservoir which is a limitation that the higher frequency dipolar heating does not experience. Simulations have also been used to assess the technically recoverable hydrocarbons for future field tests. A numerical simulation was run specific to the tar sands of the Ugnu formation in Alaska where the result was a recovery of over 50% (Wadadar and Islam 1994). Opportunities for downhole dielectric heating in Venezuela were also simulated for medium, heavy, and extra heavy oil reservoirs. Results showed an increase in cumulative oil production of 86% (Ovalles et al. 2002). Therefore, the presence of the MW is very effective as a heating agent in the reservoir as expounded by both pilot testing and numerical studies.

Microwaves travel in the reservoir and interact with the material where energy loss relative to the wave occurs as a function of absorption. Wave propagation dictates that as energy is gradually absorbed by the material, the remaining energy content of the wave must diminish. Energy is neither created nor destroyed so as the wave propagates through the material any heat generation directly corresponds to less remaining energy to continue propagation. Vast quantities of generated heat must accordingly correspond to

lower penetration depth as there is less remaining energy to continue wave propagation. Higher frequency waves in the MW range offer the benefit of very high heat generation but at the cost of penetration depth. Future implementation of the EM process for enhanced oil recovery warrants discovery of a way to both maintain the heat generation of the high-frequency range while also increasing the lateral penetration of the wave. Economic implementation of EM technology hinges on accessing adequate reservoir volume to increase the amount of heated oil; so, the direct piezoelectric effect becomes integral as a means of increasing stimulated reservoir volume in sandstones.

Piezoelectricity is a phenomenon where certain materials will experience a change in voltage and polarity when under the influence of mechanical stress which is denoted the direct piezoelectric effect (Curie and Curie 1880b). This phenomenon is reversible where mechanical stress is produced when an electric current propagates through the element and is denoted the converse piezoelectric effect (Lippmann 1881). Imposing the element to external mechanical force creates a slight deformation in the respective positions of the positive and negative center of the molecule (Arnau and Soares 2009; Ikeda 1996). For the petroleum industry, the implication of the direct piezoelectric effect is the potential to change in the polarity of the reservoir, thus increasing the penetration depth of the MW. Lowering the absorptive capacity of the wave corresponds to an increase in the energy content, enabling the wave to travel further into the formation and access greater volume of reservoir.

Taking advantage of inherent piezoelectricity in quartz crystals provides the means of increasing the depth of penetration thus increasing the volume of heated oil generating more attractive project economics. The concept is illustrated in Figure 1.1 to better visualize the potential implementation in the field. The economic implications would suggest implementing this technology can increase the stimulated reservoir volume and accordingly increase the quantity of produced oil which increases economic viability. Penetration depth is a direct function of the complex permittivity of the material. By introducing a mechanical stress element to the rock the direct piezoelectric effect in terms of complex permittivity can be investigated (Chung 2007; Krupka 2006). Any dependency on piezoelectricity would manifest itself in an alteration of the permittivity; so penetration depth will serve as a pseudo measurement for piezoelectricity.

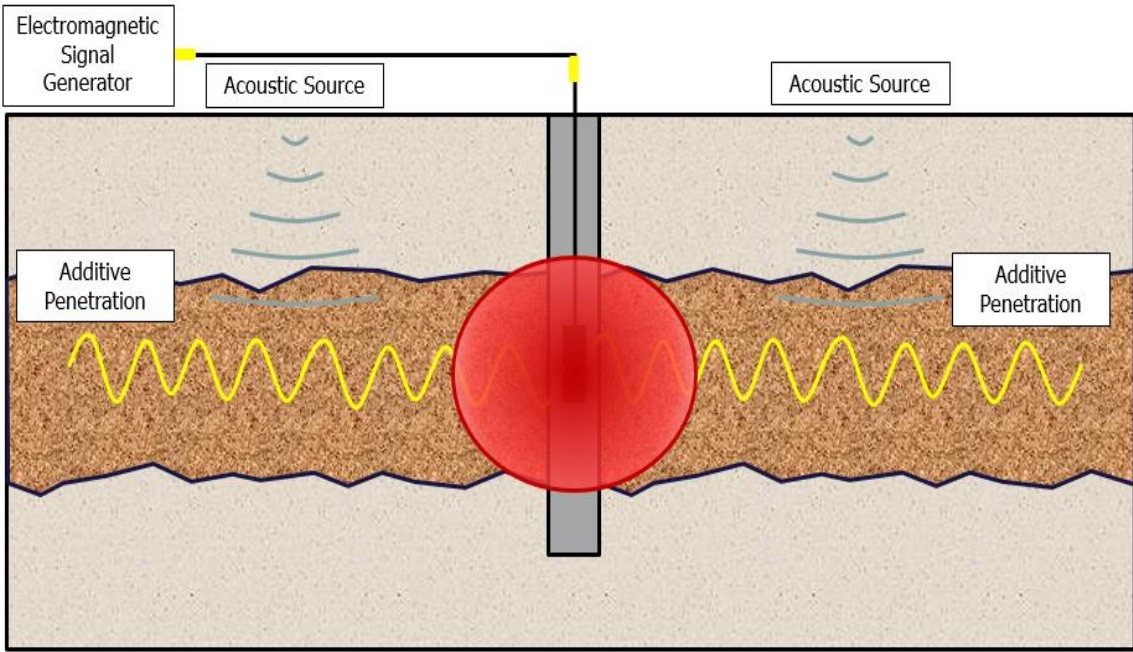


Figure 1.1 - Illustration of the concept with additive penetration being achieved by the presence of the mechanical stress from the acoustic wave

The attractive potential of microwave implementation for enhanced oil recovery is not only limited by penetration depth issues but also by concerns arising from controlling the wave propagation. Interactions between the wave form with the complex and dynamic environment of the reservoir are difficult to define. Very few fundamental studies have been published about the polarization behavior of oil sands and this lack of research has created operational disadvantages slowing progress on commercialization (Abraham et al. 2016). The ability of the material to absorb the heat-creating energy is dependent on the polarity of the medium, where polarity can be defined on the basis of the material property of complex permittivity (Metaxas and Meredith 1983; Von Hippel 1954). Therefore, the material in the reservoir uniquely interacts with the microwave owing to the individual polarity of each component.

The magnitude of the interaction, whether strong or weak, creates a classification system where material can be reflective (metals), transparent (quartz), or absorbent (water) (Jackson 2002; Martinez and Byrnes 2001; Thostenson and Chou 1999). Greater polarity corresponds to superior wave absorption; so, more polar molecules such as water intrinsically benefit from wave absorption to a greater extent than their transparent counterparts. Temperature increase in the reservoir through microwave heating is directly dependent on absorption and, by extension, the complex permittivity of the reservoir (Kar and Hascakir 2015). The state of the system regarding the physical properties such as temperature, pressure, mineralogy, etc. changes stemming from reservoir heterogeneity, so it becomes necessary to capture these dependencies in the reservoir (Hascakir and Akin 2009). The integral nature of the complex permittivity in the reservoir is seen through a

historical perspective of the utilization of EM technology in the petroleum industry. This material property extends well beyond the scope of exclusively heating the reservoir and has been of primary interest in numerous applications for decades (Abernethy 1976; Bera and Babadagli 2015; Doll 1949; Russell 1944).

For example, the performance of logging applications have taken advantage of EM technology and are performed routinely, becoming a major component of every petroleum play. The unique ability of the waveform to permeate through the bulk material is an advantage that is well suited for down-hole usage. Limited access to the reservoir inhibits proper description of the reservoir environment where physical sampling is very difficult owing to the extreme depths of operation. Exploratory and investigative practices that bypass the need for physical introduction of mass are therefore very attractive and ideal for the petroleum industry. The spectrum in the frequency range of 300 EHz defined as gamma radiation can be introduced into the reservoir where the interaction with the wave is indicative of material in the reservoir. Logging takes advantage of the interaction of the EM wave with the unique complex permittivity of the material in the reservoir. Naturally occurring radioactive elements such as uranium, potassium, and thorium found in the reservoir interact with the introduced gamma-ray (Wahl 1983). Strong correlations can then be developed between the mineralogy of the target zone which enables the interpretation of the lithology (Russell 1944).

Proper estimation of the reservoir properties hinges upon on accurate interpretation and measurement of the complex permittivity of the system. Correlations are only valid if the measured value is true and accurate. The nature of complex permittivity as a material

property creates an opportunity to identify the material in the reservoir owing to the overall sample complex permittivity. By extension, the fluid in the pore space is identified as a function of the unique molecular interaction of the wave. Measurements of the complex permittivity of the system are indicative of the water-filled pore space as the disparity between the permittivity of the water and all other materials is so large and distinctive. Materials in the reservoir can be characterized by their dielectric permittivity which is a constitutive property. Water is a polar molecule that exhibits a high dielectric constant. Comparatively, oil is a non-polar molecule that exhibits a dielectric constant twenty times lower than that of water. The difference in the two fluids is quite dramatic when analyzing the complex permittivity of each fluid. The dielectric response of the reservoir can then be stated to be primarily a function of the water volume in the pore space (Snyder and Fleming 1985; Wharton et al. 1980). The large disparity between the oil and water dielectric permittivity enables a correlation to estimate the water saturation in the reservoir (Freedman and Vogiatzis 1979; Meador and Cox 1975). The ability to estimate the water saturation of the reservoir as indicated by the complex permittivity of the reservoir is an invaluable tool. The fluid saturation is of primary importance as knowledge of the volume of oil in the target zone allows for the economics of the project to be determined with overall profit being the screening criteria. Dielectric behavior is seen in both the radio frequency range with implemented frequencies of approximately 10-50 MHz and the microwave frequency range with a frequency of 1 GHz.

Resistivity and induction logging techniques were employed to provide insight into the fluids that occupy the pore space. Induction logging directly takes advantage of

the radio frequency in the kHz range with operating frequencies ranging from tens to hundreds of kilohertz based on the depth of investigation. Resolution can be optimized through utilization of multiple coil arrays. Induction tools operate on the foundation of Eddy currents where an introduced electric current creates a primary magnetic field (Doll 1949; Faraday 1839; Foucault 1878; Maxwell 1865; Moran and Kunz 1962). Eddy currents flow in a continuous circular distribution in reference to the borehole and the current intensity is proportional to the formation conductivity (Foucault 1878). However, the utilization of radio frequency for dielectric logging is limited due to the fundamental behavior of the radio frequency range resulting in increased attenuation from ionic activity. Lower frequency probes are very sensitive to salinity and the rock matrix properties relative to the high-frequency probes. So, high-frequency waves in the range of 1 GHz are used as they experience the phenomenon of effective homogenization, making them more capable of withstanding substantial near-wellbore heterogeneity. Homogenization of the medium increases with frequency which results in the MW region being more desirable as a dielectric logging frequency (Snyder and Fleming 1985).

Beyond well logging, complex permittivity dependent applications were further engrained into the petroleum industry, furthering the importance of accurate estimation of this parameter. Introducing MW energy to induce compositional changes of crude oil was achieved through preferential targeting of the polar asphaltenes. Crude oil can be fractionated into the asphaltenes fraction and the maltenes fraction with the asphaltenes being heavier with higher polarity. EM waves interact preferentially with high polarity materials so the asphaltene absorbs an increased proportionality of the wave energy,

defined by the complex permittivity of the system. Microwave irradiation produces changes in the colloidal orientation of the asphaltene molecules and breaks down the molecules through thermal cracking (Gunal and Islam 2000; Jackson 2002). Greater concentration of asphaltenes corresponds to an increase in the steady-state temperature achieved. The role of asphaltene during viscosity increase is reversed during microwave irradiation. So, the composition of the crude oil can be enhanced by taking advantage of the constituent complex permittivity of the asphaltene.

Compared to the solid asphaltene and reservoir rock, fluids interact to a much greater extent with the nature of the incident wave and many applications of EM technology accordingly target fluids. One such application is the breaking of oil and water emulsions, owing to the large disparity in complex permittivity between the two fluids. Destabilization of the emulsions is performed by reduction in the viscosity of the continuous phase and breaking the outer film of the material. Coalescence is achieved revolving around the rearrangement of the charge distribution of the water molecules due to preferential interaction with the water molecules (Vega and Delgado 2002) The absorption phenomenon alluded to can be extended to encompass gas reservoirs with problematic water blocking. The relative permeability of gas to water can result in the blocking of pore channels which inhibits production of hydrocarbon. The gases in the reservoir are considered transparent to the EM wave and transmit the wave energy whereas the water highly absorbs the heat-creating energy. Therefore, the wave targets the water phase and ignores the transparent gases so all temperature gain is felt by the liquid water

phase. Phase change associated with temperature rise is achieved and the liquid water blocking the channel readily flows in gaseous form (Li et al. 2006).

In addition to enabling the creation of MW specific applications to benefit the petroleum industry, taking advantage complex permittivity driven EM heating creates an opportunity to enhance well-established processes such as pyrolysis. The extremely efficient nature of the energy conversion instead of energy transfer creates the potential to dielectrically heat any material with significant water content (Gasner et al. 1986; Monsef-Mirzai et al. 1995). Pyrolysis of both coal and oil shales have been performed with EM waves and offers great potential due to the volumetric heating (Chanaa et al. 1994; Hascakir and Akin 2009; Mokhlisse et al. 2000). Furthermore, microwave technology offers the ability to achieve temperature increase in a variety of materials and processes. For example, soil contaminants can be targeted with MW technology to greatly accelerate the remediation of soil, conventionally a very long and costly process that requires a very energy intensive system. Acceleration of the removal of many contaminants can be done as a function of increasing temperature. Microwave heating offers much more rapid and efficient heating of the soil compared to conventional thermal processes (Kawala and Atamańczuk 1998). Contaminants are organic compounds of high volatility with higher relative complex permittivity. Additive heat as a result of the preferential interaction with the wave forces the molecules into the vapor phase, greatly enhancing the transmissibility of the fluid (Vermeulen and McGee 2000). The vaporized hydrocarbons are then removed from the formation by extraction wells (Chien 2012; Vermeulen and McGee 2000).

All of the above applications of EM technology hinge upon understanding and accurately characterizing the complex permittivity of the material. Variable complex permittivity must be accounted for to adequately estimate penetration and absorption for the purpose of temperature increase estimation. Therefore, it is important to understand the change in permittivity associated with microwave propagation as well as the implications it has in the reservoir. Complex permittivity is a material property that governs the ability of electromagnetic energy to be absorbed or transmitted. Greater absorption of wave energy directly corresponds to greater quantity of heat generation and temperature rise. Accordingly, processes involving the electromagnetic heating mechanism are very sensitive to complex permittivity or dielectric parameters (Singh and Heldman 2001; Sun 2014). It then becomes necessary to illuminate the dependencies of dielectric parameters on both the pore space and rock matrix.

The simplest description of a composite material is a volumetric proportion of each constituent part. Conventionally, mixing rules are utilized to estimate the dielectric behavior of a composite. However, the interaction between the pore space and the rock matrix prohibits the utilization of a simple mixing rule relationship. Mutual interactions between the constituent components of a composite prevent the utilization of simple mixing rules as a volumetric proportionality cannot be achieved. For porous media, the two constituent components, namely the rock matrix and pore space, are not mutually exclusive and therefore are not adequately described by mixing rules. However, the contribution of each component is inherently captured by the measured complex permittivity as the electromagnetic wave propagates through all material. This

contribution must be accurately defined to provide for a realistic estimation of heat generation in the reservoir.

Volumetrically the samples consist of the rock matrix and the void space which is represented by the porosity parameter. Intricacies within the pore space as well as the skeletal frame, or rock matrix, are described in this study as relationships between water saturation, oil saturation, rock mineralogy, pressure, temperature, porosity, and oil permittivity. The culmination of all the experimental findings will result in the integration of the contribution of both the skeletal frame and pore space to the dielectric response. Defining relationships enables the estimation of the performance of any electromagnetic treatment specific to identified reservoirs on the basis of rock mineralogy and fluid saturations.

Expansive distributions of heavy oil and bitumen throughout the world dictate that efficient means of extraction be explored and optimized. Fundamental mechanisms of heating using microwave energy offer distinct advantage with increased efficiency compared to conventional heating. However, poor penetration depth and the inability to adequately predict complex permittivity as a function of space and time in the reservoir prove prohibitive in terms of economic implementation. This study addressed these issues by focusing on increasing the penetration depth using the direct piezoelectric effect and presenting new predicting equations for complex permittivity.

References

- Abernethy, E. 1976. Production Increase of Heavy Oils by Electromagnetic Heating. *Journal of Canadian Petroleum Technology* **15** (03).
- Abraham, T., Afacan, A., Dhandharia, P. et al. 2016. Conduction and Dielectric Relaxation Mechanisms in Athabasca Oil Sands with Application to Electrical Heating. *Energy & Fuels* **30** (7): 5630-5642.
- Alomair, O.A., Alarouj, M.A., Althenayyan, A.A. et al. 2012. Improving Heavy Oil Recovery by Unconventional Thermal Methods. In *SPE Kuwait International Petroleum Conference and Exhibition*: Society of Petroleum Engineers. ISBN 1613992637.
- Alvarado, V. and Manrique, E. 2010. Enhanced Oil Recovery: An Update Review. *Energies* **3** (9): 1529-1575.
- Arnau, A. and Soares, D. 2009. Fundamentals of Piezoelectricity. In *Piezoelectric Transducers and Applications*: Springer.
- Bera, A. and Babadagli, T. 2015. Status of Electromagnetic Heating for Enhanced Heavy Oil/Bitumen Recovery and Future Prospects: A Review. *Applied Energy* **151**: 206-226.
- Bientinesi, M., Petarca, L., Cerutti, A. et al. 2013. A Radiofrequency/Microwave Heating Method for Thermal Heavy Oil Recovery Based on a Novel Tight-Shell Conceptual Design. *Journal of Petroleum Science and Engineering* **107**: 18-30.
- Bjorndalen, N. and Islam, M. 2004. The Effect of Microwave and Ultrasonic Irradiation on Crude Oil During Production with a Horizontal Well. *Journal of petroleum Science and Engineering* **43** (3-4): 139-150.
- Bjorndalen, N., Mustafiz, S., and Islam, M. 2003. Numerical Modeling of Petroleum Fluids under Microwave Irradiation for Improved Horizontal Well Performance. *International communications in heat and mass transfer* **30** (6): 765-774.
- Carrizales, M.A., Lake, L.W., and Johns, R.T. 2008. Production Improvement of Heavy-Oil Recovery by Using Electromagnetic Heating. In *SPE Annual Technical Conference and Exhibition*: Society of Petroleum Engineers. ISBN 1555631479.
- Chanaa, M.B., Lallemand, M., and Mokhlisse, A. 1994. Pyrolysis of Timahdit, Morocco, Oil Shales under Microwave Field. *Fuel* **73** (10): 1643-1649.
- Chhetri, A. and Islam, M. 2008. A Critical Review of Electromagnetic Heating for Enhanced Oil Recovery. *Petroleum Science and Technology* **26** (14): 1619-1631.
- Chien, Y.-C. 2012. Field Study of in Situ Remediation of Petroleum Hydrocarbon Contaminated Soil on Site Using Microwave Energy. *Journal of hazardous materials* **199**: 457-461.
- Chung, B.-K. 2007. Dielectric Constant Measurement for Thin Material at Microwave Frequencies. *Progress In Electromagnetics Research* **75**: 239-252.
- Curie, J. and Curie, P. 1880. On Electric Polarization in Hemihedral Crystals with Inclined Faces. *Comptes Rendus* **91**: 383-386.
- Das, S.K. 2008. Electro Magnetic Heating in Viscous Oil Reservoir. In *International Thermal Operations and Heavy Oil Symposium*: Society of Petroleum Engineers. ISBN 1555631991.

- Davison, R.J. 1995. Electromagnetic Stimulation of Lloydminster Heavy Oil Reservoirs: Field Test Results. *The Journal of Canadian Petroleum Technology*. DOI: 10.2118/95-04-01
- Davletbaev, A., Kovaleva, L., and Babadagli, T. 2011. Mathematical Modeling and Field Application of Heavy Oil Recovery by Radio-Frequency Electromagnetic Stimulation. *Journal of petroleum science and engineering* **78** (3): 646-653.
- Doll, H.G. 1949. Introduction to Induction Logging and Application to Logging of Wells Drilled with Oil Base Mud. *Journal of Petroleum Technology* **1** (06): 148-162.
- Fanchi, J.R. 1990. Feasibility of Reservoir Heating by Electromagnetic Irradiation. Society of Petroleum Engineers. DOI: 10.2118/20483-MS.
- Faraday, M. 1832. Experimental Researches in Electricity. *Philosophical transactions of the Royal Society of London* **122**: 125-162.
- Faraday, M. 1839. Experimental Researches in Electricity. Fifteenth Series. *Philosophical Transactions of the Royal Society of London* **129**: 1-12.
- Foucault, L. 1878. *Recueil Des Travaux Scientifiques De Léon Foucault: Texte*: Gauthier-villars. Original edition. ISBN.
- Freedman, R. and Vogiatzis, J.P. 1979. Theory of Microwave Dielectric Constant Logging Using the Electromagnetic Wave Propagation Method. *Geophysics* **44** (5): 969-986.
- Gasner, L.L., Denloye, A., and Regan, T.M. 1986. Microwave and Conventional Pyrolysis of a Bituminous Coal. *Chemical Engineering Communications* **48** (4-6): 349-354.
- Gauss, C.F. 1813. *Observationes Cometae Secundi, Observatorio Gottingensi Factae, Adjectis Nonnullis Adnotationibus Circa Calculum Orbitalium Parabolicarum*. In: Göttingen.
- Gauss, C.F. 1867. *Allgemeine Theorie Des Erdmagnetismus (1838)*. *Werke* **5**: 127-193.
- Gunal, O.G. and Islam, M. 2000. Alteration of Asphaltic Crude Rheology with Electromagnetic and Ultrasonic Irradiation. *Journal of Petroleum Science and Engineering* **26** (1-4): 263-272.
- Hasanvand, M. and Golparvar, A. 2014. A Critical Review of Improved Oil Recovery by Electromagnetic Heating. *Petroleum Science and Technology* **32** (6): 631-637.
- Hascakir, B., Acar, C., and Akin, S. 2009. Microwave-Assisted Heavy Oil Production: An Experimental Approach. *Energy & Fuels* **23** (12): 6033-6039.
- Hascakir, B. and Akin, S. 2009. Recovery of Turkish Oil Shales by Electromagnetic Heating and Determination of the Dielectric Properties of Oil Shales by an Analytical Method. *Energy & Fuels* **24** (1): 503-509.
- Hascakir, B., Babadagli, T., and Akin, S. 2008. Experimental and Numerical Simulation of Oil Recovery from Oil Shales by Electrical Heating. *Energy & Fuels* **22** (6): 3976-3985.
- Hiebert, A., Vermeulen, F., Chute, F. et al. 1986. Numerical Simulation Results for the Electrical Heating of Athabasca Oil-Sand Formations. *SPE reservoir engineering* **1** (01): 76-84.
- Ikeda, T. 1996. *Fundamentals of Piezoelectricity*: Oxford university press. Original edition. ISBN 0198564600.

- Islam, M.R. and Wadadar, S.S. 1991. Enhanced Oil Recovery of Ugnu Tar Sands of Alaska Using Electromagnetic Heating with Horizontal Wells. Society of Petroleum Engineers. DOI: 10.2118/22177-MS.
- Jackson, C. 2002. Upgrading a Heavy Oil Using Variable Frequency Microwave Energy. Society of Petroleum Engineers. DOI: 10.2118/78982-MS.
- Jha, K. and Chakma, A. 1999. Heavy-Oil Recovery from Thin Pay Zones by Electromagnetic Heating. *Energy Sources* **21** (1-2): 63-73.
- Joule, J.P. 1850. Iii. On the Mechanical Equivalent of Heat. *Philosophical Transactions of the royal Society of London* **140**: 61-82.
- Kar, T. and Hascakir, B. 2015. The Role of Resins, Asphaltenes, and Water in Water–Oil Emulsion Breaking with Microwave Heating. *Energy & Fuels* **29** (6): 3684-3690.
- Kasevich, R., Price, S., Faust, D. et al. 1994. Pilot Testing of a Radio Frequency Heating System for Enhanced Oil Recovery from Diatomaceous Earth. In *SPE Annual Technical Conference and Exhibition*: Society of Petroleum Engineers. ISBN 155563463X.
- Kawala, Z. and Atamańczuk, T. 1998. Microwave-Enhanced Thermal Decontamination of Soil. *Environmental science & technology* **32** (17): 2602-2607.
- Kokal, S. and Al-Kaabi, A. 2010. Enhanced Oil Recovery: Challenges & Opportunities. *World Petroleum Council: Official Publication* **64**.
- Koolman, M., Huber, N., Diehl, D. et al. 2008. Electromagnetic Heating Method to Improve Steam Assisted Gravity Drainage. In *International Thermal Operations and Heavy Oil Symposium*: Society of Petroleum Engineers. ISBN 1555631991.
- Kovaleva, L., Nasyrov, N., and Khaidar, A. 2004. Mathematical Modeling of High-Frequency Electromagnetic Heating of the Bottom-Hole Area of Horizontal Oil Wells. *Journal of Engineering Physics and Thermophysics* **77** (6): 1184-1191.
- Krupka, J. 2006. Frequency Domain Complex Permittivity Measurements at Microwave Frequencies. *Measurement Science and Technology* **17** (6): R55.
- Li, G., Meng, Y., and Tang, H. 2006. Clean up Water Blocking in Gas Reservoirs by Microwave Heating: Laboratory Studies. In *International Oil & Gas Conference and Exhibition in China*: Society of Petroleum Engineers. ISBN 1555631835.
- Lippmann, M. 1881. On the Principle of the Conservation of Electricity. *The London, Edinburgh, and Dublin Philosophical Magazine and Journal of Science* **12** (73): 151-154.
- Martinez, A. and Byrnes, A.P. 2001. *Modeling Dielectric-Constant Values of Geologic Materials: An Aid to Ground-Penetrating Radar Data Collection and Interpretation*: Kansas Geological Survey Lawrence, Kansas. Original edition. ISBN.
- Maxwell, J.C. 1865. A Dynamical Theory of the Electromagnetic Field. *Philosophical transactions of the Royal Society of London* **155**: 459-512.
- McGee, B.C. and Vermeulen, F.E. 2007. The Mechanisms of Electrical Heating for the Recovery of Bitumen from Oil Sands. *Journal of canadian petroleum technology* **46** (01).
- Meador, R.A. and Cox, P. 1975. Dielectric Constant Logging, a Salinity Independent Estimation of Formation Water Volume. In *Fall Meeting of the Society of*

- Petroleum Engineers of AIME: Society of Petroleum Engineers.* ISBN 1555637531.
- Metaxas, A.a. and Meredith, R.J. 1983. *Industrial Microwave Heating*: IET. Original edition. ISBN 0906048893.
- Meyer, R.F., Attanasi, E.D., and Freeman, P.A. 2007. *Heavy Oil and Natural Bitumen Resources in Geological Basins of the World*.
- Mokhlisse, A., Chanâa, M.B., and Outzourhit, A. 2000. Pyrolysis of the Moroccan (Tarfaya) Oil Shales under Microwave Irradiation. *Fuel* **79** (7): 733-742.
- Monsef-Mirzai, P., Ravindran, M., McWhinnie, W.R. et al. 1995. Rapid Microwave Pyrolysis of Coal: Methodology and Examination of the Residual and Volatile Phases. *Fuel* **74** (1): 20-27.
- Moran, J. and Kunz, K. 1962. Basic Theory of Induction Logging and Application to Study of Two-Coil Sondes. *Geophysics* **27** (6): 829-858.
- Mukhametshina, A. and Martynova, E. 2013. Electromagnetic Heating of Heavy Oil and Bitumen: A Review of Experimental Studies and Field Applications. *Journal of Petroleum Engineering* **2013**.
- Mutyala, S., Fairbridge, C., Paré, J.J. et al. 2010. Microwave Applications to Oil Sands and Petroleum: A Review. *Fuel Processing Technology* **91** (2): 127-135.
- Oliveira, H.J.M.d., Barillas, J.L.M., da Mata, W. et al. 2009. Energetic Optimization to Heavy Oil Recovery by Electromagnetic Resistive Heating (Erh). In *Latin American and Caribbean Petroleum Engineering Conference*: Society of Petroleum Engineers. ISBN 1555632556.
- Ovalles, C., Fonseca, A., Lara, A. et al. 2002. Opportunities of Downhole Dielectric Heating in Venezuela: Three Case Studies Involving Medium, Heavy and Extra-Heavy Crude Oil Reservoirs. In *SPE International Thermal Operations and Heavy Oil Symposium and International Horizontal Well Technology Conference*: Society of Petroleum Engineers. ISBN 1555639496.
- Owen, N.A., Inderwildi, O.R., and King, D.A. 2010. The Status of Conventional World Oil Reserves—Hype or Cause for Concern? *Energy policy* **38** (8): 4743-4749.
- Pizarro, J. and Trevisan, O. 1990. Electrical Heating of Oil Reservoirs: Numerical Simulation and Field Test Results. *Journal of Petroleum Technology* **42** (10): 1,320-321,326.
- Rehman, M.M. and Meribout, M. 2012. Conventional Versus Electrical Enhanced Oil Recovery: A Review. *Journal of Petroleum Exploration and Production Technology* **2** (4): 169-179.
- Rice, S., Kok, A., and Neate, C. 1992. A Test of the Electric Heating Process as a Means of Stimulating the Productivity of an Oil Well in the Schoonebeek Field. In *Annual Technical Meeting*: Petroleum Society of Canada. ISBN 1555634680.
- Russell, W.L. 1944. The Total Gamma Ray Activity of Sedimentary Rocks as Indicated by Geiger Counter Determinations. *Geophysics* **9** (2): 180-216.
- Sahni, A., Kumar, M., and Knapp, R.B. 2000. Electromagnetic Heating Methods for Heavy Oil Reservoirs. In *SPE/AAPG Western Regional Meeting*: Society of Petroleum Engineers. ISBN 1555633455.

- Sarathi, P.S. and Olsen, D.K. 1992. *Practical Aspects of Steam Injection Processes: A Handbook for Independent Operators*. National Inst. for Petroleum and Energy Research, Bartlesville, OK (United States).
- Singh, R.P. and Heldman, D.R. 2001. *Introduction to Food Engineering*: Gulf Professional Publishing. Original edition. ISBN 0080574491.
- Snyder, D.D. and Fleming, D.B. 1985. Well Logging—a 25-Year Perspective. *Geophysics* **50** (12): 2504-2529.
- Sorrell, S., Speirs, J., Bentley, R. et al. 2010. Global Oil Depletion: A Review of the Evidence. *Energy Policy* **38** (9): 5290-5295.
- Sresty, G.C., Dev, H., Snow, R.H. et al. 1986. Recovery of Bitumen from Tar Sand Deposits with the Radio Frequency Process. *SPE Reservoir Engineering* **1** (01): 85-94.
- Sun, D.-W. 2014. *Emerging Technologies for Food Processing*: Elsevier. Original edition. ISBN 0124104819.
- Thostenson, E. and Chou, T.-W. 1999. Microwave Processing: Fundamentals and Applications. *Composites Part A: Applied Science and Manufacturing* **30** (9): 1055-1071.
- Vega, C. and Delgado, M. 2002. Treatment of Waste-Water/Oil Emulsions Using Microwave Radiation. In *SPE International Conference on Health, Safety and Environment in Oil and Gas Exploration and Production*: Society of Petroleum Engineers. ISBN 155563947X.
- Vermeulen, F. and McGee, B. 2000. In-Situ Electromagnetic Heating for Hydrocarbon Recovery and Environmental Remediation. *Journal of Canadian Petroleum Technology* **39** (08).
- Von Hippel, A.R. 1954. *Dielectric Materials and Applications*: Artech House on Demand. Original edition. ISBN 0890068054.
- Wacker, B., Karmeileopardus, D., Trautmann, B. et al. Electromagnetic Heating for in-Situ Production of Heavy Oil and Bitumen Reservoirs. Society of Petroleum Engineers. DOI: 10.2118/148932-MS.
- Wadadar, S. and Islam, M. 1994. Numerical Simulation of Electromagnetic Heating of Alaskan Tar Sands Using Horizontal Wells. *Journal of Canadian Petroleum Technology* **33** (07).
- Wahl, J. 1983. Gamma-Ray Logging. *Geophysics* **48** (11): 1536-1550.
- Wattenbarger, R. and McDougal, F. 1988. Oil Production Response to in Situ Electrical Resistance Heating (Erh). *Journal of Canadian Petroleum Technology* **27** (06).
- Wharton, R.P., Rau, R.N., and Best, D.L. 1980. Electromagnetic Propagation Logging: Advances in Technique and Interpretation. In *SPE Annual Technical Conference and Exhibition*: Society of Petroleum Engineers. ISBN 1555636934.
- Wilson, A. 2012. Comparative Analysis of Electromagnetic Heating Methods for Heavy-Oil Recovery. DOI: 10.2118/0612-0126-JPT

2. PART 1: PENETRATION DEPTH OF MICROWAVES UNDER THE INFLUENCE OF STATIC MECHANICAL STRESS: THE DIRECT PIEZOELECTRIC EFFECT

Abstract

Electromagnetic waves as the mechanism of heat generation for enhanced oil recovery is a concept that offers advantage as a means of overcoming shortcomings of steam. However, poor penetration depth of the wave inhibits economic exploitation. Inherent piezoelectricity in quartz enables additive penetration to be achieved through an introduction of a static mechanical load. The maximization of the wave penetration accordingly results in much greater stimulated volume and therefore more viable economic return.

The direct piezoelectric effect asserts that the polarity of the material will change under the influence of an imposed stress state. A static load through coaxial compression was introduced where the polarization of the material was measured and represented by variation in the complex permittivity of the sample. Both absorption and penetration characteristics are directly dependent upon the complex permittivity so manipulation of this parameter by mechanical loading changes the penetration of the wave. Measurements were performed both with and without the imposed static load to provide for direct comparison.

The benefit of piezoelectricity is portrayed in all investigated samples where the utilization of both sandstone (quartz-rich) and limestone (quartz-poor) cores isolates the causality of additive penetration to the direct piezoelectric effect. The differential stress applied to the cores was capable of activating the transformation of the polar state of the

materials. The modification of the polarity generated a more favorable penetration environment where the remaining energy content of the wave was increased. The static load that is introduced is analogous to overburden stress and will represent the pressure component present in any reservoir. Increased penetration of the wave equates to greater heated volume of oil and enhanced transmission of oil to the producing well.

Poor penetration depth of electromagnetic waves hinders economic implementation of what is otherwise a technically feasible heating mechanism in the reservoir. Adopting a strategy that practices the direct piezoelectric effect made possible by the quartz content in sandstones increases the volume of oil that is heated. Additive penetration depth by static loading of the cores in this study elucidates the potential to benefit from this phenomenon.

Introduction

Utilization of electromagnetic (EM) waves is a process that has been gaining traction in the industry as an effective mechanism of heat introduction to the reservoir. Predominately, steam injection is implemented in thermal EOR as a means of imparting heat energy to lower viscosity but steam is situationally inefficient. (Fanchi 1990; Mukhametshina and Martynova 2013; Sarathi and Olsen 1992). The nature of steam as a heat-transporting agent renders it incapable of generating heat in the reservoir, instead essentially serving as a conduit which carries heat energy into the reservoir. The mechanism of heat exchange with steam is convection, requiring contact between the steam and oil at the interface which has implications in the reservoir. A temperature gradient is established between the inside volume of the mass and the heated interface of

the material which contacted the steam. The fluidity of steam dictates propagation through the path of least resistance and is governed by the physical characteristics of the reservoir (Carrizales et al. 2008; Hasanvand and Golparvar 2014). Injected steam travels through the pore space along the path of least resistance and owing to variability in the horizontal and vertical permeability; the steam often propagates out of the target zone. Lack of directional control of the fluid results in minimal efficiency as any steam that leaves the system is accordingly a loss of additive energy, providing no benefit in terms of increased flow potential (Hascakir et al. 2009).

Thin reservoirs realize prohibitive losses of steam and deep reservoirs are also poor candidates for steam introduction as steam quality decreases with increasing depth (Sahni et al. 2000). In contrast, the irradiation of the reservoir with EM waves takes advantage of volumetric heating. The ability of the waveform to travel through a material instead of to the contact at the interface is an advantage unique to EM heating (Jha and Chakma 1999; Mutyala et al. 2010). The entirety of the volume of the material is instantaneously heated resulting in faster and more efficient localized temperature gain. Therefore, EM waves can be situationally more effective as a mechanism of heat introduction than steam in the presence of both thin and deep reservoirs.

The potential of EM waves to heat the reservoir has warranted numerous pilot tests to investigate the technical feasibility of the concept. Additive heat to the reservoir was attained and the projects achieved a measurable increase in the temperature of the reservoir as a function of the radiation (Davison 1995; Kasevich et al. 1994; Sresty et al. 1986). However, prohibitive wave attenuation results in poor depth of penetration of the wave

and the accessed reservoir is not sufficient to produce an economically viable volume of hydrocarbon. Mathematically, absorption and penetration depth are inversely related where high absorption necessarily equates to low penetration depth resulting in minimized treated oil volume. Large magnitudes of absorption correspond to less remaining incident wave energy to continue propagation into the reservoir. The degree of absorption of the incident wave by the fluids in the pore space is excessive considering the necessity to penetrate deep into the reservoir, marginalizing the technology in terms of economics (Carrizales et al. 2008; Das 2008; Koolman et al. 2008). Implementation on a field-scale hinges upon harnessing the absorptive capacity in the dielectric heating frequency range while increasing the penetration depth of the incident wave.

Heat generation in the dielectric frequency range is governed by the inability of the material charges in the medium to maintain phase with a rapidly oscillating field. The natural polar state of the sample is changed from the interaction of the wave with the reservoir material (Hill 1969). This phenomenon is compounded under the presence of mechanical stress governed by piezoelectricity. The direct piezoelectric effect is a phenomenon where certain materials will undergo a change in polarity and voltage as a function of an applied external mechanical stress (Curie and Curie 1880a). The behavior is reversible where the influence of an electric current through the element will result in a mechanical stress, referred to as the converse piezoelectric effect (Lippmann 1881). Quartz is a piezoelectric material and is the fundamental principle behind the interest in introducing mechanical stress into a consolidated sandstone core to manipulate microwave penetration depth (Tuck et al. 1977). Any material that is constituted of a piezoelectric

element has the potential to display piezoelectric behavior; so sandstone reservoirs, constituted predominately of quartz, have the ability to exhibit the identified phenomenon.

Subjecting a piezoelectric element to an external force corresponds to a slight deformation in the position of the negative and positive centers of the molecule, thus increasing polarity (Arnau and Soares 2009; Ikeda 1996). Asymmetry in the crystalline structure of the unit cell of the quartz mineral creates non-uniform deformation of the electrical potential of the element. This deformation creates dipoles in the molecule where deviance from an electrically neutral molecule changes the polarization (Cady 1946). The change in the polar state of the molecule is reflected in corresponding change in the complex permittivity of the material, defined as a measure of resistance encountered when forming an electric field in a medium (Metaxas and Meredith 1983; Van Beek 1967). Penetration depth of the microwave is related to the polarity of the medium and so by changing the complex permittivity of the interface as a result of the polarization, the depth of the wave propagation can be manipulated. Therefore, penetration depth and complex permittivity will be pseudo measurements for the effect and magnitude of piezoelectricity.

Realization of this behavior is predicated on the presence of a differential mechanical stress through a piezoelectric element, which in the case of the sandstone cores in the quartz crystal (Bishop 1981). Inherent piezoelectricity in the quartz crystals found in sandstone rocks provides the means of manipulating the penetration depth of the microwave to access more reservoir. Increasing the stimulated reservoir volume directly equates to an increased volume of heated oil, generating more attractive project economics. Exploiting the potential benefit of the piezoelectric effect in the context of

enhanced oil recovery offers the ability to address concerns regarding relatively poor penetration depth of microwaves.

Experimental Procedure

The experimental procedure consisted of measuring the complex permittivity of consolidated core samples in a natural state and then doing the same measurement while a static mechanical stress state was imposed. Overburden stress inherent to any reservoir introduces a pressure component and a mechanical stress. This stress state is simulated in this study by means of an applied coaxial compression and represents the pressure domain of the experiments (Morte et al. 2018). Piezoelectricity dictates that the electric potential of the sample will change in the presence of a mechanical stress. Any polarization achieved by the coaxial compression is then indicative of the contribution of piezoelectric behavior, thereby illustrating the viability of the concept.

The equipment required consisted of a N9923A FieldFox Handheld RF vector network analyzer (VNA), a computer, a dielectric probe, coaxial cable, and a vice. The VNA generates a wave in the frequency of interest which is then transmitted by the coaxial cable to the dielectric probe (Keysight 2013). The signal emanates out of the probe which simultaneously acts as the transmitter and receiver and directs the wave into the consolidated core samples (Kaatze 2010; Marsland and Evans 1987). The probe operates on the basis of the S-parameters or scattering parameters which is an interfacial measurement. The incident wave propagates to the interface of the core and is either reflected or transmitted as a function of the complex permittivity of the sample (Baker-

Jarvis et al. 1990; Krupka 2006; Weir 1974). The complex permittivity of the sample is directly calculated by the VNA as a result of the proportion of reflected and transmitted wave (Ghodgaonkar et al. 1989; Varadan et al. 1991). The VNA model along with the dielectric probe kit are depicted in Figure 2.1.



Figure 2.1 - Both the vector network analyzer and dielectric probe kit utilized to measure the complex permittivity of the sample

Complex permittivity is the parameter that controls both the penetration and absorption characteristics and describes the capabilities of the material as a microwave receptor (Singh and Heldman 2001; Sun 2014). It is a complex number that consists of both a real and imaginary component as is evidenced by Eq 2.1. The real portion is called dielectric constant and describes the ability of the material to store energy (Clarke et al. 2003; Von Hippel 1954). The imaginary component is called loss index which defines the ability of the material to convert electrical energy to heat energy (Gross 1941; Hill 1969). Both of these parameters are vital to EM heating and entail the success or failure of high-frequency heating implementation. The loss tangent as displayed in Eq 2.2 defines the ability of the material to store microwave energy and represents the efficacy of the material

as a microwave absorber. The rate of attenuation of the wave is calculated by means of Eq 2.3 where α is the attenuation constant. The penetration depth can be found as a result of the inverse nature of attenuation and penetration using Eq 2.4. Absorbed power is described by Eq 2.5 where both the magnitude of the applied electric field as well as the complex permittivity are independent parameters. Absorbed power directly correlates to heat introduction and temperature gain.

$$\varepsilon_r^* = \frac{\varepsilon^*}{\varepsilon_0} = \varepsilon' - j\varepsilon'' \quad \text{Eq 2.1}$$

$$\tan(\delta) = \frac{\varepsilon'}{\varepsilon''} \quad \text{Eq 2.2}$$

$$\alpha = \frac{2*\pi*f}{2,998*10^8} * \sqrt{\frac{\varepsilon'}{2} \left[\sqrt{1 + \tan(\delta)^2} - 1 \right]} \quad \text{Eq 2.3}$$

$$d_p = \frac{1}{2\alpha} \quad \text{Eq 2.4}$$

$$P_d = 2\pi f \varepsilon_0 \varepsilon'' |E|^2 \quad \text{Eq 2.5}$$

Increase in penetration depth calculated from equation 2.4 will be considered indicative of the influence of piezoelectricity. However, before the experimental equipment could be confidently applied in quartz-bearing rock (sandstone), the accuracy and validity of the procedure needed to be validated. Therefore, it became necessary to establish a control to elucidate the effect of piezoelectricity in the context of enhanced oil recovery. Complex permittivity values as a function of frequency were taken for a pure quartz crystal which will serve as the control. Investigation into the contribution of the fundamental mechanism of polarization of the quartz crystal creates the ability to attribute additive penetration of the sandstone to the direct piezoelectric effect.

The crystal has very little pore space where the contribution of air in the pore space is negligible so the data recorded reflects the true behavior of solely the quartz crystal. The behavior that is illustrated in Figure 2.2 in terms of dielectric constant and loss tangent exhibited by the crystal are corroborated by literature and help to validate the fundamental approach taken in the experimental procedure. The control experiment definitively shows the impact of the direct piezoelectric effect as there is a marked increase in penetration depth under the influence of mechanical stress which provides validation in the governing physics behind the project. The loss tangent is low as quartz is a low loss material and the dielectric constant is accordingly higher relative to the sandstone. Utilization of the quartz crystal enables the direct comparison of measured data with what is fundamentally known and expected which validates the accuracy of the measurements on the other samples.

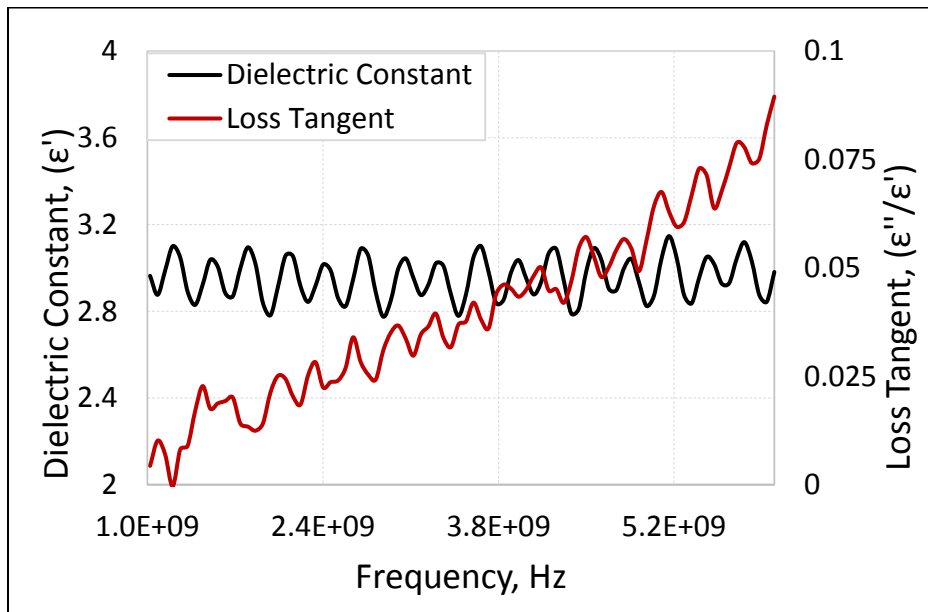


Figure 2.2 - Real and imaginary components of relative permittivity as a function of frequency for the quartz control crystal

Penetration depth as a function of frequency is illustrated in Figure 2.3 for both the stressed and the unstressed cases where the expected behavior of increased penetration depth for the stressed core is evident. In accordance with the piezoelectric effect, the mechanical stress introduced to the core employing compressive force alters the polarity distribution vector resulting in increased penetration depth. Quartz is the component of sandstone which contributes to piezoelectricity so a pure quartz crystal would experience the largest gain in penetration depth with stress. Figure 2.3 displays a large increase in penetration depth at the lower frequencies where the phenomenon of piezoelectricity would be more prominent.

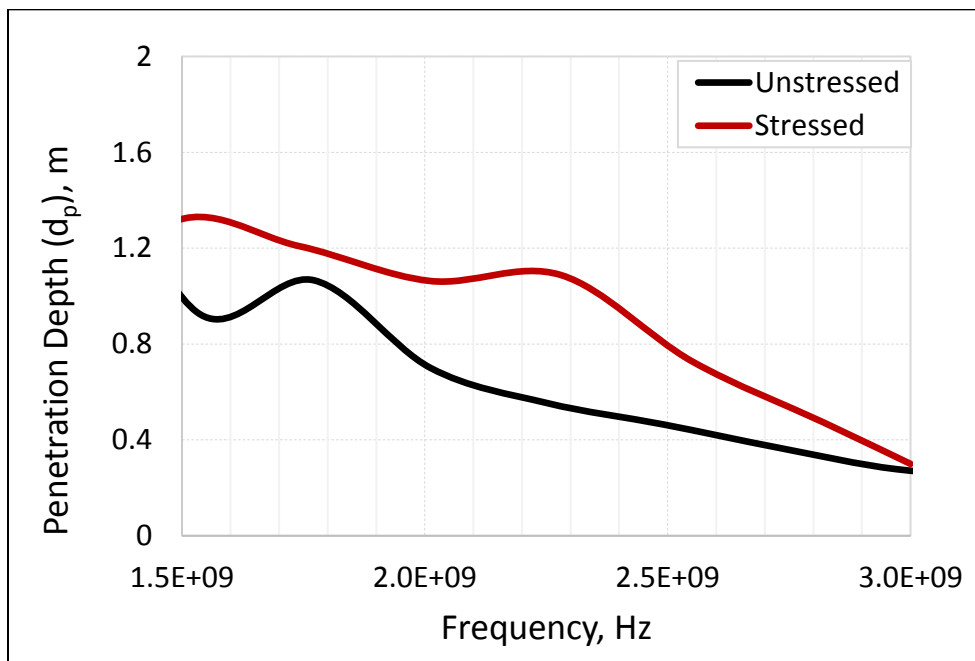


Figure 2.3 - Penetration depth of unstressed and stressed quartz crystal

Once the fundamental mechanism of piezoelectricity was validated by the control experiments, the experimental procedure was expanded to consolidated cores to be more

analogous to reservoir conditions. This provides for closer examination into the in-situ behavior of the reservoir in a more comprehensive and robust manner. The mineralogy of the rock is pertinent to the experiments as no benefit will be achieved without the presence of the piezoelectric material (quartz). Therefore, two sandstone samples which consist of mostly quartz will be used along with one limestone which has mostly calcium carbonate. Sample 1 is a core taken from an outcrop of the Bandera sandstone with a quartz content of 77.1% and a porosity value of 21% (Shehata and Nasr-El-Din 2014). Sample 2 is a core taken from an outcrop of the Berea sandstone with a quartz content of 85.2% and a porosity value of 17% (Churcher et al. 1991; Shehata and Nasr-El-Din 2014). Sample 3 is a core taken from an Indiana limestone outcrop that contains 99% calcite with a porosity of 14% (Churcher et al. 1991). The presence of the limestone core will serve to isolate the foundational contribution of piezoelectricity as the lack of any quartz content should correspond to no dependency of penetration depth on the stress state imposed. Table 2.1 displays the properties of the three different rock samples selected.

Table 2.1 - Properties of core samples including quartz content

Cores	Lithology	Quartz (%)	Limestone (%)	Kaolinite (%)	Illite (%)	Albite (%)	Porosity (%)	Perm (mD)
Sample 1	Sandstone	77.1	2.3	5.1	2.8	12.7	21	30
Sample 2	Sandstone	85.2	0.8	11.8	2.2	0	17	80
Sample 3	Limestone	1	99	0	0	0	14	4

Cores were saturated with three different oils along with water where fluid in the pore space is more representative and analogous of in-situ conditions and provides for

more suitable analysis. The relatively incompressible nature of the fluids in comparison to air allows the core to maintain pore pressure to essentially oppose the compressive force. The mechanical stress is therefore distributed primarily through the rock matrix instead of through the pore space. The load of the coaxial compression changes the electric potential of the sample through a dynamic polarization which increases the penetration depth significantly over the frequency range provided. Consistency in the rock lithology will be used to further elucidate the impact and contribution of the saturating fluid to the complex permittivity response.

The oil samples were selected based on viscosity, composition, and dielectric response to achieve the greatest diversity in the samples. The first oil selected (C1) has a lower dielectric constant of 2.61, more manageable viscosity of 496 cP at room temperature, and a moderate loss tangent of .0226. These parameters were deemed vital to the relative amount of microwave penetration as loss tangent is a measure of the efficacy of the material to absorb microwaves. The second oil selected (C2) has a higher trace metals content which results in a higher dielectric constant of 3.84 and a higher loss tangent of .0295 along with a higher viscosity of 53,146 cP. The high loss tangent in conjunction with the high dielectric constant is indicative of an increased capacity to absorb microwave energy relative to the other oils making oil two a prime candidate. The third oil selected (C3) has a moderate dielectric constant of 2.69 and a lower loss tangent of .0192, corresponding to a greater transmissibility of the incident MW. By utilizing three different oil samples, the response that is achieved will be able to capture heterogeneity in the pore space. The varying oil dielectric properties will also give an inclination as to the

dependencies of penetration depth on complex permittivity properties of the fluid volume. The properties of the three oils selected along with water can be seen in greater detail in Table 2.2.

Table 2.2 - Properties of all reservoir fluid samples including complex permittivity

Sample	API Gravity	Viscosity cP	Dielectric Constant	Loss Index	Loss Tangent
Oil C1	17.12	496	2.61	0.0598	0.0226
Oil C2	8.19	53146	3.84	0.1127	0.0295
Oil C3	12.09	10139	2.69	0.0528	0.0192
Water	10	1	77.1	9.32	0.121

Experimental Results and Discussion

In accordance with piezoelectricity, manipulation of the imposed stress state of the cores directly affects the calculated penetration depth of the EM wave. The presence of measurable disparity in the absorptive capacity of the samples corroborates the fundamental contribution of the polarized quartz crystal. Additive stress activated a transformation of the polarity of the material, manifesting in an enhanced penetration of the wave. Penetration depth as a function of frequency is illustrated in Figure 2.4 for both the stressed and the unstressed experiments for the oil-saturated sample 1 core. The expected behavior of increased penetration depth for the stressed core is evident. Piezoelectricity is realized where there is a significant increase in penetration depth under the influence of mechanical stress in the lower frequency range.

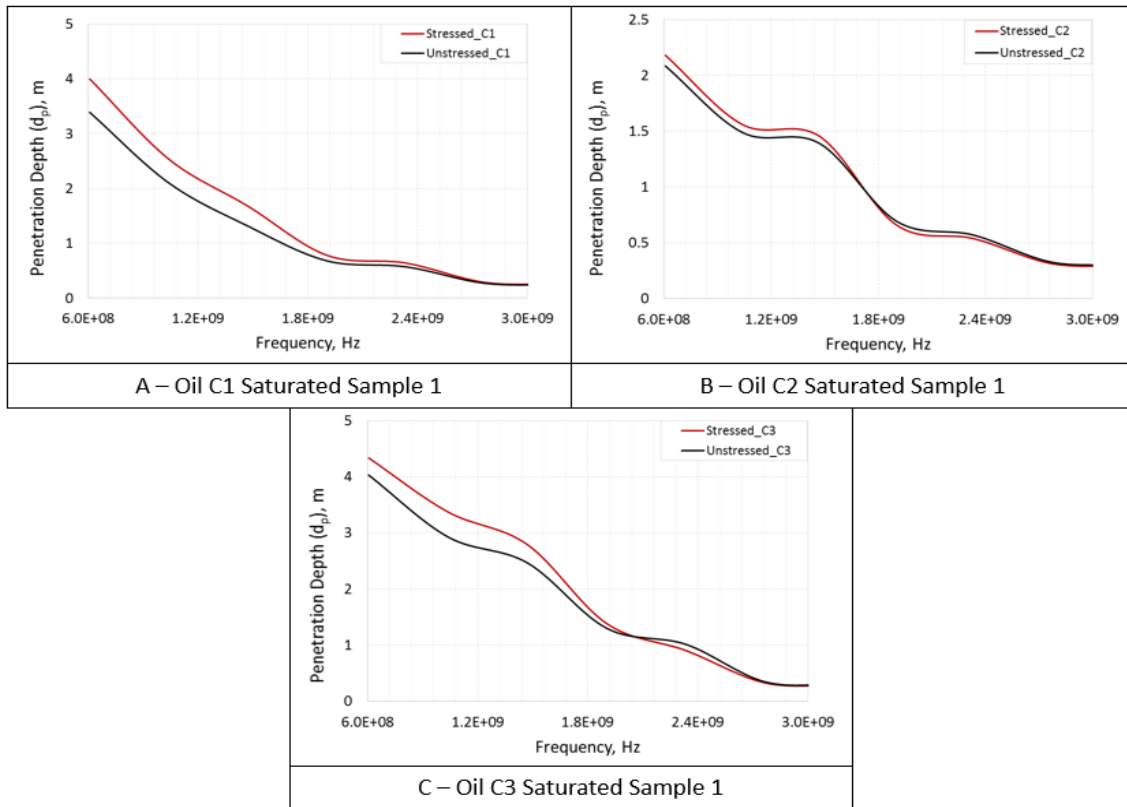


Figure 2.4 - Penetration depth of unstressed and stressed Sample 1 core saturated with oils (A) C1, (B) C2, and (C) C3

The large component of quartz in the sample is sufficient to enable the core to take advantage of piezoelectricity. The presence of the mechanical stress element introduced by the static load causes deviance from an electrically neutral molecule. The polarity distribution vector is altered which corresponds to a relative decrease in wave attenuation. As less incident wave is absorbed, remaining energy content of the wave is greater to continue propagation. The penetration depth of Sample 1 exhibits the same relationship as that of the control but to a lesser extent in regard to the increase realized with the introduction of mechanical stress. The lithology of sandstone contains a majority percent of quartz so the behavior of sandstone samples correlates well to that of the pure quartz.

Inspection of the figure depicts a significant range in penetration depth dependent upon the fluid that occupies the pore space. The saturating oil C2 has a much higher loss tangent than the other two fluids and therefore has a greater predisposition to absorb microwave energy. The relative increase in absorbed wave content by the pore space for the C2 saturated sample is illustrated by the lower penetration depth in comparison to the other two oils. The relationship identified adheres to what would be expected by purely looking at the dielectric response of the fluids themselves. The figure indicates that the dielectric response of the sample as a whole is sensitive to the contribution of the pore space as variation in the loss tangent of the saturating fluid has a large effect on penetration depth (Liao et al. 2018). By changing the loss tangent of the pore space even slightly, the penetration of the wave is greatly affected.

The piezoelectric effect is frequency-dependent and more prominent at lower frequencies. The relaxation time of the quartz crystal has to be sufficiently small to maintain phase with the oscillating EM wave or they are not capable of rotating, so the increase in penetration depth should be largest at the lower end of the spectrum (Titov et al. 2010). Larger frequencies correspond to faster oscillations and less time for the particles to rotate to keep phase with the wave and so the benefit of piezoelectricity is realized only at lower frequencies. This is evident in Figure 2.4 and Figure 2.5 where there is a disparity between the penetration depths of the samples at the lower frequency range. The same relationship identified in Figure 2.4 is once again evidenced in Figure 2.5 which is the oil-saturated sample 2. The samples from the two figures are both sandstones and so the consistency achieved in the result provides confidence in the data and the

conclusions being drawn. The behavior realized in the penetration depth is once again indicative of the benefit of the direct piezoelectric effect.

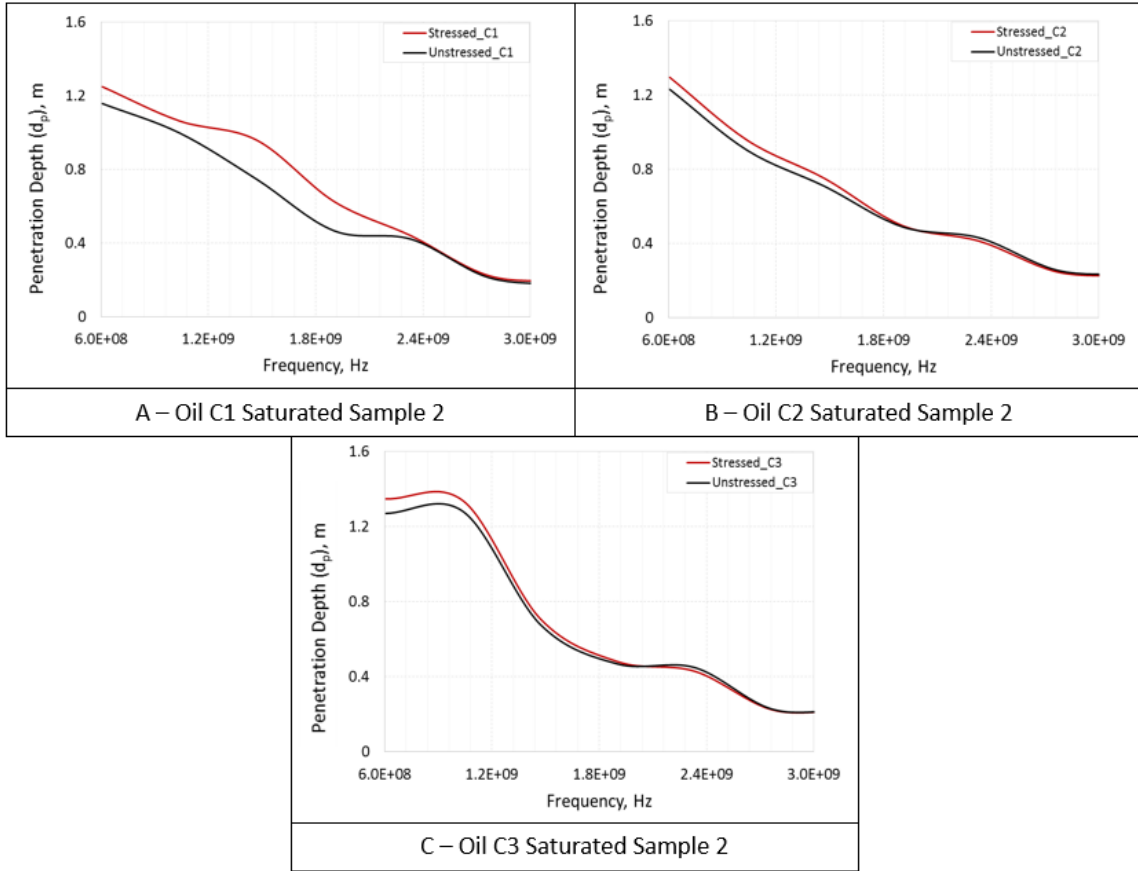


Figure 2.5 - Penetration depth of unstressed and stressed Sample 2 core saturated with oils (A) C1, (B) C2, and (C) C3

Quartz is the piezoelectric element present in the sandstone cores enabling the additive penetration. Limestone is primarily calcium carbonate with very little quartz content. The constituent components of the limestone core lack a piezoelectric material so the limestone core is not capable of experiencing the benefit of additive penetration depth with mechanical stress. Robust measurements were taken over the frequency range of interest where the lack of significant and measurable piezoelectricity within the limestone

cores is indisputable. Figure 2.6 definitively shows no dependency on the coaxial compression, expounding the foundational impact of additive penetration from Figure 2.4 and Figure 2.5 being the direct piezoelectric effect. All things being equal besides the quartz content of the cores, the sandstone achieved measurable disparity in penetration depths while the limestone achieved no change. Utilization of the limestone cores as a control allows for the isolation of the quartz content dependency and helps to explicate a causal relationship. Direct comparison of the responses of the loaded sandstone and limestone cores allows attribution of all additive penetration to piezoelectricity.

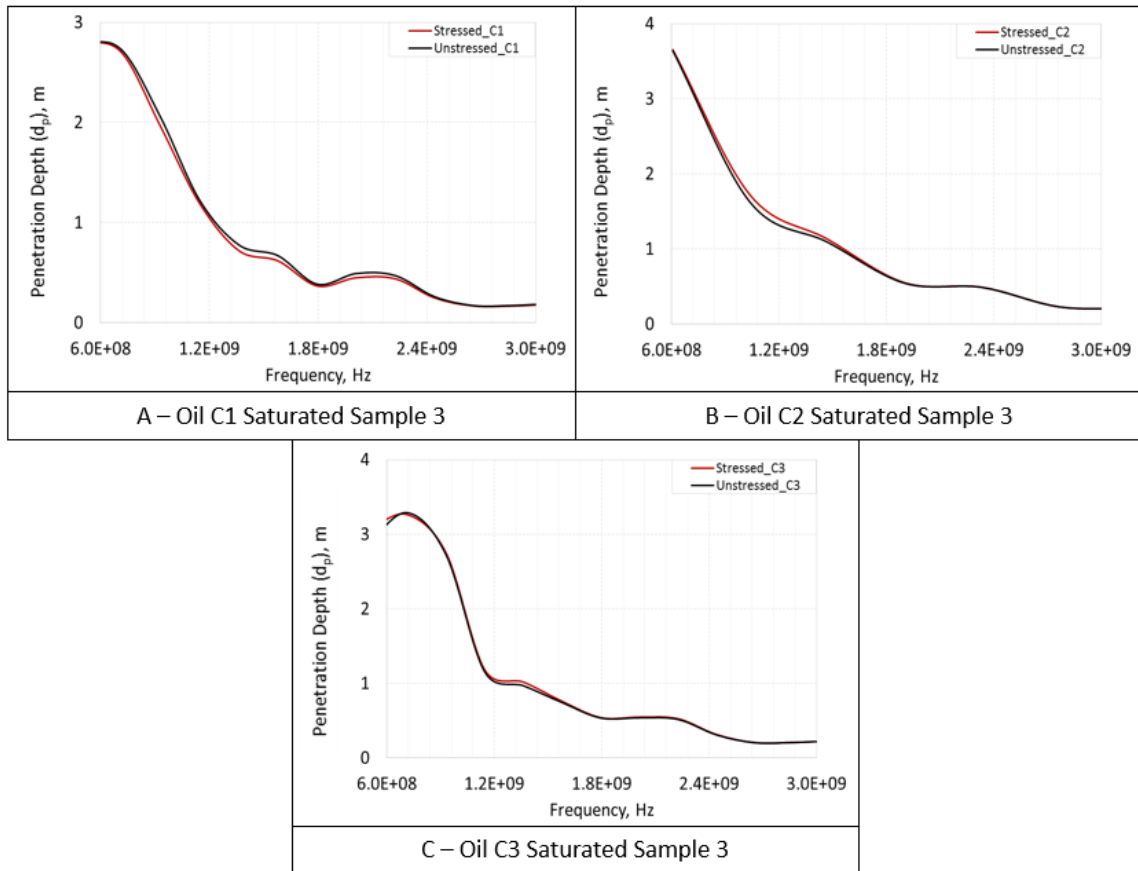


Figure 2.6 - Penetration depth of unstressed and stressed Sample 3 core saturated with oils (A) C1, (B) C2, and (C) C3

Once the response of the pore space with oil as the saturating fluid had been captured, it became necessary to introduce water to extend the domain of the experiments to include a preferential absorber of microwaves. Water is the reservoir fluid that serves as the primary absorber of microwaves owing to very large polarity. Absorption and penetration run directly contrary to each other where large absorption must necessarily equate to lower wave penetration. Looking at the penetration depth of the water sample in juxtaposition to the oils clearly illustrates this relationship. The water-saturated cores experience a much lower penetration relative to the oils as is seen in Figure 2.7. The penetration depth of the water-saturated cores is roughly half that of the oil-saturated cores and so changing the dielectric response of the pore space can change the penetration depth significantly. However, disparity in the penetration depths of the unstressed and stressed sandstones is still achieved. The predisposition of the water towards absorption of the wave does not prohibit the benefit of the imposed stress. Therefore, the piezoelectric effect is capable of creating a more desirable microwave receptive environment in the reservoir irrespective of the fluids that occupy the pore space.

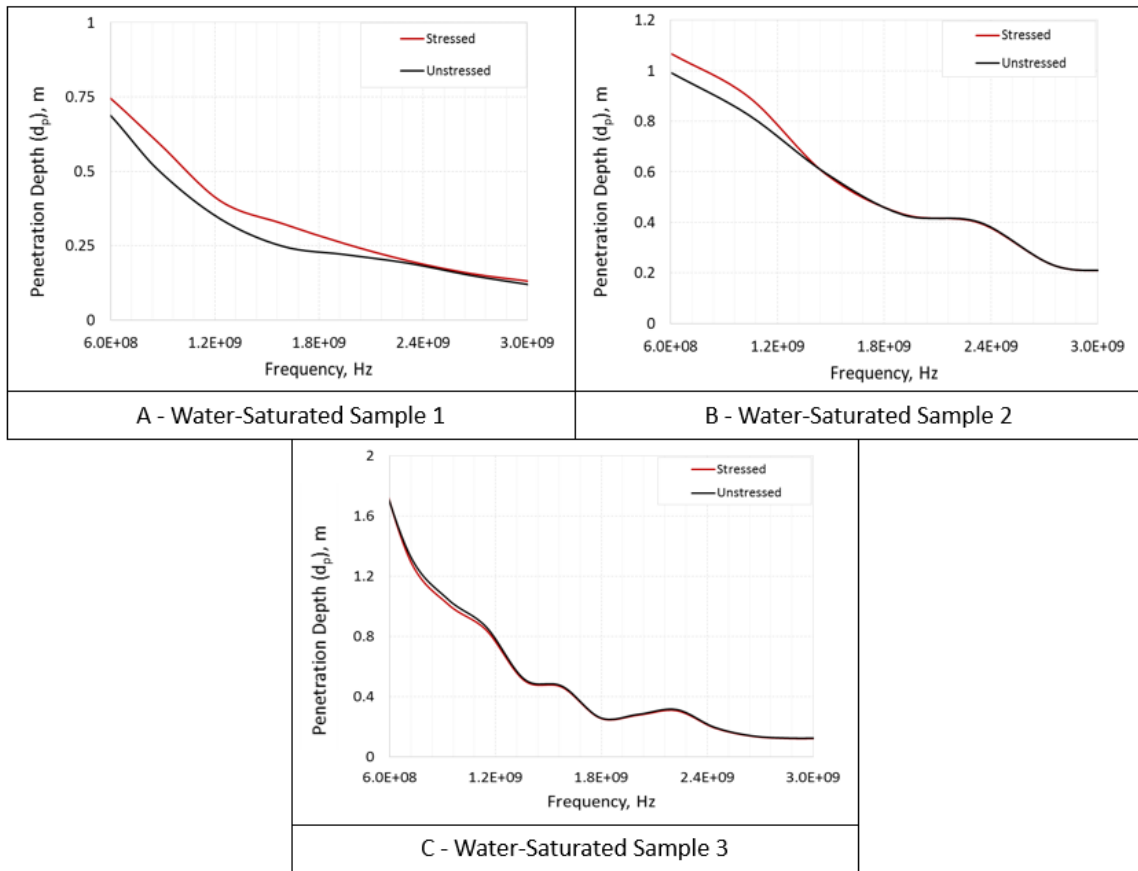


Figure 2.7 - Penetration depth of unstressed and stressed water-saturated cores for lithological cores (A) Sample 1, (B) Sample 2, and (C) Sample 3

The behavior of both water and oil samples corroborates the idea that to take advantage of inherent piezoelectricity, the skeletal frame or rock matrix must be inundated with mechanical stress. Simply placing a differential pressure on the sample is not adequate to achieve piezoelectric behavior as the system also necessitates that an incompressible load-bearing fluid be present in the pore space. The application of compressive force to any sample incapable of maintaining pore space integrity will result in the overall response becoming necessarily more similar to the rock matrix response. The ability of the fluid to oppose stress and strain allow for pressure to dissipate through

the pore space along with the rock matrix. The stress propagating through the rock matrix is partially alleviated as the pore space compresses to accommodate the differential stress applied. Coaxial compressive force on the core introduces a stress component throughout the entire volume. The pore space is slightly compressible as a result of the fluid that fills the void space so there is a component of the stress dissipated through slight reduction in pore space. However, the rock matrix serves as the frame of the sample and experiences a load similar to that within the pore space, ensuring a differential loading of the quartz crystals. The aforementioned load-bearing quartz crystals undergo a dynamic polarization resulting in change in the complex permittivity of the system.

Conclusions

The polar state of the rock was recorded as a function of varying frequency as well as with different stress states. Compressive force applied to the saturated cores results in a stress component throughout the entirety of the core where both the rock matrix and the pore space experience a load. Load-bearing quartz crystals are then polarized resulting in a change in the complex permittivity of the sample. The relationship that is exhibited provides evidence to the foundational concept of the study and supports the claim that the direct piezoelectric phenomenon has an effect on penetration depth in quartz-bearing formations. Additive penetration is portrayed in all sandstone samples regardless of the saturating fluid. This consistency in the response helps to corroborate the experimental findings and is indicative of sound experimental procedure. Coupling both the mineralogical contribution and the fluid saturation while under a static load to represent pressure creates a more realistic approach to the estimation of dielectric properties.

Limestones have no element that exhibits piezoelectricity; so no dependency on the imposed stress state in terms of penetration is achieved. Limestone cores expound the causality of piezoelectricity to the additive penetration realized in the sandstone samples where the lack of quartz corresponds to no additive wave penetration. The response of all limestone cores comparatively isolates the quartz content where any increase in wave penetration of the sandstone samples can be attributed to piezoelectricity. Utilization of the different lithological samples and fluids allows for the direct comparison of measured data with what is fundamentally known which validates the accuracy of the measurements.

Technical feasibility of heat introduction by utilization of EM waves has been proven with various field studies. However, poor penetration depth is prohibitive in terms of economic implementation, resulting in current marginalization of the technology. The ability to increase the penetration depth is then an integral and valuable tool to realize the vast potential that EM waves offer. For sandstone reservoirs with heavy oil, a static load introduced by coaxial compression triggers the direct piezoelectric effect enabling additive incident wave penetration. Any increase in wave penetration directly corresponds to more oil being heated, increasing the economics of the project. Adopting a strategy that exploits innate piezoelectricity in the quartz content helps to make electromagnetic waves more viable as an enhanced oil recovery technique.

References

- Arnau, A. and Soares, D. 2009. Fundamentals of Piezoelectricity. In *Piezoelectric Transducers and Applications*: Springer.
- Baker-Jarvis, J., Vanzura, E.J., and Kissick, W.A. 1990. Improved Technique for Determining Complex Permittivity with the Transmission/Reflection Method. *IEEE Transactions on microwave theory and techniques* **38** (8): 1096-1103.

- Bishop, J. 1981. Piezoelectric Effects in Quartz-Rich Rocks. *Tectonophysics* **77** (3): 297-321.
- Cady, W.G. 1946. Piezoelectricity: An Introduction to the Theory and Applications of Electromechanical Phenomena in Crystals.
- Carrizales, M.A., Lake, L.W., and Johns, R.T. 2008. Production Improvement of Heavy-Oil Recovery by Using Electromagnetic Heating. In *SPE Annual Technical Conference and Exhibition*: Society of Petroleum Engineers. ISBN 1555631479.
- Churcher, P., French, P., Shaw, J. et al. 1991. Rock Properties of Berea Sandstone, Baker Dolomite, and Indiana Limestone. In *SPE International Symposium on Oilfield Chemistry*: Society of Petroleum Engineers. ISBN 1555635342.
- Clarke, R., Gregory, A., Cannell, D. et al. 2003. A Guide to the Characterisation of Dielectric Materials at Rf and Microwave Frequencies. *Institute of Measurement and Control/National Physical Laboratory*.
- Curie, J. and Curie, P. 1880. Development, Via Compression, of Electric Polarization in Hemihedral Crystals with Inclined Faces. *Bull. Soc. Minéralogique Fr* **3**: 90-93.
- Das, S.K. 2008. Electro Magnetic Heating in Viscous Oil Reservoir. In *International Thermal Operations and Heavy Oil Symposium*: Society of Petroleum Engineers. ISBN 1555631991.
- Davison, R.J. 1995. Electromagnetic Stimulation of Lloydminster Heavy Oil Reservoirs: Field Test Results. *The Journal of Canadian Petroleum Technology*. DOI: 10.2118/95-04-01
- Fanchi, J.R. 1990. Feasibility of Reservoir Heating by Electromagnetic Irradiation. Society of Petroleum Engineers. DOI: 10.2118/20483-MS.
- Ghodgaonkar, D.K., Varadan, V.V., and Varadan, V.K. 1989. A Free-Space Method for Measurement of Dielectric Constants and Loss Tangents at Microwave Frequencies. *IEEE Transactions on Instrumentation and measurement* **38** (3): 789-793.
- Gross, B. 1941. On the Theory of Dielectric Loss. *Physical Review* **59** (9): 748.
- Hasanvand, M. and Golparvar, A. 2014. A Critical Review of Improved Oil Recovery by Electromagnetic Heating. *Petroleum Science and Technology* **32** (6): 631-637.
- Hascakir, B., Acar, C., and Akin, S. 2009. Microwave-Assisted Heavy Oil Production: An Experimental Approach. *Energy & Fuels* **23** (12): 6033-6039.
- Hill, N.E. 1969. *Dielectric Properties and Molecular Behaviour*: Van Nostrand Reinhold. Original edition. ISBN.
- Ikeda, T. 1996. *Fundamentals of Piezoelectricity*: Oxford university press. Original edition. ISBN 0198564600.
- Jha, K. and Chakma, A. 1999. Heavy-Oil Recovery from Thin Pay Zones by Electromagnetic Heating. *Energy Sources* **21** (1-2): 63-73.
- Kaatze, U. 2010. Techniques for Measuring the Microwave Dielectric Properties of Materials. *Metrologia* **47** (2): S91.
- Kasevich, R., Price, S., Faust, D. et al. 1994. Pilot Testing of a Radio Frequency Heating System for Enhanced Oil Recovery from Diatomaceous Earth. In *SPE Annual Technical Conference and Exhibition*: Society of Petroleum Engineers. ISBN 155563463X.

- Keysight. 2013. Basics of Measuring the Dielectric Properties of Materials Application Note. In.
- Koolman, M., Huber, N., Diehl, D. et al. 2008. Electromagnetic Heating Method to Improve Steam Assisted Gravity Drainage. In *International Thermal Operations and Heavy Oil Symposium*: Society of Petroleum Engineers. ISBN 1555631991.
- Krupka, J. 2006. Frequency Domain Complex Permittivity Measurements at Microwave Frequencies. *Measurement Science and Technology* **17** (6): R55.
- Liao, H., Morte, M., Bloom, E. et al. 2018. Controlling Microwave Penetration and Absorption in Heavy Oil Reservoirs. Paper presented at the SPE Western Regional Meeting, Garden Grove, California, USA. 13. Society of Petroleum Engineers. DOI: 10.2118/190089-MS.
- Lippmann, M. 1881. On the Principle of the Conservation of Electricity. *The London, Edinburgh, and Dublin Philosophical Magazine and Journal of Science* **12** (73): 151-154.
- Marsland, T. and Evans, S. 1987. Dielectric Measurements with an Open-Ended Coaxial Probe. In *IEE Proceedings H (Microwaves, Antennas and Propagation)*, 134:341-349: IET. ISBN 2053-907X.
- Metaxas, A.a. and Meredith, R.J. 1983. *Industrial Microwave Heating*: IET. Original edition. ISBN 0906048893.
- Morte, M., Bloom, E., Huff, G. et al. 2018. Factors Affecting Electromagnetic Wave Penetration in Heavy Oil Reservoirs. Paper presented at the SPE Canada Heavy Oil Technical Conference, Calgary, Alberta, Canada. 12. Society of Petroleum Engineers. DOI: 10.2118/189746-MS.
- Mukhametshina, A. and Martynova, E. 2013. Electromagnetic Heating of Heavy Oil and Bitumen: A Review of Experimental Studies and Field Applications. *Journal of Petroleum Engineering* **2013**.
- Mutyala, S., Fairbridge, C., Paré, J.J. et al. 2010. Microwave Applications to Oil Sands and Petroleum: A Review. *Fuel Processing Technology* **91** (2): 127-135.
- Sahni, A., Kumar, M., and Knapp, R.B. 2000. Electromagnetic Heating Methods for Heavy Oil Reservoirs. In *SPE/AAPG Western Regional Meeting*: Society of Petroleum Engineers. ISBN 1555633455.
- Sarathi, P.S. and Olsen, D.K. 1992. *Practical Aspects of Steam Injection Processes: A Handbook for Independent Operators*. National Inst. for Petroleum and Energy Research, Bartlesville, OK (United States).
- Shehata, A.M. and Nasr-El-Din, H.A. 2014. Role of Sandstone Mineral Compositions and Rock Quality on the Performance of Low-Salinity Waterflooding. In *International Petroleum Technology Conference*: International Petroleum Technology Conference. ISBN 1613993714.
- Singh, R.P. and Heldman, D.R. 2001. *Introduction to Food Engineering*: Gulf Professional Publishing. Original edition. ISBN 0080574491.
- Sresty, G.C., Dev, H., Snow, R.H. et al. 1986. Recovery of Bitumen from Tar Sand Deposits with the Radio Frequency Process. *SPE Reservoir Engineering* **1** (01): 85-94.

- Sun, D.-W. 2014. *Emerging Technologies for Food Processing*: Elsevier. Original edition. ISBN 0124104819.
- Titov, K., Tarasov, A., Ilyin, Y. et al. 2010. Relationships between Induced Polarization Relaxation Time and Hydraulic Properties of Sandstone. *Geophysical Journal International* **180** (3): 1095-1106.
- Tuck, G., Stacey, F., and Starkey, J. 1977. A Search for the Piezoelectric Effect in Quartz-Bearing Rocks. *Tectonophysics* **39** (4): T7-T11.
- Van Beek, L. 1967. Dielectric Behaviour of Heterogeneous Systems. *Progress in dielectrics* **7** (71): 113.
- Varadan, V.V., Hollinger, R.D., Ghodgaonkar, D.K. et al. 1991. Free-Space, Broadband Measurements of High-Temperature, Complex Dielectric Properties at Microwave Frequencies. *IEEE Transactions on Instrumentation and Measurement* **40** (5): 842-846.
- Von Hippel, A.R. 1954. *Dielectric Materials and Applications*: Artech House on Demand. Original edition. ISBN 0890068054.
- Weir, W.B. 1974. Automatic Measurement of Complex Dielectric Constant and Permeability at Microwave Frequencies. *Proceedings of the IEEE* **62** (1): 33-36.

3. PART 2: INCREASING THE PENETRATION DEPTH OF MICROWAVE RADIATION USING ACOUSTIC STRESS TO TRIGGER PIEZOELECTRICITY *

Abstract

Electromagnetic waves as a mechanism of heat generation in the reservoir is a concept that has great potential to efficiently produce heavy oil and bitumen. However, as a result of large wave attenuation, the penetration depth of the wave is relatively small. This limits the economic viability of an otherwise technically proven technology. Taking advantage of the inherent piezoelectric phenomenon in quartz crystals enables the manipulation of the penetration depth of the wave.

Acoustic waves were introduced simultaneously with a microwave to the core samples where the presence of the mechanical wave generated an infinitesimal stress. Mechanical stress achieved by the acoustic wave triggered piezoelectricity in two sandstone samples with a limestone sample serving as the control. All consolidated core samples were fully saturated with either oil or water to capture the effect of the pore space. The incremental stress manifests itself through change in the complex permittivity of the sample measured with a vector network analyzer. Penetration depth of the microwave was calculated as a function of the measured complex permittivity. Comparative analysis of the penetration depth of the varying imposed stress states illustrates the additive penetration achieved due to piezoelectricity. Piezoelectricity as the fundamental

* Reprinted with permission from Morte, M., Dean, J., Kitajima, H. and Hascakir, B., 2019. Increasing the Penetration Depth of Microwave Radiation Using Acoustic Stress to Trigger Piezoelectricity. *Energy & Fuels*, 33(7): 6327-6334. Copyright 2019 American Chemical Society

mechanism of penetration increase was further demonstrated by isolation of the quartz contribution through use of the limestone.

An increase in penetration depth was realized for all oil-saturated sandstone cores. The presence of the acoustic wave introduced a stress component across the quartz crystals, generating a change in the electric potential. This created a dynamic polarization which corresponded to an absorption environment more conducive to microwave penetration.

Introduction

Electromagnetic (EM) heating of heavy oil reservoirs is an enhanced oil recovery technique that offers innate advantage. Prohibitively high viscosity values intrinsic to heavy oil require additive energy in the form of heat to effectively increase the transmission of the fluid. Generally, steam is introduced to the reservoir as the heating mechanism, however, the foundation of steam as a heat-transporting fluid in conjunction with innate fluidity can limit the efficacy of the treatment (Carrizales et al. 2008). Lack of control often corresponds to injected steam bypassing the target zone and being lost to the overburden. Any steam that leaves the targeted region is accordingly loss of additive energy; so, no benefit is realized in terms of temperature rise by the steam introduction. The associated directionality necessary for effective steam treatment corresponds to EM waves being situationally attractive for thin and deep reservoirs where steam is inefficient.

Along with superiority in directional control, EM waves offer faster heating owing to instantaneous volumetric heating. Imparting heat to the reservoir when utilizing a heat-transporting fluid such as steam requires contact as heat is exchanged at the interface.

Comparatively to steam, EM waves propagate through the entirety of the material instead of just the pore space, volumetrically heating the sample instead of just the surface. The distinction of avoiding the interfacial convective heating of a heat-transporting fluid makes implementation of electromagnetic waves desirable (Chhetri and Islam 2008; Hasanvand and Golparvar 2014; Kasevich et al. 1994). Furthermore, the implication of instantaneous heating of the entirety of the volume is the ability to target specific locations while avoiding energy loss to the overburden, producing a more a more efficient introduction of energy (Fanchi 1990; Mukhametshina and Martynova 2013). Therefore, the propagation of a high-frequency wave such as those utilized in this study is locally efficient with minimal energy loss to the wellbore. Attenuation of the wave occurs within the formation and manifests itself as heat transfer. The localized efficiency of the EM process is attractive and desirable where there is greater return on energy input with this technique relative to other thermal methods (Alomair et al. 2012; Bera and Babadagli 2015). As a result, the potential of EM waves to address the shortcomings of steam has been expounded by various numerical studies (Bogdanov et al. 2011; Koolman et al. 2008; Wacker et al. 2011; Wang et al. 2008).

However, implementation of electromagnetic waves as a heating mechanism in the petroleum industry is marginalized by poor penetration depth of the wave. As incident wave energy is absorbed by the reservoir, less energy must remain to continue propagation further into the formation. Poor penetration depth directly corresponds to lower stimulated reservoir volume so project economics dictates maximization of this parameter. More oil being accessed by the heat generation directly equates to greater volume being transmitted

to the producing well. By utilizing the direct piezoelectric effect inherent to quartz the penetration depth can be optimized and maximized resulting in more expansive stimulated area. The change in polarity associated with the direct piezoelectric effect stems from the influence of mechanical stress through the element. Additive mechanical stress by means of coaxial compression was investigated where the results established the validity of the fundamental concept. However, a differential mechanical load through coaxial compression has limited applicability in the industry as a means of illustrating the fundamental viability of piezoelectricity. Overburden in place for every reservoir prohibits the direct introduction of mechanical stress through utilization of coaxial compression so coaxial compression is not plausible. Therefore, it became necessary to tailor the introduction of the mechanical stress to be analogous to the field-scale.

A more useful method to capture the intrinsic value of piezoelectricity relative to the industry is to introduce a mechanical stress by propagating a mechanical wave through the sample (Auld 1973; Mason 1956). This alternative means of stress introduction provides a better representation of the capabilities of the industry to take advantage of the direct piezoelectric effect. The ability to introduce mechanical waves through the formation is widely established in seismic surveys and therefore offers value if proven to activate any benefit to the lateral penetration of the microwave (Badley 1985; Ben-Menahem and Singh 2012; McQuillin et al. 1984; Wu and Aki 1988). Acoustic waves are mechanical waves that are associated with the vibration of the material; so an infinitesimal mechanical stress is introduced to the material through the propagation of the wave (Ikushima et al. 2006; Okada 1980). The presence of the acoustic wave creates a stress in

the rock matrix and accordingly provides the potential to realize change in the polar nature of the rock (Bishop 1981). However, the quantitative significance of the differential mechanical stress needs to be sufficient to register in terms of piezoelectricity.

The spectrum of microwave heating relies heavily on the dielectric rotation of the dipole response to an oscillating electric and magnetic field. The generation of heat stems from the inability of the material charges to maintain phase with the rapidly oscillating field. The magnitude of the polarization of the material is proportional to the displacement of the electrons from the nuclei. The deviance from an electrically neutral molecule results in surface charges on the molecule; so the electric potential of the surface is manipulated. Differential stress applied to the cores results in a dynamic polarization of the material which reorients the polarity distribution vector and accordingly changes the capability of the material to efficiently absorb microwaves. Induced dipoles are generated as the applied field disturbs the particles, forcing deviation from the equilibrium state. Polarity is a byproduct of the complex permittivity of the material with complex permittivity serving as the primary driver of absorption dynamics. Heat is generated in the reservoir as a function of both the induced polarity as well as the natural polar state of the reservoir. Manipulation of the polarity distribution vector of the material must then equate to a change in the absorption of the wave. The incident wave propagates through the material where the oscillating electric field causes rotation of particles in an attempt to maintain phase with the corresponding negative or positive half-cycle (Davletbaev et al. 2011; Rehman and Meribout 2012; Sresty et al. 1986; Wacker et al. ; Wilson 2012). Transfer of heat as a function of the absorbed wave energy results in viscosity reduction and enhanced

transmissibility of the fluid to the producer. Absorbed wave energy by the material is loss of energy relative to the wave with associated decreases in both amplitude and size as it travels. Reduction in incident wave energy necessarily results in reduction in the distance the wave can travel.

Absorption and penetration depth are inversely related and the economic feasibility of the electromagnetic technology hinges on the ability to adequately control this relationship. Therefore, by manipulating the absorptive capacity of the rock through the presence of the acoustic wave, the penetration depth can be enhanced. The distance the microwave travels is mathematically dependent upon the complex permittivity of the material. Alteration of the complex permittivity of the samples as a result of the introduced acoustic stress is considered a response to the presence of the direct piezoelectric effect. So, the parameter of penetration depth is a direct indicator of the magnitude of piezoelectricity achieved by the experiments. In accordance with piezoelectricity, additive stress to the core samples will alter the polarity and change the absorption of the wave (Morte et al. 2018). Reduced absorptive capacity will allow the wave to maintain higher energy content and travel further into the reservoir.

Experimental Procedure

The contribution of piezoelectricity is captured and represented through the parameter of penetration depth which is denoted d_p . Penetration depth is defined as distance traveled before the wave reaches an arbitrary threshold of reduction in incident power. All penetration depths reported in this study use a threshold of e^{-1} or roughly 63%

which represents the distance the wave travels before 63% of the energy is absorbed by the sample (Metaxas and Meredith 1983). Dictated by piezoelectricity, additive mechanical stress to the system will redistribute the electrical charges in the element creating a net dipole (Arnau and Soares 2009). Complex permittivity is highly sensitive to polarity so any contribution of piezoelectricity will be captured by variations in the complex permittivity.

The material property of complex permittivity describes the microwave absorptive behavior and captures the interaction of the material under the influence of the externally applied electric field. Complex permittivity is defined by both a real and imaginary component where the real portion is denoted dielectric constant (ϵ') and the imaginary component is denoted loss index (ϵ'') as seen in Eq 2.1 (Debye 1934; Gross 1941; Wyman 1936). Dielectric constant can be thought of as the ability of the material to store energy while the loss index is the ability of the material to convert electrical energy to heat energy (Chang et al. 2010; Krupka et al. 1994). The loss tangent as defined in Eq 2.2 is a ratio of the two components of complex permittivity and is representative of how well microwave energy is absorbed (Holland 1967). The components are coupled in nature as is evident in Eq 2.3 which provides the means of calculating attenuation (Heston Jr et al. 1950; Koubaa et al. 2008; Weir 1974). The attenuation constant, α , represents the rate of absorption of the wave into the sample. Finally, the output of penetration depth is achieved by using Eq 2.4 where the depth is inversely related to the attenuation (Metaxas and Meredith 1983). The penetration depth response is highly frequency-dependent where the relationship is governed by exponential decay. Intuitively, the distance the wave is capable of traveling

must be inversely related to the absorption of the incident wave energy. The Law of Conservation of Energy dictates that any energy absorbed by the reservoir must equate to the same energy lost to the wave. As the wave loses energy to the surrounding through heat transfer, there remains less energy content to maintain propagation through the reservoir. The identified relationship is evidenced in all figures of penetration depth.

A N9923A FieldFox Handheld vector network analyzer in conjunction with a Keysight N1501A dielectric probe was used to measure the complex permittivity of the sample which can be seen in Figure 2.1. Microwave frequency is generated by the network analyzer, transmitted through a coaxial cable and emanated from the probe. The probe directs the wave into the material under test and serves as both the transmitter and receiver (Marsland and Evans 1987). At the interface of the material the microwave is either transmitted or reflected as a function of the permittivity of the sample (Chung 2007; Krupka 2006). The probe receives the proportionality of reflected wave in the form of scattering parameters which enables the network analyzer to output the desired parameters of complex permittivity (Ghodgaonkar et al. 1989).

The cores were simultaneously inundated with both microwaves and acoustic waves to trigger the benefit of the direct piezoelectric effect. As discussed above the microwave component was introduced through the use of the vector network analyzer. The mechanical wave required the use of transducers to convert an electrical signal to a mechanical wave. The equipment used for the acoustic wave component consisted of a Tektronix TDS 210 oscilloscope, a Panametrics Pulser Receiver Model 5055PR signal generator, and two transducers along with the pressure vessel used to simulate overburden.

All of the equipment utilized to introduce the acoustic wave is pictured in Figure 3.1. The top right depicts the signal generator while the bottom right illustrates the oscilloscope that was used. Both pictures on the left hand side are of the pressure vessel that introduces both the coaxial compression and the acoustic wave. The transducers are governed by a discrete resonant frequency of 1 MHz and are limited to operating at resonance.

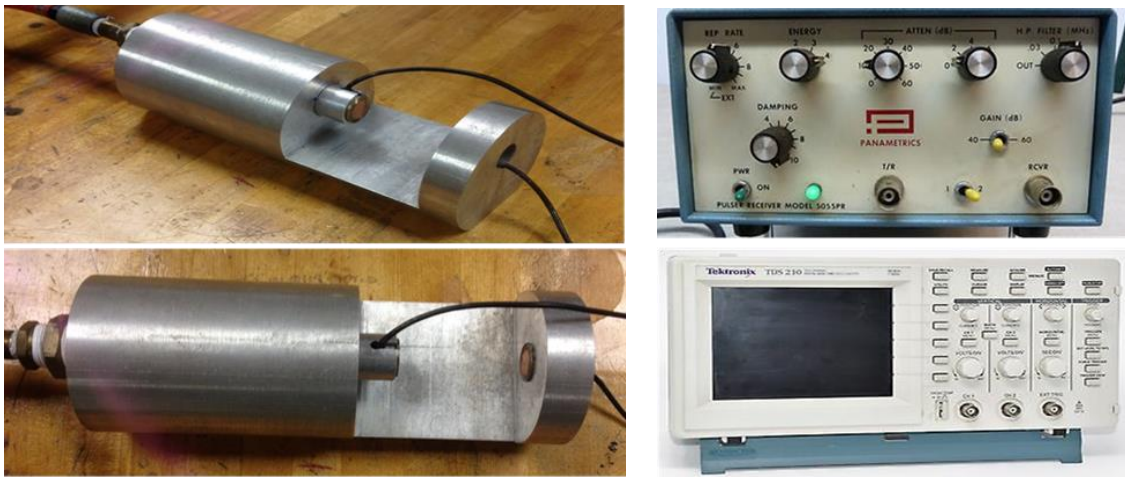


Figure 3.1 - The experimental equipment used to generate and introduce the acoustic signal into the core volume while simultaneously imposing the pressure state

The electric signal is converted to a mechanical wave at the resonant frequency of 1 MHz by the first transducer, then directed through the core sample, and finally converted back to an electric signal by the secondary transducer so the digital data can be recorded by the oscilloscope. The experimental set-up for the simultaneous introduction of both the microwave and acoustic wave is depicted in Figure 3.2. The core holder itself serves as the means of introducing small differential pressure to the core through coaxial compression. The coaxial compression is introduced as a result of a piston that protrudes from a chamber connected to a compressed air outlet.

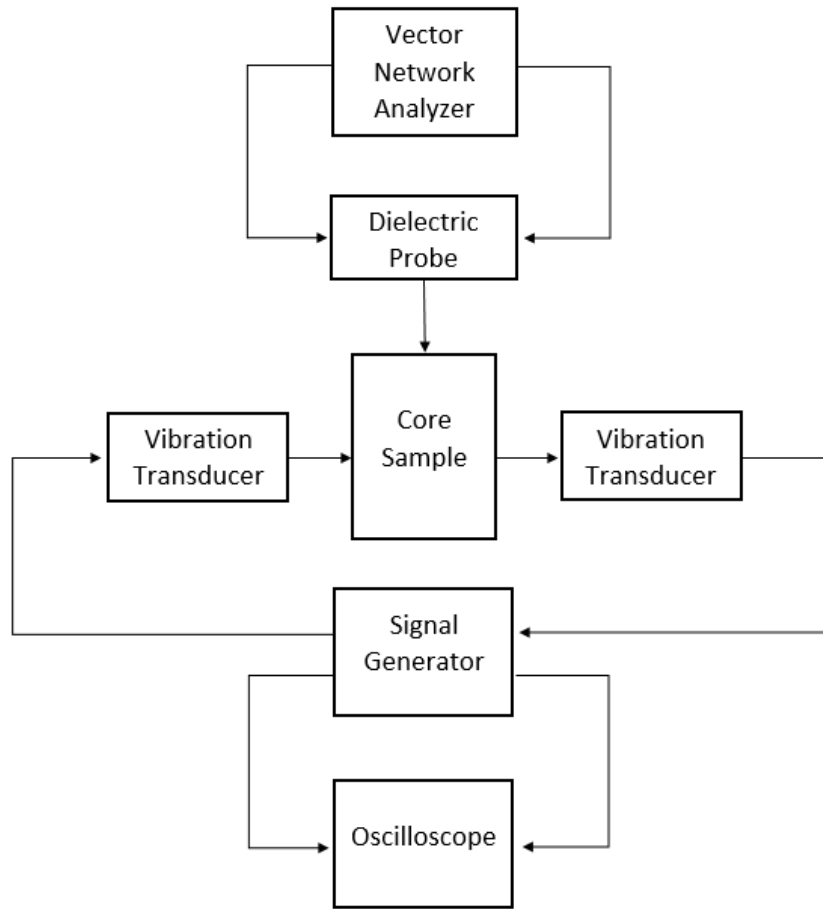


Figure 3.2 - Experimental setup for the simultaneous introduction of the microwave and acoustic wave

The skeletal frame (rock matrix) of the reservoir will be investigated by varying lithology while the pore space contribution will be captured by varying saturating fluid. Three different cores comprising two sandstone and one limestone lithology have been saturated both with water and three different oils and then tested. The lithologies, namely the two sandstones and the limestone, remained consistent for all saturating fluids as the cores were all cut from the same outcrops. The composition of all three core samples along with the porosity and permeability can be seen in Table 2.1.

The cores are depicted in Figure 3.3 and show the consolidated nature of the samples. As a result, the cores were able to maintain their own structural integrity when introduced directly into the pressure apparatus. The consolidated nature of the cores enabled the introduction of the samples directly into the pressure apparatus which bypasses the need for a dielectric cell. The cores are rectangular in shape with dimensions of 2”x 1”x 1” to allow for surface measurements to be performed with the dielectric probe and also to provide for an ideal volume for measurement. Consideration to the dimensions of the cut cores was also a function of meeting the specifications of the machined apparatus seen in Figure 3.1. The pictured equipment provides a coaxial compression as the result of a piston that protrudes from a chamber connected to a compressed air outlet. The cores are rectangular in shape to allow for surface measurements to be performed with the dielectric probe.

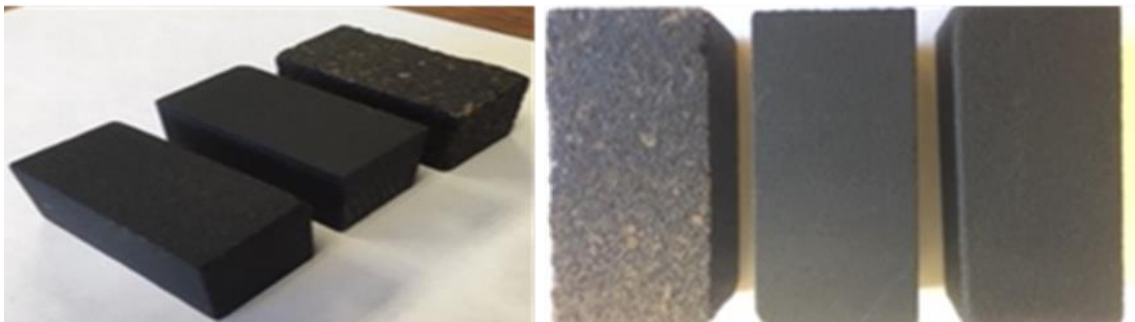


Figure 3.3 - Picture of the oil-saturated consolidated cores utilized in the experiments for all three different lithologies

Complex permittivity of the samples is to some extent a volume average of the pore space and the skeletal frame of the sample. Varying the fluid properties helps to clarify dependencies of the overall response on the pore space itself, while simultaneously

testing the applicability of the concept with fluids routinely seen in reservoir rock (Liao et al. 2018). The presence of reservoir fluids allows for illumination of the response of cores with greater applicability to the industry to provide for more robust analysis and expand the domain of the experiments. Properties of the fluids that were used are included in Table 2.2 which describes the oils in terms of the dielectric parameters. The viscosity presented was measured at room temperature while the API gravity was measured at standard conditions. The fluid in the pore space is the primary contributor to heat generation from MW absorption and the usage of different oils helps to delineate that contribution.

Along with the fluid in the pore space, the rock mineralogy plays a vital role for the proposed concept. The behavior and therefore the additive benefit is dependent upon the presence of quartz. Therefore, any lithological layer which does not contain a significant amount of quartz or some other piezoelectric material is unable to display the dependency discussed in the paper. However, the proposed technique would be valid with any lithology that contains quartz. Quartz is a dominant mineral commonly found not only in sandstones but also in shale layers. This allows for the extension of the displayed phenomenon to include shale layers which typically contain a significant volumetric percentage of organic matter. As displayed in the study, limestone layers with low quartz content will not display any benefit of piezoelectricity.

Repeatability in the measurements is established through the multitude of measurements taken at the various locations on the surface of the cores. The presented data is an average of three measurements taken at each of five different locations along the same plane of the core sample, providing confidence in the values that are measured.

The tolerance of the probe is $\pm .1 |\epsilon_r^*|$ taken directly from Keysight which falls well within the threshold of the changes in the penetration. The additive penetration can therefore be attributed to piezoelectricity as the tolerance of the probe doesn't account for the magnitude of change. All reservoirs experience overburden to some extent so the presence of the pressure component will simulate the contribution of overburden stress. The pressure and the acoustic wave are coupled in the reservoir and investigating both simultaneously provides a more realistic window into the true permittivity response.

Experimental Results and Discussion

The piezoelectric effect would dictate that differential stress states imposed on the element would result in a change in the polar state. Quartz is the component of sandstone which contributes to piezoelectricity, therefore, we would expect to see change in the penetration depth of the sandstone cores but no change in the limestone cores. As piezoelectricity is the governing mechanism of the dynamic polarization of the core samples, the lack of a piezo element in the limestone cores necessarily would result in no stress state dependency. All figures representing the different fluid saturations and lithologies adhere to the expected trends. Differential penetration is achieved for each of the sandstone samples for all fluid saturations while the limestone cores experience no differential penetration regardless of the stress state imposed.

Figure 3.4 illustrates the penetration performance of the Sample 1 cores saturated with oil C1 (A), oil C2 (B), and oil C3 (C). The propagation of the acoustic wave through the material is coupled with pressure so both were investigated simultaneously as well as

separately. The pressure component is representative of the overburden present for all reservoirs and closely resembles what would be expected on a field-scale. The yellow curve is the original unstressed response and will serve as the control.

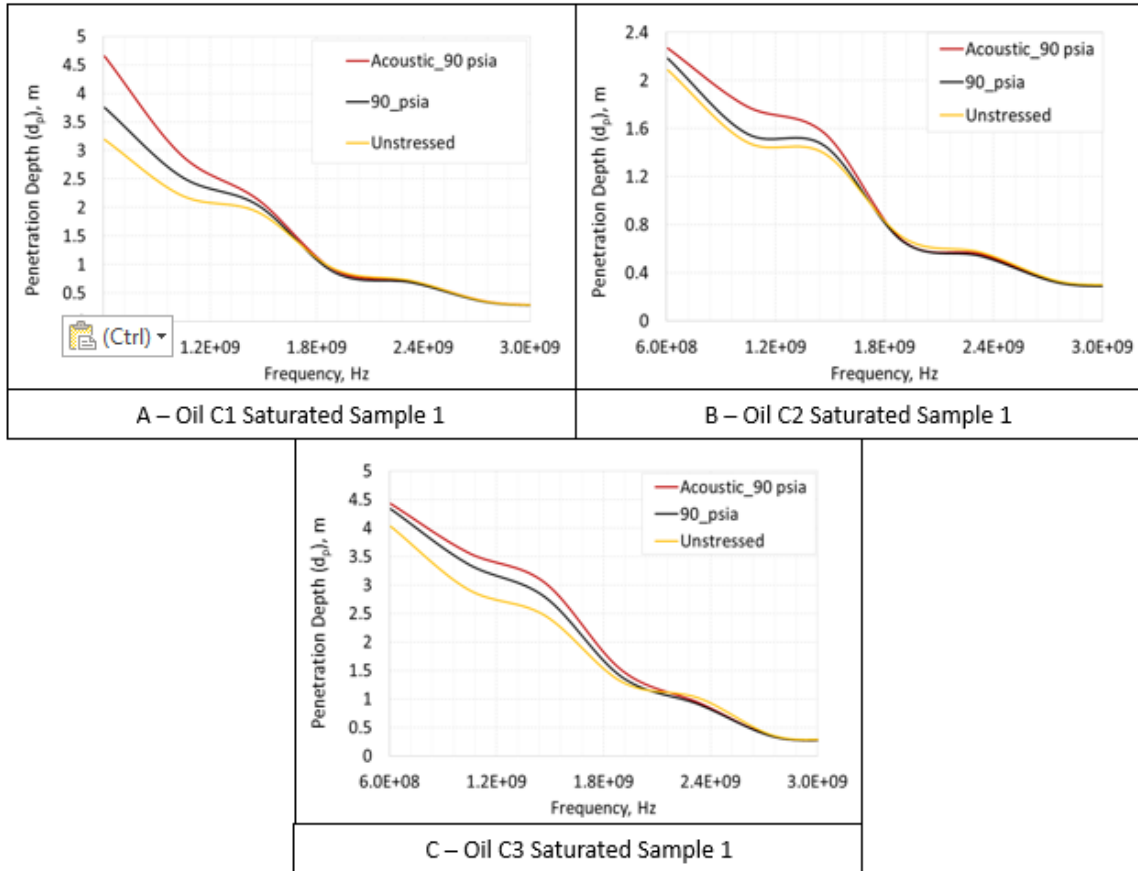


Figure 3.4 - Penetration depth of oil-saturated sample 1 (quartz rich sandstone) cores with the unstressed and imposed stress states

Examination of the figure illustrates that the acoustic wave (red curve) experiences the largest penetration depth and the unstressed (yellow curve) achieves the smallest. This is indicative of the ability of the acoustic wave to provide enough mechanical stress to overcome any threshold required to take advantage of piezoelectricity. For all investigated oil samples, the introduction of the acoustic wave was capable of triggering a measurable

response in the penetration depth of the samples as the acoustic experiment exhibited greater penetration depth than the control. The infinitesimal stress achieved through propagation of the mechanical wave was large enough to create a dynamic polarization of the quartz crystals. The magnitude of the penetration disparity between the acoustic stress and the unstressed state is above the tolerance of the dielectric probe which provides confidence in the result that is achieved.

With the driver of the direct piezoelectric effect being mechanical stress, it became important to attribute the additive stress to only the acoustic wave and not external sources such as the local stress field. Introduction of EM waves produces preferential heating due to enhanced capacity of certain materials to absorb heat which leads to expansion of materials and induced localized stress (Li et al. 2006). For example, certain minerals such as pyrite have a higher proclivity for microwave absorption and will therefore experience greater heat exchange. This creates heat dependent localized stress conditions as there are non-uniform expansions. However, unlike the steam processes, the EM technique does not introduce any mass into the reservoir. The waveform is a source of energy to the reservoir but does not have mass so the local stress condition is relatively unaffected by the presence of the microwave. Therefore, the mechanical stress element through the quartz crystals is wholly attributed to the presence of the acoustic wave.

Figure 3.5 provides the trends for the oil-saturated sample 2 cores and illustrates similar behavior as in Figure 3.4. The acoustic wave achieved the greatest benefit in terms of the penetration depth. The smallest penetration depth response was once again achieved by the unstressed core without the acoustic wave which is in line with what would be

expected. Consistency is established when directly comparing both figures as the established trends for both are similar. Both Figure 3.4 and Figure 3.5 are sandstone cores which have a considerable amount of quartz so they contain an inherent potential to experience the direct piezoelectric effect. The figures help to corroborate the existence of the benefit of piezoelectricity to the petroleum industry as well as the ability to trigger this effect with the mechanical wave.

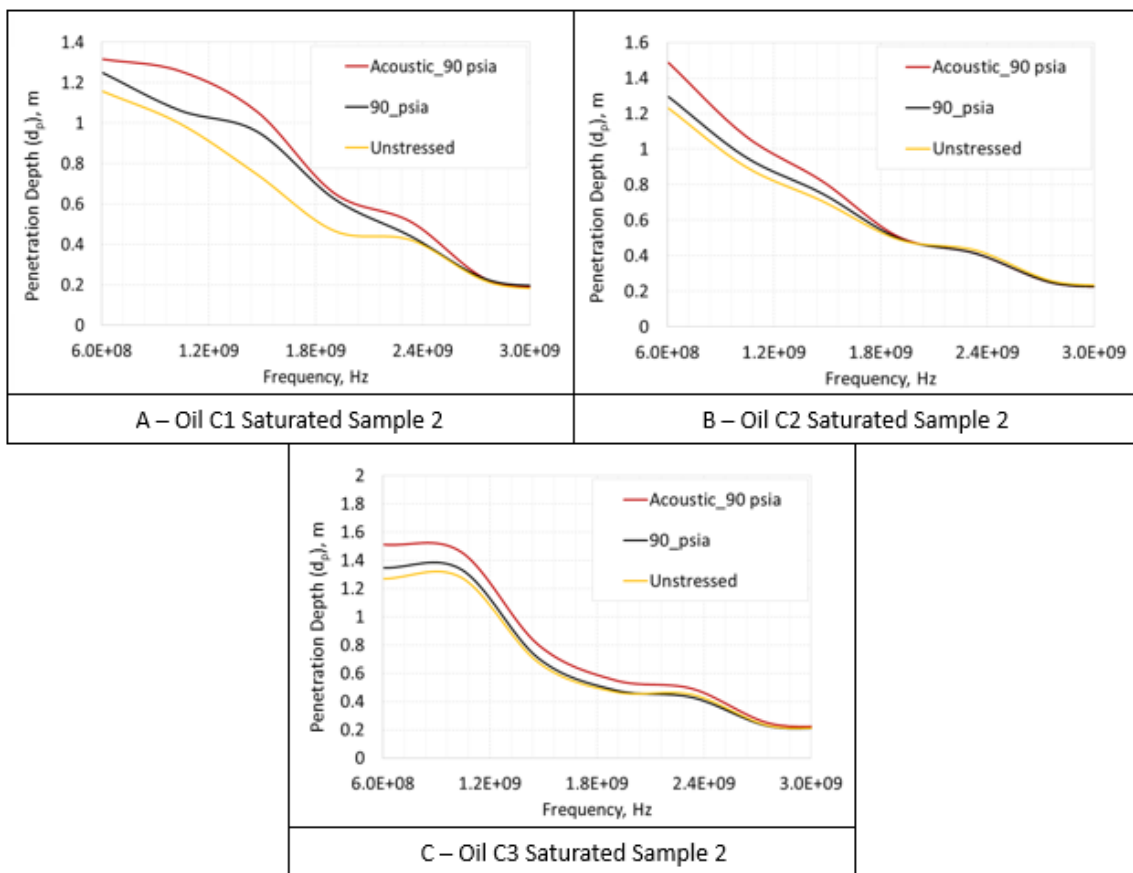


Figure 3.5 - Penetration depth of oil-saturated sample 2 (quartz rich sandstone) cores with the unstressed and imposed stress states

To provide realistic benefit to the industry, the disparity between the penetration depths with the addition of the acoustic waves must be large enough to provide economic

incentive. Justification for the introduction of the acoustic wave in terms of additive penetration is made through examination of the increase in the accessed reservoir volume. The penetration depth shown is radial where any increase in penetration depth becomes volumetrically more significant through the near-spherical radiation pattern. Any percentage increase in penetration is amplified by non-linearity in the irradiation of the wave in all directions. Figure 3.6 graphically represents the new stimulated volume of the reservoir as a function of percentage of penetration depth increase. The volume multiplier is described mathematically as the new accessed reservoir volume over the original accessed reservoir volume. The non-linearity is easily seen in the figure where simply doubling the penetration depth of the wave equates to a new stimulated reservoir volume eight times larger than the original. Increase in penetration depth of the magnitude seen in this study in terms of additive volume of accessed reservoir would be very beneficial.

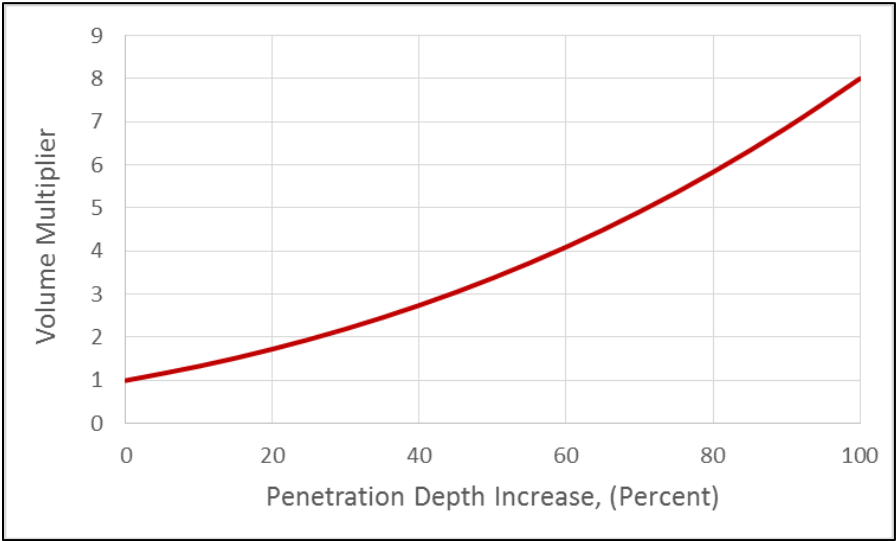


Figure 3.6 - Magnitude of increased reservoir volume as a function of percent increase in penetration depth

The presence of a piezoelectric element is an integral component of the system. No additive penetration would be achieved without it. This is evidenced by Figure 3.7 which depicts the penetration depth of the oil-saturated sample 3 or carbonate cores. The absence of quartz content results in little to no change in the penetration of the wave regardless of the stress state imposed. Acoustic stress in conjunction with the mechanical load provides no advantage without the presence of a piezoelectric element. Regardless of the saturating fluid, all limestone cores display no sensitivity to the imposed stress state. The lack of disparity in the responses of Figure 3.5 conforms to what would be expected according to the direct piezoelectric effect.

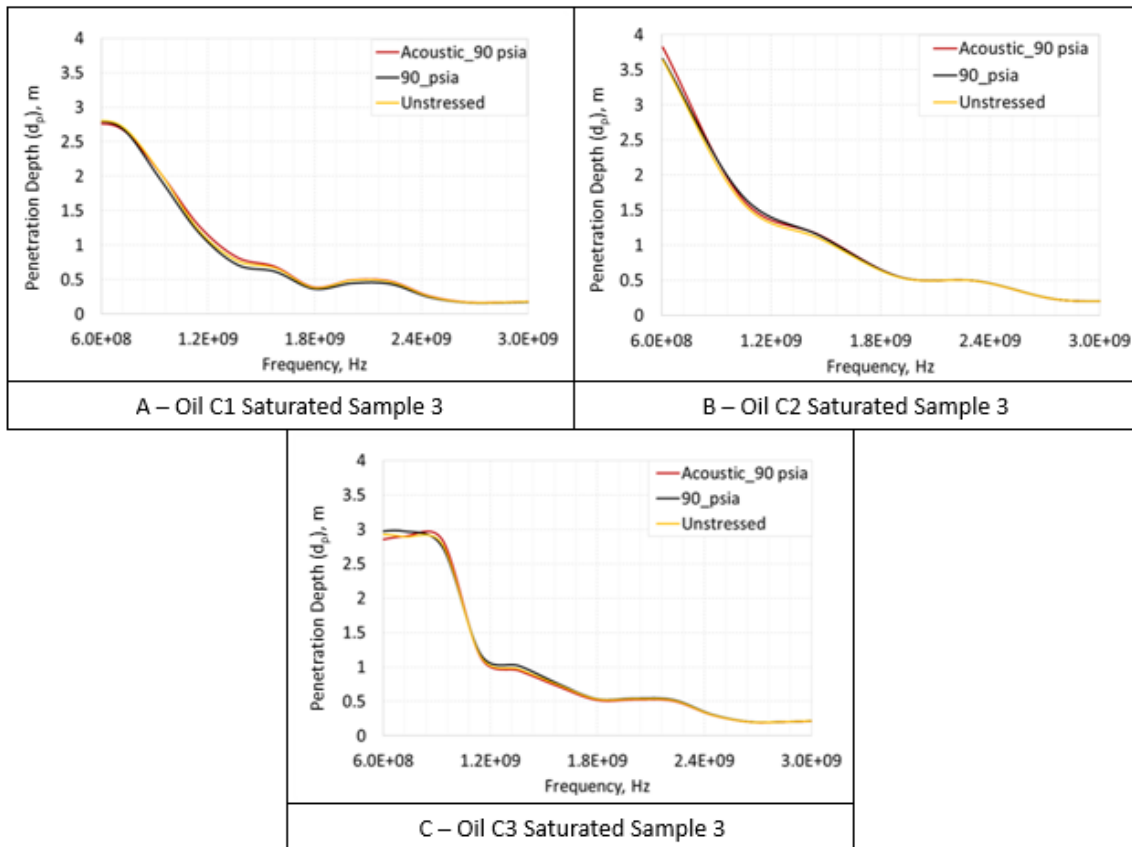


Figure 3.7 - Penetration depth of oil-saturated sample 3 (carbonate rich) cores with the unstressed and imposed stress states

After capturing the response of the oil-saturated cores, the responses of the water-saturated cores were measured. The proclivity of water for microwave absorption corresponds to a decrease in the penetration depth of the wave as a function of increasing water content. As a rule, the greater volume of water will result in greater microwave absorption, greater temperature rise, but lower penetration depth. Figure 3.8 describes the behavior of the microwave penetration for all water-saturated samples. The relationship demonstrates the increased capacity of the sample to absorb microwave energy. The significance of the contribution of piezoelectricity is smaller for sample 1 shown in Figure 3.8 (A), but slight variation in penetration depth does occur in the frequency of interest. Figure 3.8 (B) depicts the water-saturated sample 2 (sandstone) and exhibits the expected behavior with the acoustic waves achieving the largest penetration depth. Water has a polar nature and accordingly is very efficient at absorbing microwave energy. This propensity for microwave absorption manifests itself when comparing the penetration depths of the oil and water-saturated cores. The more transparent nature of oil corresponds to increased remaining energy content of the wave relative to the water. This is illustrated by the much smaller penetration depth of the water compared to that of oil. The incident wave is more effectively absorbed by the polar water molecules so less energy remains to continue propagation into the reservoir. The predisposition for microwave energy established by the lower penetration depth of the water-saturated sample delineates the contribution of the pore space to the overall penetration response. The presence of a fluid which preferentially absorbs microwaves decreases the penetration depth significantly.

Therefore, the composition of the pore space is very important when considering the utilization of microwave energy.

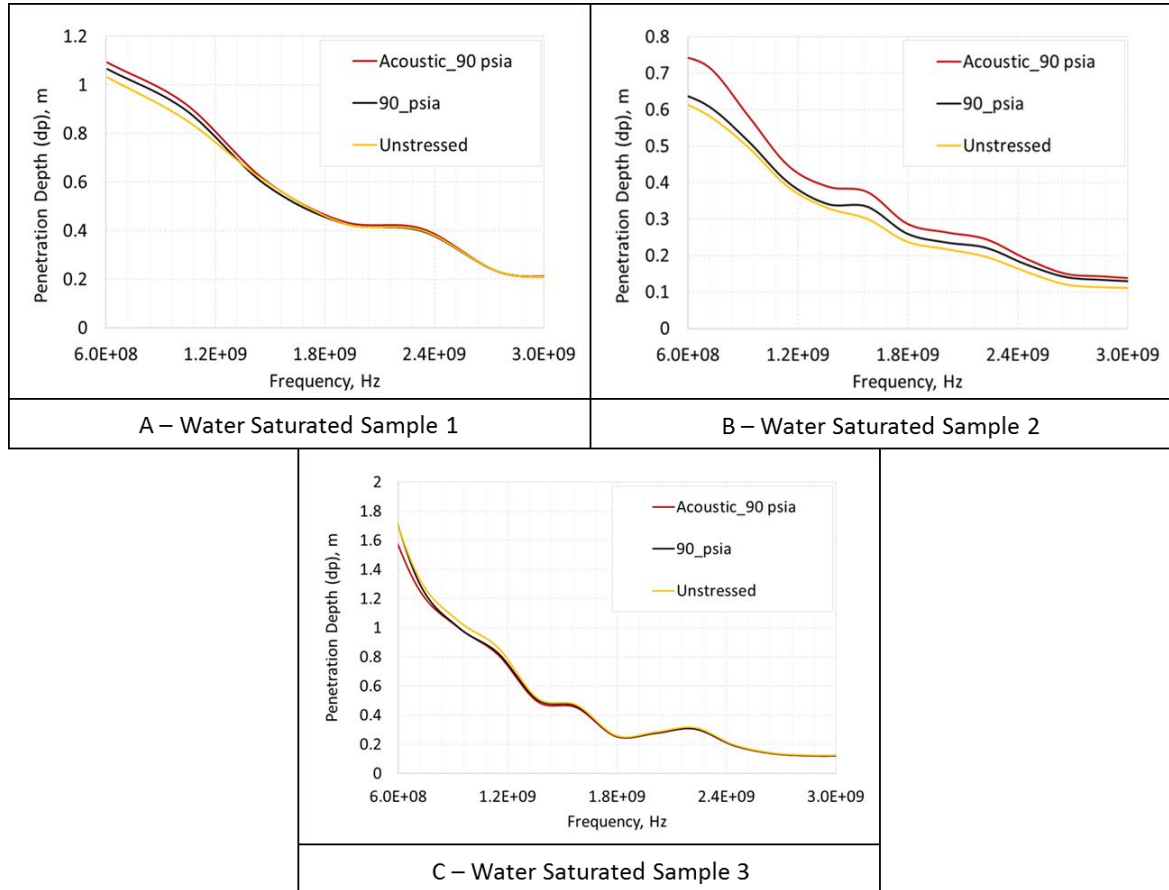


Figure 3.8 - Penetration depth of all water-saturated cores with the unstressed and imposed stress states

Figure 3.8 (C) illustrates the behavior of the limestone saturated with water where the trends identified are consistent with the oil-saturated cores. The lack of a stress dependency for the limestone cores supplies further evidence of the foundational contribution of the piezoelectric effect for the sandstone cores. All things being equal besides the quartz content, the limestone achieves no change in penetration depth with

stress while the sandstones experience an increase in penetration depth with stress. Therefore, any disparity achieved by varying the stress state of the sandstone cores is a function of the piezoelectric effect.

The magnitude of the dynamic polarization of the quartz crystal is dependent upon the magnitude of the differential stress and also the volume of the piezoelectric element. The presented works involved the use of consolidated cores taken from various outcrops with defined properties. This prohibits the direct manipulation of the core as all properties are intrinsic. Intuitively, any correlation would be limited to the lithology of the three cores that were used, only two of which contained quartz. The scope of the analysis involves the two sandstone cores and is essentially a comparison of two discrete values. The sample 2 lithology has a greater quartz content and would be expected to achieve greater differential penetration. Investigation into the identified relationship reveals that all but one of the core samples adheres to the anticipated trend. For the water-saturated cores, the sample 2 core experiences substantially more disparity in penetration between the acoustic stress state and the coaxial stress. The same is true for both Oil C2 and Oil C3.

The acoustic waves serve as an incremental stress to the core so the mechanism of penetration depth increase experienced by both the wave and the confining pressure are the same. The mechanical stress does not differentiate between the acoustic source and the coaxial compression. Therefore, the frequency range that the differential penetration is seen should be the same for both the static load as well as the dynamic load. The effect for both the acoustic stress and the confining pressure is seen at the lower frequency range as a result of dielectric relaxation. At very high-frequency, the molecules are no longer able

to maintain phase with the oscillating electric field and relaxation occurs. The Debye relaxation is the response of the population of dipoles no longer interacting with the external electric field. This phenomenon behaves irrespective of the stress that is applied which is why both the acoustic stress and the confining pressure behave similarly. The values that are achieved are essentially ϵ_{∞} which is the relative permittivity at the high-frequency limit. The differential penetration of the sandstone cores is limited to the lower frequency range of the project (Debye 1954; Hoekstra and Delaney 1974; Jonscher 1999).

Conclusions

The acoustic wave provides a realistic approach to dynamically applying mechanical stress to the reservoir, thus triggering the benefit of the piezoelectric effect. The potential benefit realized by taking advantage of inherent piezoelectricity in sandstone cores has been experimentally validated and would directly correspond to increased production. The proof of concept provided explicitly demonstrates the differential increase in penetration of microwaves when supplemented by acoustic wave stimulation. In accordance with the piezoelectric effect, the mechanical stress introduced to the core by means of the mechanical wave alters the polarity distribution vector resulting in increased penetration depth. Comparison of the acoustic stress to the confining pressure yielded an average differential increase in penetration of 10.5% with values as high as 24% (Figure 3.4 A). The benefit of the mechanical stress was not limited to the acoustic wave as the confining pressure alone experienced an increase of an average of 7.2%. However, the acoustic wave was consistently more capable of creating a polarization of the quartz

crystal; so the introduction of the acoustic wave offers a viable means of triggering piezoelectricity in the field.

The impact of the direct piezoelectric effect was much more prominent for the oil-saturated cores relative to water as a result of the high affinity of microwave energy by the polar water molecule. Higher absorption of the wave is realized with increasing water content due to the very polar nature of the water molecule. Absorption of the wave equates to less remaining energy content of the incident wave to continue propagation and accordingly lower penetration. Reservoirs with very high water saturation will experience faster temperature rise as the wave is quickly attenuated but at the cost of a lower stimulated reservoir volume. The average of the disparity in the penetration depth for the two water-saturated sandstone cores was 7.8 % owing to the large difference in Figure 3.8 (B).

Both limestone and sandstone cores were used to isolate the foundational contribution of the quartz crystal to the overall response. The responses of each core sample were consistent with what this phenomenon would dictate. Piezoelectricity is dependent upon the volume of the element which was corroborated by the results. The mineralogy of the Sample 1 cores had significantly more quartz content and as a result, realized a greater penetration depth dependency on stress. The lack of dependency of the limestone cores adheres to what would be expected and provides further evidence and support of the direct piezoelectric effect as the governing phenomenon. Considering both the results of the limestone and sandstone cores establishes the validity of the fundamental concept. The largest disparity between the responses of the stressed and unstressed

polarity state consistently occurred at the lower frequency range which is a result of dielectric relaxation. The simultaneous propagation of the microwave and acoustic wave effectively increase the stimulated reservoir volume generating more attractive project economics.

The technical feasibility of EM wave implementation to heat the reservoir has been established by various field trials. However, the technology is marginalized as economic implementation has not been achieved. The cost of a microwave frequency project is significant with estimated costs in the range of \$10 million CAD. The economics of the project dictate that expansive reserves are stimulated so any increase in penetration depth is vital to the implementation of EM technology in the field. Piezoelectricity in sandstone reservoirs has the potential to take the very limited technology of microwave heating for EOR and make it more plausible for the industry. As displayed in the study, limestone layers with low quartz content will not display any benefit of piezoelectricity. Quartz is a dominant mineral commonly found not only in sandstones but also in shale layers, expanding the domain of the experiments to include shale with high quartz content. The value of the presented concept lies in the identification of the ability to dynamically trigger the direct piezoelectric effect with the potential to gain enhanced penetration of an electromagnetic wave.

References

- Alomair, O.A., Alarouj, M.A., Althenayyan, A.A. et al. 2012. Improving Heavy Oil Recovery by Unconventional Thermal Methods. In *SPE Kuwait International Petroleum Conference and Exhibition*: Society of Petroleum Engineers. ISBN 1613992637.
- Arnau, A. and Soares, D. 2009. Fundamentals of Piezoelectricity. In *Piezoelectric Transducers and Applications*: Springer.
- Auld, B.A. 1973. *Acoustic Fields and Waves in Solids*: Рипол Классик. Original edition. ISBN 5885013438.
- Badley, M.E. 1985. Practical Seismic Interpretation.
- Ben-Menahem, A. and Singh, S.J. 2012. *Seismic Waves and Sources*: Springer Science & Business Media. Original edition. ISBN 1461258561.
- Bera, A. and Babadagli, T. 2015. Status of Electromagnetic Heating for Enhanced Heavy Oil/Bitumen Recovery and Future Prospects: A Review. *Applied Energy* **151**: 206-226.
- Bishop, J. 1981. Piezoelectric Effects in Quartz-Rich Rocks. *Tectonophysics* **77** (3): 297-321.
- Bogdanov, I., Torres, J., Kamp, A.M. et al. 2011. Comparative Analysis of Electromagnetic Methods for Heavy Oil Recovery. In *SPE Heavy Oil Conference and Exhibition*: Society of Petroleum Engineers. ISBN 1613991509.
- Carrizales, M.A., Lake, L.W., and Johns, R.T. 2008. Production Improvement of Heavy-Oil Recovery by Using Electromagnetic Heating. In *SPE Annual Technical Conference and Exhibition*: Society of Petroleum Engineers. ISBN 1555631479.
- Chang, C.-M., Chen, J.-S., and Wu, T.-B. 2010. Dielectric Modeling of Asphalt Mixtures and Relationship with Density. *Journal of Transportation Engineering* **137** (2): 104-111.
- Chhetri, A. and Islam, M. 2008. A Critical Review of Electromagnetic Heating for Enhanced Oil Recovery. *Petroleum Science and Technology* **26** (14): 1619-1631.
- Chung, B.-K. 2007. Dielectric Constant Measurement for Thin Material at Microwave Frequencies. *Progress In Electromagnetics Research* **75**: 239-252.
- Davletbaev, A., Kovaleva, L., and Babadagli, T. 2011. Mathematical Modeling and Field Application of Heavy Oil Recovery by Radio-Frequency Electromagnetic Stimulation. *Journal of petroleum science and engineering* **78** (3): 646-653.
- Debye, P. 1934. Part I. Dielectric Constant. Energy Absorption in Dielectrics with Polar Molecules. *Transactions of the Faraday Society* **30**: 679-684.
- Debye, P.J.W. 1954. Collected Papers of Peter Jw Debye.
- Fanchi, J.R. 1990. Feasibility of Reservoir Heating by Electromagnetic Irradiation. Society of Petroleum Engineers. DOI: 10.2118/20483-MS.
- Ghodgaonkar, D.K., Varadan, V.V., and Varadan, V.K. 1989. A Free-Space Method for Measurement of Dielectric Constants and Loss Tangents at Microwave Frequencies. *IEEE Transactions on Instrumentation and measurement* **38** (3): 789-793.
- Gross, B. 1941. On the Theory of Dielectric Loss. *Physical Review* **59** (9): 748.

- Hasanvand, M. and Golparvar, A. 2014. A Critical Review of Improved Oil Recovery by Electromagnetic Heating. *Petroleum Science and Technology* **32** (6): 631-637.
- Heston Jr, W., Franklin, A., Hennelly, E. et al. 1950. Microwave Absorption and Molecular Structure in Liquids. V. Measurement of the Dielectric Constant and Loss of Low-Loss Solutions. *Journal of the American Chemical Society* **72** (8): 3443-3447.
- Hoekstra, P. and Delaney, A. 1974. Dielectric Properties of Soils at Uhf and Microwave Frequencies. *Journal of geophysical research* **79** (11): 1699-1708.
- Holland, R. 1967. Representation of Dielectric, Elastic, and Piezoelectric Losses by Complex Coefficients. *IEEE transactions on Sonics and Ultrasonics* **14** (1): 18-20.
- Ikushima, K., Watanuki, S., and Komiyama, S. 2006. Detection of Acoustically Induced Electromagnetic Radiation. *Applied physics letters* **89** (19): 194103.
- Jonscher, A.K. 1999. Dielectric Relaxation in Solids. *Journal of Physics D: Applied Physics* **32** (14): R57.
- Kasevich, R., Price, S., Faust, D. et al. 1994. Pilot Testing of a Radio Frequency Heating System for Enhanced Oil Recovery from Diatomaceous Earth. In *SPE Annual Technical Conference and Exhibition*: Society of Petroleum Engineers. ISBN 155563463X.
- Koolman, M., Huber, N., Diehl, D. et al. 2008. Electromagnetic Heating Method to Improve Steam Assisted Gravity Drainage. In *International Thermal Operations and Heavy Oil Symposium*: Society of Petroleum Engineers. ISBN 1555631991.
- Koubaa, A., Perré, P., Hutcheon, R.M. et al. 2008. Complex Dielectric Properties of the Sapwood of Aspen, White Birch, Yellow Birch, and Sugar Maple. *Drying Technology* **26** (5): 568-578.
- Krupka, J. 2006. Frequency Domain Complex Permittivity Measurements at Microwave Frequencies. *Measurement Science and Technology* **17** (6): R55.
- Krupka, J., Geyer, R.G., Kuhn, M. et al. 1994. Dielectric Properties of Single Crystals of Al_2O_3 , LaAlO_3 , NdGaO_3 , SrTiO_3 , and MgO at Cryogenic Temperatures.
- Li, G., Meng, Y., and Tang, H. 2006. Clean up Water Blocking in Gas Reservoirs by Microwave Heating: Laboratory Studies. In *International Oil & Gas Conference and Exhibition in China*: Society of Petroleum Engineers. ISBN 1555631835.
- Liao, H., Morte, M., Bloom, E. et al. 2018. Controlling Microwave Penetration and Absorption in Heavy Oil Reservoirs. Paper presented at the SPE Western Regional Meeting, Garden Grove, California, USA. 13. Society of Petroleum Engineers. DOI: 10.2118/190089-MS.
- Marsland, T. and Evans, S. 1987. Dielectric Measurements with an Open-Ended Coaxial Probe. In *IEE Proceedings H (Microwaves, Antennas and Propagation)*, 134:341-349: IET. ISBN 2053-907X.
- Mason, W.P. 1956. Physical Acoustics and the Properties of Solids. *The Journal of the Acoustical Society of America* **28** (6): 1197-1206.
- McQuillin, R., Bacon, M., and Barclay, W. 1984. An Introduction to Seismic Interpretation-Reflection Seismics in Petroleum Exploration.

- Metaxas, A.a. and Meredith, R.J. 1983. *Industrial Microwave Heating*: IET. Original edition. ISBN 0906048893.
- Morte, M., Bloom, E., Huff, G. et al. 2018. Factors Affecting Electromagnetic Wave Penetration in Heavy Oil Reservoirs. Paper presented at the SPE Canada Heavy Oil Technical Conference, Calgary, Alberta, Canada. 12. Society of Petroleum Engineers. DOI: 10.2118/189746-MS.
- Mukhametshina, A. and Martynova, E. 2013. Electromagnetic Heating of Heavy Oil and Bitumen: A Review of Experimental Studies and Field Applications. *Journal of Petroleum Engineering* **2013**.
- Okada, K. 1980. Stress-Acoustic Relations for Stress Measurement by Ultrasonic Technique. *Journal of the Acoustical Society of Japan (E)* **1** (3): 193-200.
- Rehman, M.M. and Meribout, M. 2012. Conventional Versus Electrical Enhanced Oil Recovery: A Review. *Journal of Petroleum Exploration and Production Technology* **2** (4): 169-179.
- Sresty, G.C., Dev, H., Snow, R.H. et al. 1986. Recovery of Bitumen from Tar Sand Deposits with the Radio Frequency Process. *SPE Reservoir Engineering* **1** (01): 85-94.
- Wacker, B., Karmeileopardus, D., Trautmann, B. et al. Electromagnetic Heating for in-Situ Production of Heavy Oil and Bitumen Reservoirs. Society of Petroleum Engineers. DOI: 10.2118/148932-MS.
- Wacker, B., Karmeileopardus, D., Trautmann, B. et al. 2011. Electromagnetic Heating for in-Situ Production of Heavy Oil and Bitumen Reservoirs. In *Canadian Unconventional Resources Conference*: Society of Petroleum Engineers. ISBN 1613991495.
- Wang, J., Bryan, J.L., and Kantzas, A. 2008. Comparative Investigation of Thermal Processes for Marginal Bitumen Resources. In *International Petroleum Technology Conference*: International Petroleum Technology Conference. ISBN 1555632068.
- Weir, W.B. 1974. Automatic Measurement of Complex Dielectric Constant and Permeability at Microwave Frequencies. *Proceedings of the IEEE* **62** (1): 33-36.
- Wilson, A. 2012. Comparative Analysis of Electromagnetic Heating Methods for Heavy-Oil Recovery. DOI: 10.2118/0612-0126-JPT
- Wu, R.-S. and Aki, K. 1988. Introduction: Seismic Wave Scattering in Three-Dimensionally Heterogeneous Earth. In *Scattering and Attenuations of Seismic Waves, Part I*: Springer.
- Wyman, J. 1936. The Dielectric Constant of Solutions of Dipolar Ions. *Chemical Reviews* **19** (3): 213-239.

4. PART 3: CHARACTERIZATION OF COMPLEX PERMITTIVITY FOR CONSOLIDATED CORE SAMPLES BY UTILIZATION OF MIXING RULES *

Abstract

Candidacy of any reservoir as a microwave absorber is predicated on the complex permittivity of the sample. Modeling both the penetration and absorption dynamics of the electromagnetic wave in the reservoir is dependent on realistic estimation of this parameter. Therefore, it becomes necessary to understand the inherent intricacies of complex permittivity in the reservoir. Reservoirs are comprised of both a void space represented by the porosity parameter as well as the rock matrix and can be treated as a binary mixture of the two. Mixing rules can then be introduced and have been shown to be a viable means of estimating the dielectric response. The behavior of the bulk material is considered to be an extension of the isolated contribution of the separate parts. Therefore, by characterizing the response of the individual components of the mixture, the overall response can be estimated. Utilization of mixing rules enables efficient estimation of the dielectric properties anywhere in the reservoir as a function of the rock matrix, fluid saturation, and porosity. The absorptive capacity of the reservoir can then be described which is used to screen the efficacy of the material for microwave introduction. Both the real and imaginary components of complex permittivity are measured on nine consolidated core samples of varying lithology and fluid saturation over the frequency

* Reprinted with permission from Morte, M. and Hascakir, B. 2019. Characterization of Complex Permittivity for Consolidated Core Samples by Utilization of Mixing Rules. *Journal of Petroleum Science and Engineering* **181**. DOI: <https://doi.org/10.1016/j.petrol.2019.06.042> Copyright 2019 Elsevier

range of 400 MHz to 6 GHz. Experimental data is compared to various mixing rules commonly implemented to determine validity and viability of the estimation of complex permittivity for consolidated samples.

Introduction

Recoverable heavy oil and bitumen occur in expansive worldwide distributions available to be exploited. This creates strong potential to bolster current production levels to mitigate concerns about diminishing conventional resources. Diminishing conventional resources arising from preferential production due to ease of access has created an ever-growing importance for unconventional reserves such as bitumen and heavy oil (Bera and Babadagli 2015; Owen et al. 2010). Because of continued increase in demand, we must now identify an economically viable means of producing these unconventional hydrocarbon sources (Meyer et al. 2007; Sorrell et al. 2010). Heavy oil and bitumen resources are defined as unconventional because of their high viscosity which prevents the transmission of the fluid through the reservoir. Therefore, additive energy to the system is required (Alvarado and Manrique 2010; Kokal and Al-Kaabi 2010). This is primarily done by taking advantage of heat, typically steam (Fanchi 1990; Mukhametshina and Martynova 2013; Sarathi and Olsen 1992). Electromagnetic waves (EM) for thermal enhanced oil recovery have gained prominence as an alternative to steam as they are able to target thin reservoirs and alleviate the inherent inefficiency in steam processes.

Steam as a heat-transporting fluid propagates through the reservoir transferring heat energy convectively at the interface with the oil. At this point, the associated viscosity reduction allows for the transmission of the liquid oil to the producing well. Steam is

principally utilized due to the greater capacity to exchange heat, owing to the presence of innate latent heat. However, there are limitations associated with the usage of steam. The fluid nature of steam as the heat transporter has implications in the reservoir itself (Carrizales et al. 2008). Steam propagates through the path of least resistance; so steam loss relative to the system may occur in some thin and deep reservoirs (Hasanvand and Golparvar 2014; Hascakir et al. 2009). Any benefit achieved by the additive energy is lost as the heat transporting fluid leaves the system, corresponding to poor overall efficiency. Utilization of microwaves bypasses issues that exist with a heat-transporting fluid as the mechanism of heat introduction is not reliant on convection (Jha and Chakma 1999; Mutyala et al. 2010). The wave travels through the material and volumetrically heats through dipole rotation which offers distinct advantages over the interfacial heating of steam (Chhetri and Islam 2008; Kasevich et al. 1994). Electromagnetic wave introduction as an enhanced oil recovery process takes advantage of the ability of the material to convert wave energy to heat the reservoir. Wave absorption is defined on the basis of the complex permittivity of the material which is a measure of the polarity of the medium (Metaxas and Meredith 1983; Morte et al. 2018; Von Hippel 1954).

Therefore, processes involving the dielectric heating mechanism are very sensitive to this parameter (Singh and Heldman 2001; Sun 2014). Complex permittivity is composed of both a real component denoted as the dielectric constant and an imaginary component denoted as the loss index as is seen in Eq 2.1 (Debye 1922; Von Hippel 1954; Wyman 1936). Dielectric constant describes the ability of the material to store energy while loss index describes the ability of the material to convert electrical energy to heat

energy (Chang et al. 2010; Debye 1934; Ghodgaonkar et al. 1989; Gross 1941). Loss tangent is a parameter that is used to relate both the imaginary and real components and is a measure of the efficacy of the material to absorb microwave energy shown by Eq 2.2 (Holland 1967; Krupka et al. 1994). Both attenuation, α , depicted in Eq 2.3 and absorbed power, P_a , defined in Eq 2.5 are dependent upon permittivity. So, both the real and imaginary components are integral to the performance of any microwave treatment. Deriving from the fact that both the real and imaginary components of complex permittivity are materials properties, they are accordingly a function of the material in the reservoir. Sensitivity to the reservoir environment as well as mutual interactions make it necessary to illuminate the dependencies on both the skeletal frame as well as the void space of the rock (Han et al. 2017; Liao et al. 2018; Punase and Hascakir 2016; San-Roman-Alerigi et al. 2017).

Reservoir rock is comprised of the rock matrix and the pore space and can therefore be treated as a mixture of the two. Mixing rules can then be utilized to quantify the contribution of each to the overall dielectric response, and therefore offer an efficient means of predicting the dielectric properties of the rock (Chute et al. 1979; Seleznev et al. 2004; Sihvola 1999). The foundation of the mixing rules is governed by a volumetric proportionality where the overall response is to some extent a function of a volume average of each constituent part (Martinez and Byrnes 2001). Volumetric models are attractive and advantageous as they have simplistic relationships with input parameters that are easily obtained or defined (Martinez and Byrnes 2001; Seleznev et al. 2004). The practicality of the volumetric models parallels the focus of this study in terms of

investigating the applicability of commonly used mixing rules for estimation of the dielectric parameters of reservoir rocks. The use of mixing rules as a predictive tool is predicated on a mutually exclusive relationship between the components of the mixture. Interactions changing the volumetric proportionality or involving mutual cancellation of the individual responses create an environment where mixing rules are no longer valid. However, when viable the value of mixing rules is the ability to model very complex and dynamic environments in a much simpler and representative manner. Applicability of mixing rules to describe the reservoir environment in the context of the pore space and the rock matrix is an important tool that would simplify complex permittivity estimation considerably. The binary nature of the reservoir is illustrated in Figure 4.1.

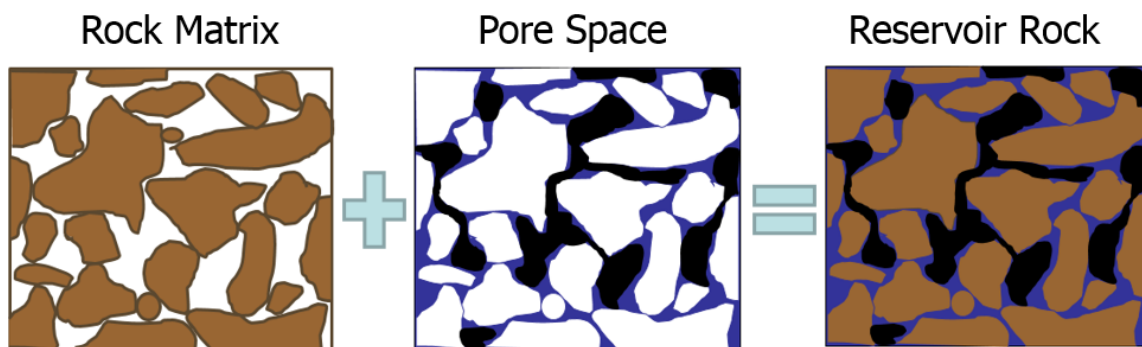


Figure 4.1 - Illustration of the binary (rock matrix and pore space) nature of the reservoir

Empirical correlations are innately valuable specifically to the modeled material but lack a globally significant representation for more widespread implementation. Simple and generic mixing rules that are more universally applicable offer the potential to efficiently characterize reservoir rock mixtures (Hu et al. 2018a). These mixing rules are

primarily implemented in the lower frequency range (radio frequency) as the wave resolution is low enough to produce sound estimates of complex permittivity. The concept of an effective permittivity increases the degree of homogenization in the lower end of the frequency range, however, with increasing frequency comes higher resolution into the medium (Chýlek and Srivastava 1983; Kouchmeshky et al. 2016; Sihvola 2000). Description of oil/sand mixtures in the higher frequency range is still incomplete especially when considering in-situ consolidated rock (Hu et al. 2018a).

Synthesized reservoir rock mixtures have value in their capability of capturing variable parameters but are inadequate at representing rock that has undergone lithification. Studies that present the complex permittivity of synthesized rock disregard the importance of the aging that all reservoirs undergo as well as the lithification process. Implementation of mixing rules is further complicated and nuanced by the presence of clays in the skeletal frame with consolidated samples. The ionic capacity of the clay results in interaction with the water phase that is present in the pore space which creates a double-layer (Feng and Sen 1985; Garrouch and Sharma 1994; Kenyon 1984; Raythatha and Sen 1986). The diffuse layer that is created is itself polarizable and therefore the measured relative real component of complex permittivity is seemingly much higher than anticipated (Adisoemarta 1999; Josh and Clennell 2015; Namdar-Khojasteh et al. 2012; Wagner and Scheuermann 2009). This study focuses on the validity of commonly implemented mixing rules for consolidated reservoir rocks saturated with both oil and water in the higher frequency range. The heterogeneity inherent to all reservoir rock is captured by volume averages of multiple measurements. Any complexity within the pore space involving the

interaction of water and bitumen is simplified by saturating the samples with only one fluid.

Measurements of the mixture are conducted to provide a direct comparison of experimental and predicted results. The implication of agreement between the estimation model and experimental data is the ability to estimate complex permittivity anywhere in the reservoir. The additive contribution from both the isolated rock matrix and the saturating fluid will be measured and experimentally defined. The volumetric nature of the EM heating requires that the wave travel through both constituent components in the reservoir and the absorption response inherently captures the contribution of each (Wagner and Scheuermann 2009). Microwave absorption characteristics are dependent on the complex permittivity so candidacy of reservoirs for electromagnetic wave introduction is determined by this parameter.

Experimental Procedure

The experimental or true quantitative values for complex permittivity were measured by utilizing a N9923A FieldFox Handheld vector network analyzer (VNA) in conjunction with a Keysight N1501A dielectric probe as is depicted in Figure 2.1. The VNA generates a sine wave in the frequency range of interest and the incident wave is then emitted from the dielectric probe (Keysight 2013). The apparatus has the capability of accurately measuring the complex permittivity in the frequency range of .5 GHz to 6 GHz. The incident wave interacts with the interface of the sample where it is either transmitted or reflected. The probe acts simultaneously as the transmitter and receiver and

reads the relative proportionality of transmitted or reflected wave (Marsland and Evans 1987). The VNA then uses these scattering parameters to output both the real and imaginary components of relative permittivity.

Both varying lithology and varying fluid saturations were accounted for to indicate dependencies on both the skeletal frame (rock matrix) as well as the fluid contribution in the pore space. The dielectric probe is capable of measuring both the synthesized reservoir rock as well as fluids. All three oil responses in terms of the measured permittivity were performed by simply immersing the probe in the identified oil samples. Comparison of the three different oil samples as the saturating fluid enables the direct investigation of the contribution of the pore space. The oil samples utilized are summarized in Table 2.2 comparatively to water where the varying dielectric properties will help to elucidate the pore space response. Oil is relatively transparent to microwaves which is evidenced by the much lower values of permittivity when compared to the very polar water. The same experimental procedure and equipment were used for both the solid interface as well as the liquid constituents themselves. The probe is ideally suited to measure both liquids and the solid interface and so the dielectric response of all constituent components was measured with the same experimental apparatus. To be more analogous to reservoir conditions, consolidated cores were measured to provide for closer examination of in situ behavior. Sandstone cores were taken from both the Berea and Bandera outcrops along with a limestone core from the Indiana outcrop which can be seen in Table 2.1.

For more robust and inclusive analysis, four different models have been investigated. Taking advantage of different models helps normalize the data without discounting any nuances or intrinsic complexity. The optimum method is considered to be the one that produces the greatest match to the measured mixture response. Adherence to the foundational relationships identified provides confidence in the capability of the mixing rule to capture inherent complexity in the mixture. Large disparity between the estimated and the measured mixture dielectric properties is indicative of the model's inadequacy to represent the dielectric response in the presence of a mixture. The four different models implemented are the Lowry, L-LN, CRIM, and LR models. Various mixing rules are derived on the basis of assumptions specific to very unique situations. Therefore Lowry's mixing rule – the most basic mixing rule - was implemented first as a function of the broader scope that can be encompassed. The foundation of Lowry's mixing rule is volumetric proportionality where the mixture's relative permittivity is considered to be the volume average of the relative permittivity of each component. The mathematical relationship is provided in Eq 4.1 where ϵ'_{rm} is the real relative permittivity of the rock matrix, v_{rm} is the volume fraction of the rock matrix, ϵ'_p is the real relative permittivity of the pore space, v_p is the volume fraction of the pore space, and ϵ'_t is the mixture's real relative permittivity (Lowry 1927).

The natural logarithmic Lichtenecker (L-LN) model accounts for a large range in data by attempting to normalize the data through usage of the natural logarithm. The normalization of the data results in less emphasis being placed on the difference in the relative permittivity of the two components of the mixture. This results in a more

representative approach as a means of capturing any small interactions that may occur between the pore space and the rock matrix. The equation for the L-LN model is seen in Eq 4.2 where denotations of parameters are consistent with Eq 4.1 (Lichtenecker 1926). The Lichtenecker-Rother (LR) model essentially normalizes the data by utilization of the power function. The equation for the LR model is seen in Eq 4.3, where the parameter c is the dimensionless fitting parameter or cementation factor. Conventionally the cementation factor is one-third which will be the quantity used in this study (Lichtenecker and Rother 1931). The LR model reduces to the Complex Refractive Index Method (CRIM) model when the cementation factor is one-half as can be seen in Eq 4.4 (Birchak et al. 1974).

$$\varepsilon'_{rm} v_{rm} + \varepsilon'_p v_p = \varepsilon'_t \quad \text{Eq 4.1}$$

$$\ln(\varepsilon'_{rm}) v_{rm} + \ln(\varepsilon'_p) v_p = \ln(\varepsilon'_t) \quad \text{Eq 4.2}$$

$$\varepsilon_m^c = \varepsilon_{rm}^c v_{rm} + \varepsilon_p^c v_p \quad \text{Eq 4.3}$$

$$\sqrt{\varepsilon_m} = \sqrt{\varepsilon_{rm}} v_{rm} + \sqrt{\varepsilon_p} v_p \quad \text{Eq 4.4}$$

The experimentally measured samples are consolidated dry cores that were taken from an outcrop and fully saturated with either oil or water. The contribution of the rock matrix cannot be directly measured as the measured response will implicitly capture the contribution of the pore space. The rock matrix contribution was found by normalizing the response of the dry cores for the contribution of the air. The pore space contribution was taken to be equal to that of the saturating fluid. Taking advantage of the known relative

permittivity of air and inputting the measured data allows for the isolation and calculation of the rock matrix relative permittivity. The contribution of the rock matrix is calculated by rearranging the above equations to solve for ϵ'_{rm} where all other parameters are known. The transparent nature of the air results in a very low relative permittivity of one, which is used to represent the contribution of the pore space. Combining the relative permittivity of the known pore space (air), and the total experimentally measured relative permittivity allows for the calculation of the rock matrix relative permittivity.

The volume fraction of each component is easily found as the mixture is binary and therefore the addition of v_{rm} and v_p must equate to one. The normalized rock matrix values calculated for the air-saturated cores are then used as an intermediary calculation for the oil-saturated cores. Taking the contribution of the rock matrix found using the air-saturated cores as well as the contribution of the pore space for the oil-saturated cores produces a calculated mixture relative permittivity. The calculated mixture relative permittivity is compared to the measured values to investigate the validity of mixing rules in describing the samples in this study. The pore space is saturated with the liquid oil or water; so the contribution of the pore is considered the dielectric response of the fluid samples themselves. The dielectric response of each of the constituent components in the utilized mixing rules is illustrated in Figure 4.2. The figure graphically represents the contribution of each of the constituent components in the binary mixing rules employed where the bulk response in terms of real relative permittivity and loss tangent can be seen for all three oils and all three rock matrices.

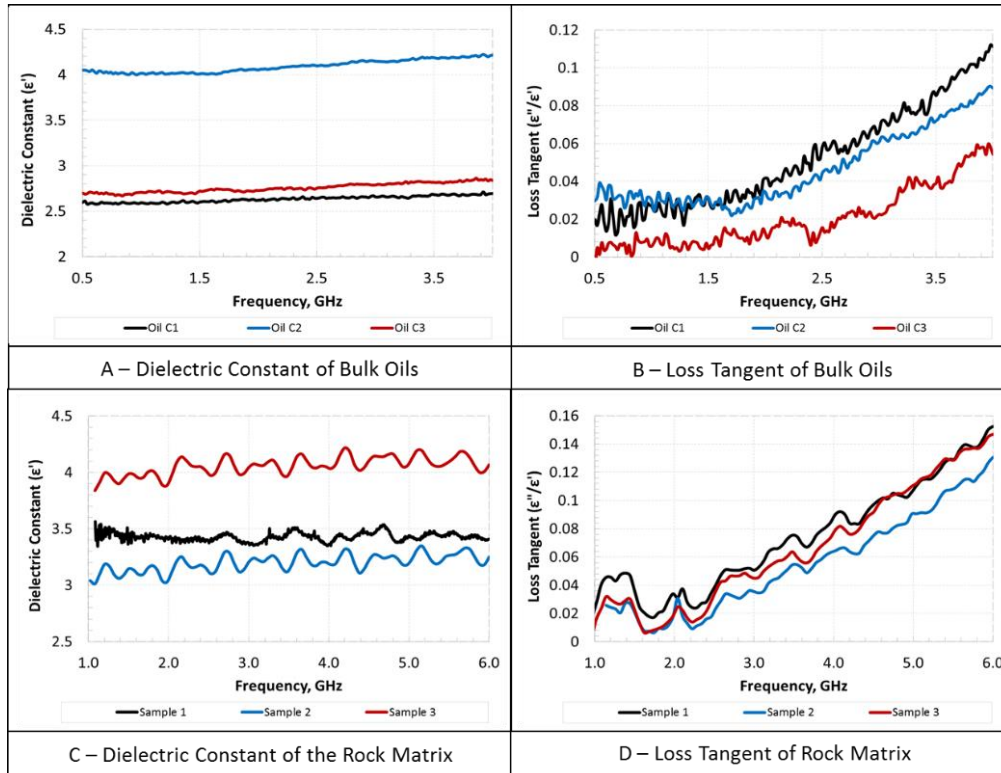


Figure 4.2 - Experimentally measured dielectric properties of the constituent components of bulk oil and rock matrix

Experimental Results and Discussion

The value in implementing mixing rules is only realized under the assumption that the estimation provided is valid. Therefore, for each specific scenario it is vital that the correct mixing rule be utilized (i.e., the mixing rule which results in the greatest agreement between measured and estimated quantities). The results of all four models for the oil-saturated samples can be seen in Table 4.1, Table 4.2, and Table 4.3 for oil C1, C2, and C3 respectively. The values in the tables are averages over the frequency range of interest from .5 GHz to 6 GHz. There is very little disparity between the measured real relative permittivity and the calculated values for all four models. When oil is the primary

saturating fluid, both components of the binary mixture have a real relative permittivity that is very close in quantity. This results in the volumetric mixing rule implemented by Lowry being able to capture the behavior as there is little discrepancy between measured and estimated values. However, the CRIM model is also very capable as evidenced in the table and the increased complexity in the model corresponds to a higher degree of applicability. As the constituent component dielectric response varies with the addition of other fluids to the pore space, the CRIM model is better suited to account for the increasing divergence between the pore space and rock matrix. Microwaves travel through the bulk of the material and will therefore interact with the irreducible water content of the reservoir. The added complexity of irreducible water content in conjunction with the presence of a small initial water saturation in most reservoirs makes the CRIM model better suited for estimation.

Table 4.1 - Experimental and calculated real relative permittivity for all four models pertaining to the C1 saturated core samples

	Real Relative Permittivity, ϵ'								
	Exp	Lowry	Error, %	CRIM	Error, %	L-LN	Error, %	LR	Error, %
Oil C1	Mix	Mix (calc)		Mix(calc)		Mix (calc)		Mix (calc)	
Sample 1	2.928	3.103	5.956	2.740	6.416	3.384	15.581	3.261	11.359
Sample 2	2.914	3.123	7.164	2.815	3.426	3.374	15.763	3.257	11.755
Sample 3	3.849	3.876	0.707	3.501	9.035	4.186	8.758	4.045	5.101

Table 4.2 - Experimental and calculated real relative permittivity for all four models pertaining to the C2 saturated core samples

	Real Relative Permittivity, ϵ'								
	Exp	Lowry	Error, %	CRIM	Error, %	L-LN	Error, %	LR	Error, %
Oil C2	Mix	Mix (calc)		Mix(calc)		Mix (calc)		Mix (calc)	
Sample 1	3.063	3.387	10.574	3.000	2.071	3.676	20.018	3.543	15.657
Sample 2	2.942	3.353	13.981	3.026	2.864	3.591	22.066	3.484	18.413
Sample 3	4.016	4.063	1.175	4.172	3.878	4.423	10.131	4.268	6.278

Table 4.3 - Experimental and calculated real relative permittivity for all four models pertaining to the C3 saturated core samples

	Real Relative Permittivity, ϵ'								
	Exp	Lowry	Error, %	CRIM	Error, %	L-LN	Error, %	LR	Error, %
Oil C3	Mix	Mix (calc)		Mix(calc)		Mix (calc)		Mix (calc)	
Sample 1	2.922	3.061	4.761	2.711	7.216	3.349	14.595	3.228	10.474
Sample 2	2.932	3.090	5.375	2.791	4.824	3.330	13.564	3.231	10.180
Sample 3	3.933	3.846	2.216	3.479	11.552	4.156	5.664	4.020	2.199

The introduction of a high dielectric property fluid, namely water, creates a very different mixing rule environment than that of the oil-saturated samples. With the oil-saturated cores, all constituent dielectric properties were very similar so the simpler volumetric model was ideally suited to represent the sample. However, mixing rules in their simplest form, such as the volumetric average proposed by Lowry, are limited in scope and not as robust when data is more complex. To overcome this inadequacy, it is necessary to utilize more complex and sophisticated mixing rules. These models are better able to capture the relationship between components with a large range of quantitative values. The logarithmic nature of the LN model is more suited to handle the very large disparity of dielectric response realized in the pore space when estimating the water-

saturated sample. When water is the saturating agent, the pore space has a dielectric capacity that is many times greater than the skeletal frame. Accordingly, the LN model is more capable of estimating the actual values as seen in Table 4.4.

Table 4.4 - Experimental and calculated real relative permittivity for all four models pertaining to the water-saturated core samples

	Real Relative Permittivity, ϵ'								
	Exp	Lowry	Error, %	CRIM	Error, %	L-LN	Error, %	LR	Error, %
Water	Mix	Mix (calc)		Mix(calc)		Mix (calc)		Mix (calc)	
Sample 1	6.763	18.765	177.447	10.043	48.494	7.022	3.827	9.197	35.978
Sample 2	6.387	15.983	150.223	7.744	21.236	5.833	8.678	7.382	15.572
Sample 3	7.056	14.236	101.760	8.172	15.816	6.591	6.593	6.763	4.158

The frequency-dependent response for the real relative permittivity for all three lithological samples utilized can be seen in Figures 4.3, 4.4, and 4.5. The sound agreement between the models and the experimental data is easily seen as all models do a relatively fine job of estimating the real relative permittivity for the oil-saturated samples. The dielectric constant is the real component of the complex permittivity which is much less sensitive to frequency and accordingly relatively constant. Therefore, the estimation for dielectric constant introduces much less error and the models employed are able to produce adequate values comparatively to the measured parameters. However, it is clearly shown that the L-LN model is much more capable of representing the samples in the presence of high water content.

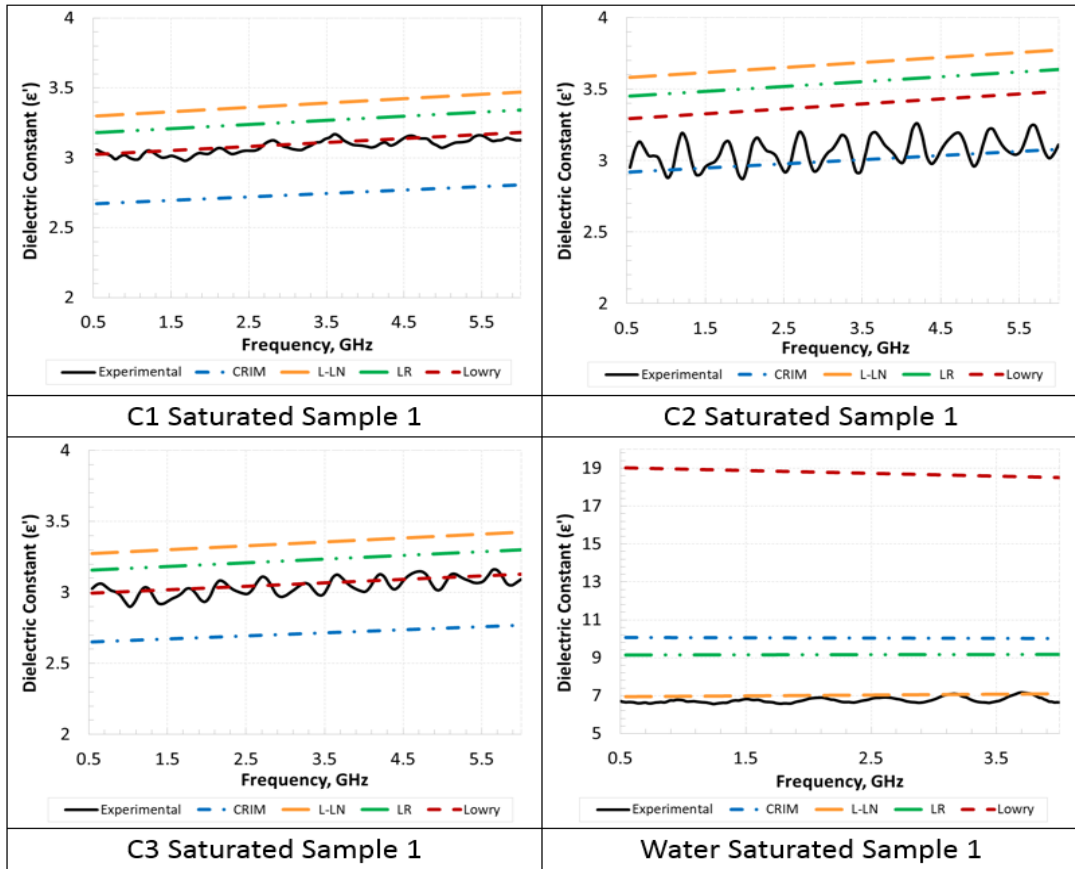


Figure 4.3 - Mixing rule relationships for the frequency-dependent real relative permittivity for sample 1 cores with all four saturating fluids

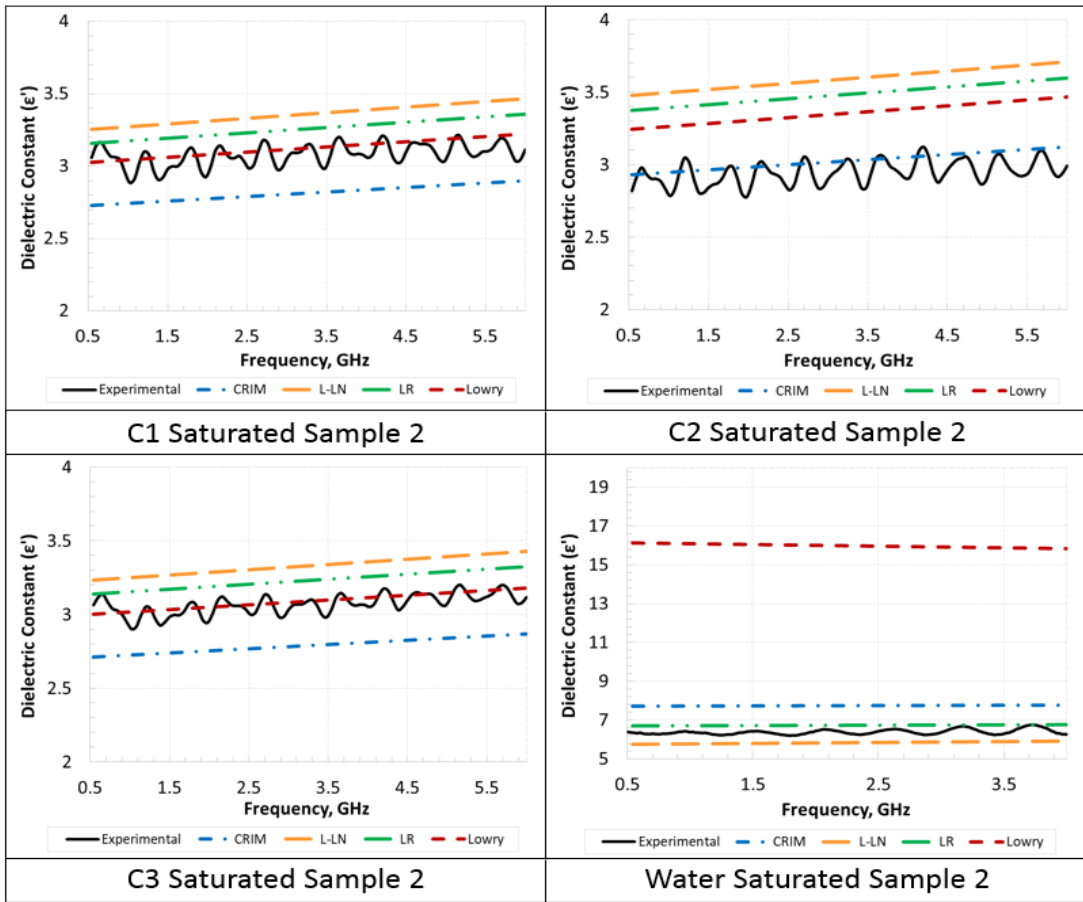


Figure 4.4 - Mixing rule relationships for the frequency-dependent real relative permittivity for sample 2 cores with all four saturating fluids

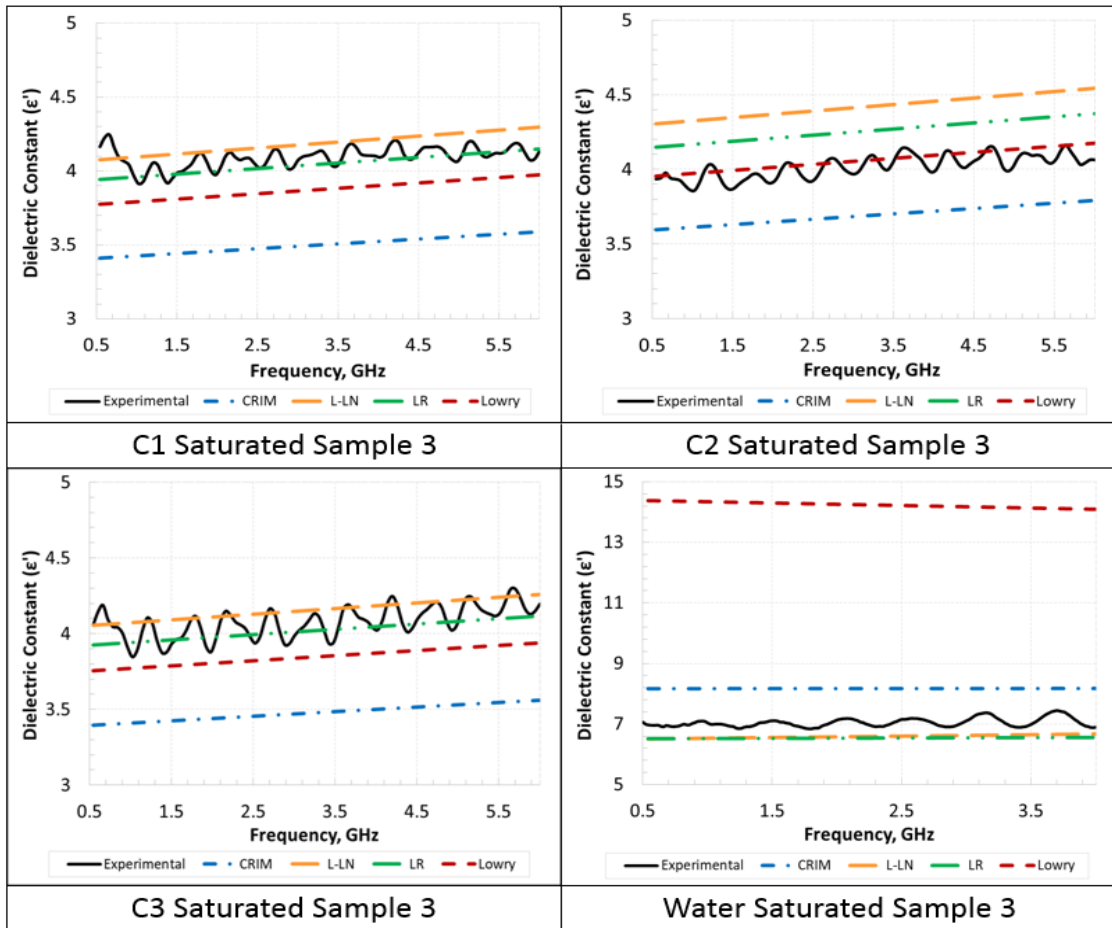


Figure 4.5 - Mixing rule relationships for the frequency-dependent real relative permittivity for sample 3 cores with all four saturating fluids

The loss index is the imaginary component of the complex permittivity and is frequency-dependent. The complex nature of the parameter and the much lower values present a challenge not experienced with the real relative permittivity. This is evidenced through the much higher error percentages realized by most of the models. Use of effective permittivity allows for the mixture to respond to electromagnetic stimulation as if it were homogenous. The loss index is associated with attenuation which makes the utilization of mixing rules much less straightforward (Sihvola 2000). The only model that comes

relatively close to consistently attaining a good fit to the experimental data is that of the CRIM. The experimentally measured and CRIM predicted response can be seen in Figure 4.6 for all three core samples. Figure 4.6 captures the loss tangent of all experimentally measured cores and presents them comparatively to the CRIM mixing rule estimation to display the match that is achieved. The CRIM was more suited for the loss tangent analysis than the other mixing rules as is evidenced by the tables which is why the figure displays only this mixing rule.

Taking into consideration both aspects of dielectric permittivity, namely the real and imaginary components, the CRIM model has the highest applicability and provides sound estimation of the dielectric parameters. Therefore, the CRIM model can be implemented with confidence when attempting to describe the dielectric behavior of reservoir rock interactions with oil. Greater confidence is placed upon the predicted values for the dielectric constant as a result of the much lower error percentages. The imaginary component is associated with the loss of energy relative to the wave through the absorption mechanism whereas the real component is governed only by energy storage. The presence of the loss mechanism for the imaginary component of complex permittivity results in added complexity and a poorer prediction of the true values comparatively to the dielectric constant.

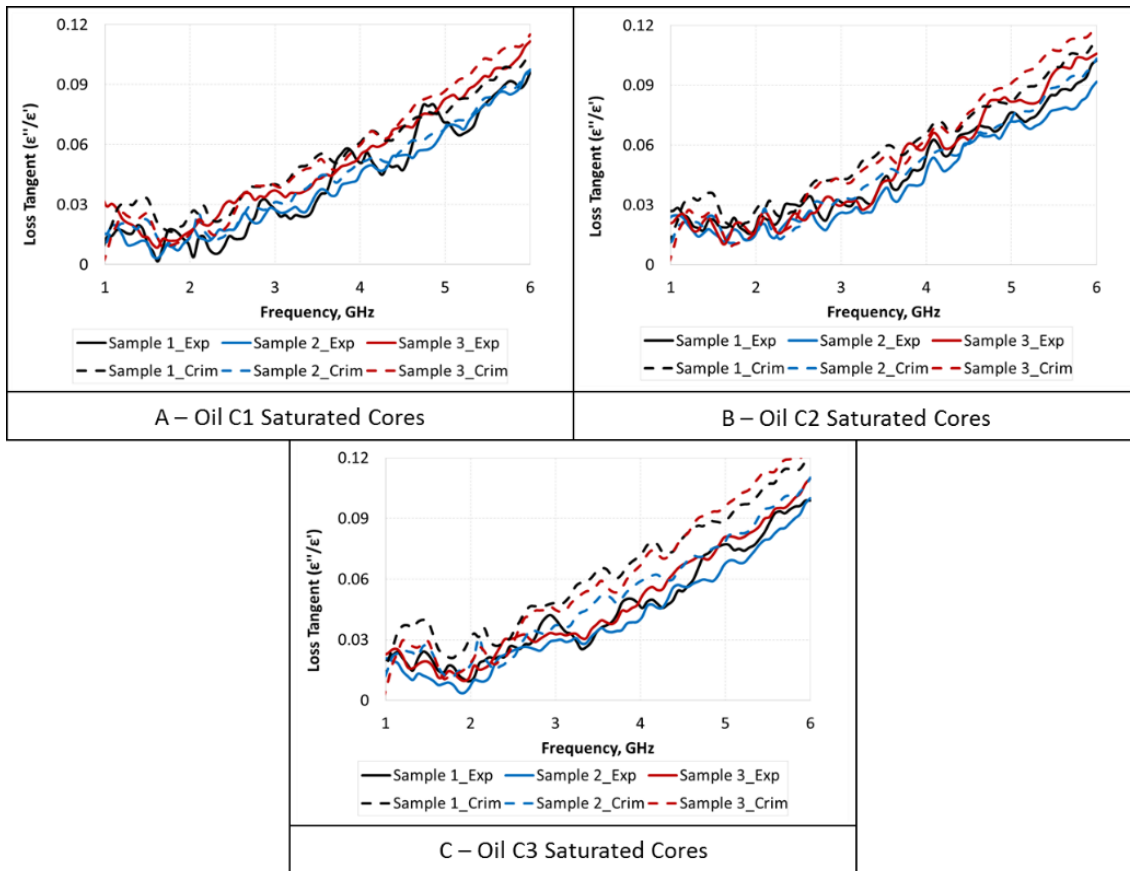


Figure 4.6 - Loss tangent of all experimentally measured cores comparatively to the estimated mixing rule utilizing the CRIM

This model provides the closest estimation of the loss index under the influence of oil as the saturating fluid as is seen in Tables 4.5, 4.6, and 4.7. The proclivity of water to absorb microwaves due to the polar nature of the molecule makes the loss index very high for the water-saturated case. Once again the disparity between the pore space and the rock matrix when high water saturation is present creates a difficult dynamic to accurately predict. The LR model is the closest in terms of error percentage shown in Table 4.8. Capturing the loss tangent response is a much greater challenge than that of the real component.

Table 4.5 - Experimental and calculated loss index for all four models pertaining to the C1 saturated core samples

	Loss Index, ϵ''								
	Exp	Lowry	Error, %	CRIM	Error, %	L-LN	Error, %	LR	Error, %
Oil C1	Mix	Mix (calc)		Mix(calc)		Mix (calc)		Mix (calc)	
Sample 1	0.123	0.192	56.973	0.146	18.851	0.195	58.743	0.317	158.628
Sample 2	0.117	0.144	23.599	0.125	7.303	0.198	69.909	0.200	71.744
Sample 3	0.200	0.218	9.085	0.195	2.682	0.292	45.951	0.281	40.254

Table 4.6 - Experimental and calculated loss index for all four models pertaining to the C2 saturated core samples

	Loss Index, ϵ''								
	Exp	Lowry	Error, %	CRIM	Error, %	L-LN	Error, %	LR	Error, %
Oil C2	Mix	Mix (calc)		Mix(calc)		Mix (calc)		Mix (calc)	
Sample 1	0.142	0.218	52.934	0.162	13.669	0.230	61.428	0.333	133.773
Sample 2	0.118	0.165	39.027	0.133	12.378	0.257	117.453	0.230	94.483
Sample 3	0.193	0.239	23.553	0.195	0.954	0.329	70.350	0.352	81.976

Table 4.7 - Experimental and calculated loss index for all four models pertaining to the C3 saturated core samples

	Loss Index, ϵ''								
	Exp	Lowry	Error, %	CRIM	Error, %	L-LN	Error, %	LR	Error, %
Oil C3	Mix	Mix (calc)		Mix(calc)		Mix (calc)		Mix (calc)	
Sample 1	0.134	0.177	32.435	0.160	19.727	0.231	72.708	0.324	141.822
Sample 2	0.120	0.136	13.460	0.133	10.861	0.254	112.645	0.230	92.147
Sample 3	0.187	0.210	12.199	0.195	4.187	0.327	74.527	0.314	67.605

Table 4.8 - Experimental and calculated loss index for all four models pertaining to the water-saturated core samples

	Loss Index, (ϵ'')								
	Exp	Lowry	Error, %	CRIM	Error, %	L-LN	Error, %	LR	Error, %
Water	Mix	Mix (calc)		Mix(calc)		Mix (calc)		Mix (calc)	
Sample 1	0.692	1.962	183.493	0.644	6.965	0.629	9.170	0.856	23.724
Sample 2	0.552	0.951	72.388	0.362	34.407	0.264	52.063	0.620	12.415
Sample 3	0.819	0.602	26.496	0.318	61.136	0.336	59.011	0.506	38.139

The validity and viability of the usage of mixing rules for this specific case are evidenced by analyzing the frequency-dependent loss index of the samples. The loss index of the saturated core experiments involving sample 1 from highest to lowest are C2, C1, and C3. This is consistent with the relationships seen of the oils before being imbibed into the cores as is evident from the quantities in Table 2.2. Therefore, the presence of the rock matrix does not alter the relationship of the dielectric response of the saturating fluids. Relationships known to be true regarding the fluids remain valid when imbibed into the core. The relationship identified illustrates that the loss index response of each sample as compared to the others adheres to what would be expected in the presence of only the liquid oils. Imbibing the oils into the pore space of the rock matrix did not change the anticipated behavior. This is indicative of minimal mutual interaction between the rock matrix and the pore space. Mixing rules are then applicable to define the samples' overall response in terms of the dielectric properties.

Conclusions

Microwaves travel as an electromagnetic wave which is absorbed by the material where the interaction is governed by the complex permittivity of the sample. Therefore, to properly and adequately estimate microwave penetration depth in a reservoir, the complex permittivity of the sample needs to be characterized. Utilization of mixing rules to accurately predict the complex permittivity of a sample is accordingly very important and offers innate advantage. Mixing rules offer the ability to estimate the bulk response of a material by analyzing the individual response of the constituent components. Analysis

of three different oils in conjunction with three different lithological cores has shown that mixing rules are valid when implemented for heavy oil reservoirs when considering the real component of complex permittivity. The implication of agreement between the estimation model and experimental data is the ability to estimate complex permittivity anywhere in the reservoir. The reservoir can be treated as a binary mixture of the rock matrix and the pore space. The contribution of the pore space is quantified by measuring the dielectric response of the saturating fluid. The rock matrix is described by normalizing the dry core response for the contribution of air in the pore space. The known dielectric properties of air allow for the back-calculation of purely the rock matrix response which is then used as an intermediary for the fluid-saturated samples.

The foundation of the work is the description of the reservoir environment in terms of the dielectric responses through utilization of mixing rules. Lack of significant clay in the rock lithology results in greater capability of describing the oil sand/rock mixture. Various models were tested to determine which model is better suited to estimate the properties specific to the reservoir rock that was utilized. The real component of complex permittivity was effectively able to be estimated by use of the mixing rules. The CRIM model specifically was able to provide an adequate description of the loss tangent for all three oils that were tested.

Prediction of the dielectric response of the reservoir in terms of the constituent components, namely the saturation fluid and rock mineralogy, offers a fast and efficient means of calculating absorption and penetration depth of the microwave introduction. These parameters are of particular interest as they directly control the heat generated in

the reservoir by electromagnetic waves. The efficacy of the heating mechanism greatly affects the economics of the project, again demonstrating the inherent value of using mixing rules. The complex permittivity in the presence of an oil dominated saturation environment can be described by implementing the CRIM model. Both the real and imaginary components of complex permittivity of the oil-saturated samples were estimated effectively with the CRIM model. The applicability of the mixing rule was extended by utilization of multiple oil samples where the CRIM mixing rule was consistently capable of providing an accurate estimation.

When a large water saturation is present, the disparity between the dielectric properties of the constituent components necessitates a more complex mixing rule. The mixing rule environment is more dynamic in the presence of water as a result of the very polar nature of water compared to the non-polar nature of the reservoir matrix. The LN model is relatively capable of accounting for the large disparity in the constituent components which makes it a better candidate as an estimation model in the presence of high water saturation.

The nature of the volumetric mixing rules that are implemented are founded upon mutual exclusivity. Therefore, the value of the mixing rule is in part tied to the interaction between the skeletal frame and the pore space. However, the real component of complex permittivity in the higher frequency range implemented in this study was found to be more than adequately described by the mixing rule. In the presence of complexities in the skeletal frame such as the contribution of expansive clays, the mixing rules do begin to break down which is evidenced by the poor match in loss tangent for this study when the

cores are saturated with water. The CRIM mixing rule was able to accurately model the complex permittivity of the oil-saturated cores and the L-LN mixing rule was able to accurately match the real relative permittivity value of the water-saturated core. The value is achieved by the match itself where the applicability of the mixing rule is evidenced by small disparity in the estimated and measured dielectric responses. Agreement between experimentally obtained and mixing rule predicted values validates the experimental procedure implemented and provides confidence in the measured parameters. Therefore, the complex and dynamic downhole environment of the reservoir can be captured in a much simpler manner through the representative homogenization of the volume. The dielectric response of the volume as a whole has been regressed to be a function of additive contributions of individual components. From these values, the wave absorption can be quantified and therefore the efficacy of the material as a microwave absorber can be categorized. The culmination of findings results in the integration of the dielectric response of both the skeletal frame and pore space to describe the viability of mixing rules in a heavy oil reservoir.

Consolidated cores are more analogous to in-situ reservoirs compared to experimentally defined unconsolidated cores so cores from various outcrops were used. The reservoir rock itself can be treated as a binary mixture of the rock matrix and pore space. Normalizing and accounting for the pore space in dry cores by treating them as air saturated allows for the isolation of the rock matrix component. The complex permittivity of the saturated samples was then measured where the volumetric contribution of the pore space is a function of the dielectric response of the saturating fluid.

References

- Adisoemarta, P.S. 1999. Complex Electrical Properties of Shale as a Function of Frequency and Water Content, Texas Tech University.
- Alvarado, V. and Manrique, E. 2010. Enhanced Oil Recovery: An Update Review. *Energies* **3** (9): 1529-1575.
- Bera, A. and Babadagli, T. 2015. Status of Electromagnetic Heating for Enhanced Heavy Oil/Bitumen Recovery and Future Prospects: A Review. *Applied Energy* **151**: 206-226.
- Birchak, J.R., Gardner, C.G., Hipp, J.E. et al. 1974. High Dielectric Constant Microwave Probes for Sensing Soil Moisture. *Proceedings of the IEEE* **62** (1): 93-98.
- Carrizales, M.A., Lake, L.W., and Johns, R.T. 2008. Production Improvement of Heavy-Oil Recovery by Using Electromagnetic Heating. In *SPE Annual Technical Conference and Exhibition*: Society of Petroleum Engineers. ISBN 1555631479.
- Chang, C.-M., Chen, J.-S., and Wu, T.-B. 2010. Dielectric Modeling of Asphalt Mixtures and Relationship with Density. *Journal of Transportation Engineering* **137** (2): 104-111.
- Chhetri, A. and Islam, M. 2008. A Critical Review of Electromagnetic Heating for Enhanced Oil Recovery. *Petroleum Science and Technology* **26** (14): 1619-1631.
- Chute, F., Vermeulen, F., Cervenán, M. et al. 1979. Electrical Properties of Athabasca Oil Sands. *Canadian Journal of Earth Sciences* **16** (10): 2009-2021.
- Chýlek, P. and Srivastava, V. 1983. Dielectric Constant of a Composite Inhomogeneous Medium. *Physical Review B* **27** (8): 5098.
- Debye, P. 1922. Methods to Determine the Electrical and Geometrical Structure of Molecules. *Nobel Lectures, Chemistry* **1941**: 383-401.
- Debye, P. 1934. Part I. Dielectric Constant. Energy Absorption in Dielectrics with Polar Molecules. *Transactions of the Faraday Society* **30**: 679-684.
- Fanchi, J.R. 1990. Feasibility of Reservoir Heating by Electromagnetic Irradiation. Society of Petroleum Engineers. DOI: 10.2118/20483-MS.
- Feng, S. and Sen, P. 1985. Geometrical Model of Conductive and Dielectric Properties of Partially Saturated Rocks. *Journal of Applied Physics* **58** (8): 3236-3243.
- Garrouch, A.A. and Sharma, M.M. 1994. The Influence of Clay Content, Salinity, Stress, and Wettability on the Dielectric Properties of Brine-Saturated Rocks: 10 Hz to 10 Mhz. *Geophysics* **59** (6): 909-917.
- Ghodgaonkar, D.K., Varadan, V.V., and Varadan, V.K. 1989. A Free-Space Method for Measurement of Dielectric Constants and Loss Tangents at Microwave Frequencies. *IEEE Transactions on Instrumentation and measurement* **38** (3): 789-793.
- Gross, B. 1941. On the Theory of Dielectric Loss. *Physical Review* **59** (9): 748.
- Han, Y., Fang, Y., San-Roman-Alerigi, D.P. et al. 2017. Numerical Modeling of Thermal-Mechanical Interaction Process in High Power Electromagnetic Heating of Rocks. Paper presented at the SPE Middle East Oil & Gas Show and Conference, Manama, Kingdom of Bahrain. 12. Society of Petroleum Engineers. DOI: 10.2118/183836-MS.

- Hasanvand, M. and Golparvar, A. 2014. A Critical Review of Improved Oil Recovery by Electromagnetic Heating. *Petroleum Science and Technology* **32** (6): 631-637.
- Hascakir, B., Acar, C., and Akin, S. 2009. Microwave-Assisted Heavy Oil Production: An Experimental Approach. *Energy & Fuels* **23** (12): 6033-6039.
- Holland, R. 1967. Representation of Dielectric, Elastic, and Piezoelectric Losses by Complex Coefficients. *IEEE transactions on Sonics and Ultrasonics* **14** (1): 18-20.
- Hu, L., Li, H.A., and Ahmadloo, M. 2018. Determination of the Permittivity of N-Hexane/Oil Sands Mixtures over the Frequency Range of 200 Mhz to 10 Ghz. *The Canadian Journal of Chemical Engineering*.
- Jha, K. and Chakma, A. 1999. Heavy-Oil Recovery from Thin Pay Zones by Electromagnetic Heating. *Energy Sources* **21** (1-2): 63-73.
- Josh, M. and Clennell, B. 2015. Broadband Electrical Properties of Clays and Shales: Comparative Investigations of Remolded and Preserved Samples broadband Electrical Properties of Clay. *Geophysics* **80** (2): D129-D143.
- Kasevich, R., Price, S., Faust, D. et al. 1994. Pilot Testing of a Radio Frequency Heating System for Enhanced Oil Recovery from Diatomaceous Earth. In *SPE Annual Technical Conference and Exhibition: Society of Petroleum Engineers*. ISBN 155563463X.
- Kenyon, W. 1984. Texture Effects on Megahertz Dielectric Properties of Calcite Rock Samples. *Journal of Applied Physics* **55** (8): 3153-3159.
- Keysight. 2013. Basics of Measuring the Dielectric Properties of Materials Application Note. In.
- Kokal, S. and Al-Kaabi, A. 2010. Enhanced Oil Recovery: Challenges & Opportunities. *World Petroleum Council: Official Publication* **64**.
- Kouchmeshky, B., Fanini, O., and Nikitenko, M. 2016. Validating Mixing Models for Dielectric Logging. Paper presented at the SPE Russian Petroleum Technology Conference and Exhibition, Moscow, Russia. 10. Society of Petroleum Engineers. DOI: 10.2118/182096-MS.
- Krupka, J., Geyer, R.G., Kuhn, M. et al. 1994. Dielectric Properties of Single Crystals of Al_2O_3 , LaAlO_3 , NdGaO_3 , SrTiO_3 , and MgO at Cryogenic Temperatures.
- Liao, H., Morte, M., Bloom, E. et al. 2018. Controlling Microwave Penetration and Absorption in Heavy Oil Reservoirs. Paper presented at the SPE Western Regional Meeting, Garden Grove, California, USA. 13. Society of Petroleum Engineers. DOI: 10.2118/190089-MS.
- Lichtenecker, K. 1926. Dielectric Constant of Natural and Synthetic Mixtures. *Phys. Z* **27**: 115.
- Lichtenecker, K. and Rother, K. 1931. Deduction of the Logarithmic Mixture Law from General Principles. *Phys. Z* **32**: 255-260.
- Lowry, H.H. 1927. The Significance of the Dielectric Constant of a Mixture. *Journal of the Franklin Institute* **203** (3): 413-439.
- Marsland, T. and Evans, S. 1987. Dielectric Measurements with an Open-Ended Coaxial Probe. In *IEE Proceedings H (Microwaves, Antennas and Propagation)*, 134:341-349: IET. ISBN 2053-907X.

- Martinez, A. and Byrnes, A.P. 2001. *Modeling Dielectric-Constant Values of Geologic Materials: An Aid to Ground-Penetrating Radar Data Collection and Interpretation*: Kansas Geological Survey Lawrence, Kansas. Original edition. ISBN.
- Metaxas, A.a. and Meredith, R.J. 1983. *Industrial Microwave Heating*: IET. Original edition. ISBN 0906048893.
- Meyer, R.F., Attanasi, E.D., and Freeman, P.A. 2007. *Heavy Oil and Natural Bitumen Resources in Geological Basins of the World*.
- Morte, M., Bloom, E., Huff, G. et al. 2018. Factors Affecting Electromagnetic Wave Penetration in Heavy Oil Reservoirs. Paper presented at the SPE Canada Heavy Oil Technical Conference, Calgary, Alberta, Canada. 12. Society of Petroleum Engineers. DOI: 10.2118/189746-MS.
- Mukhametshina, A. and Martynova, E. 2013. Electromagnetic Heating of Heavy Oil and Bitumen: A Review of Experimental Studies and Field Applications. *Journal of Petroleum Engineering* **2013**.
- Mutyala, S., Fairbridge, C., Paré, J.J. et al. 2010. Microwave Applications to Oil Sands and Petroleum: A Review. *Fuel Processing Technology* **91** (2): 127-135.
- Namdar-Khojasteh, D., Shorafa, M., and Omid, M. 2012. Evaluation of Dielectric Constant by Clay Mineral and Soil Physico-Chemical Properties. *African journal of Agricultural research* **7** (2): 170-176.
- Owen, N.A., Inderwildi, O.R., and King, D.A. 2010. The Status of Conventional World Oil Reserves—Hype or Cause for Concern? *Energy policy* **38** (8): 4743-4749.
- Punase, A. and Hascakir, B. 2016. Stability Determination of Asphaltenes through Dielectric Constant Measurements of Polar Oil Fractions. *Energy & Fuels* **31** (1): 65-72.
- Raythatha, R. and Sen, P. 1986. Dielectric Properties of Clay Suspensions in Mhz to Ghz Range. *Journal of Colloid and Interface Science* **109** (2): 301-309.
- San-Roman-Alerigi, D.P., Han, Y., Othman, H. et al. 2017. Geomechanical and Thermal Dynamics of Distributed and Far-Field Dielectric Heating of Rocks Assisted by Nano-Enablers — a Numerical Exploration. Paper presented at the Abu Dhabi International Petroleum Exhibition & Conference, Abu Dhabi, UAE. 21. Society of Petroleum Engineers. DOI: 10.2118/188790-MS.
- Sarathi, P.S. and Olsen, D.K. 1992. *Practical Aspects of Steam Injection Processes: A Handbook for Independent Operators*. National Inst. for Petroleum and Energy Research, Bartlesville, OK (United States).
- Seleznev, N., Boyd, A., Habashy, T. et al. 2004. Dielectric Mixing Laws for Fully and Partially Saturated Carbonate Rocks. In *SPWLA 45th Annual logging symposium*: Society of Petrophysicists and Well-Log Analysts.
- Sihvola, A. 2000. Mixing Rules with Complex Dielectric Coefficients. *Subsurface sensing technologies and applications* **1** (4): 393-415.
- Sihvola, A.H. 1999. *Electromagnetic Mixing Formulas and Applications*: Iet. Original edition. ISBN 0852967721.
- Singh, R.P. and Heldman, D.R. 2001. *Introduction to Food Engineering*: Gulf Professional Publishing. Original edition. ISBN 0080574491.

- Sorrell, S., Speirs, J., Bentley, R. et al. 2010. Global Oil Depletion: A Review of the Evidence. *Energy Policy* **38** (9): 5290-5295.
- Sun, D.-W. 2014. *Emerging Technologies for Food Processing*: Elsevier. Original edition. ISBN 0124104819.
- Von Hippel, A.R. 1954. *Dielectric Materials and Applications*: Artech House on Demand. Original edition. ISBN 0890068054.
- Wagner, N. and Scheuermann, A. 2009. On the Relationship between Matric Potential and Dielectric Properties of Organic Free Soils: A Sensitivity Study. *Canadian geotechnical journal* **46** (10): 1202-1215.
- Wyman, J. 1936. The Dielectric Constant of Solutions of Dipolar Ions. *Chemical Reviews* **19** (3): 213-239.

5. PART 4: MULTIVARIABLE REGRESSION OF COMPLEX PERMITTIVITY AS A FUNCTION OF RESERVOIR PROPERTIES

Abstract

Heterogeneity to some extent is realized in every reservoir. Variable properties, namely fluid saturations and lithology, make it very difficult to accurately estimate the bulk dielectric response of the reservoir. This study isolates and identifies the dependencies of the bulk dielectric response to changing water content, quartz content, limestone content, oil content, clay content, temperature, pressure, and frequency.

A multitude of experiments were run where the identified parameters were systematically isolated and varied to capture both the contribution from the rock matrix and the pore space. Reservoir rock was simulated by mixing the rock matrix components with the fluids to form unconsolidated core samples. The bulk dielectric properties, both the real and imaginary components, were measured for each of the ninety-five different samples using a vector network analyzer (VNA) in conjunction with a dielectric probe. Individual experiments were analyzed comparatively and the dielectric responses are presented as a function of each isolated parameter.

Understanding the general dependencies and sensitivity of the dielectric behavior of the reservoir is vital for various aspects of petroleum including electromagnetic heating and well logging. The complex and dynamic downhole environment creates coupled and mutual interactions making estimation of the bulk response very difficult. Isolation of each variable allows for the identification of the governing relationship of each parameter with the dielectric response. In this study, linearity is established for the dielectric

response of all investigated parameters. The sensitivity of the complex permittivity is represented by the magnitude of change as a function of variable fluid saturation or lithology. This enables the drivers of dielectric heating to be quantified, namely the increase in complex permittivity with increasing water saturation. A multivariable regression is performed on the basis of the experimental data recorded. The regressed relationships allow for the estimation of the dielectric response of the reservoir as a result of heterogeneity present. Variable properties that change with position and time are accounted for by understanding the corresponding change in the complex permittivity of the reservoir.

By illuminating the complex permittivity relationship as a function of rock mineralogy and fluid saturations, a more holistic understanding of absorption mechanics can be achieved. The study offers the unique ability to express the intrinsic relationship experienced under the influence of reservoir properties. The presented relationships also enable the estimation of dielectric properties as a function of reservoir heterogeneity.

Introduction

The utilization of EM irradiation as a stimulation tool is an attractive means of heat generation with great potential, however, issues arise in regard to controlling the wave propagation. The heat is generated at the molecular level where the particles in the medium undergo dipolar rotation with the oscillating EM wave. Rotating particles attempting to align themselves with the corresponding negative or positive half cycle of the EM wave create heat owing to the particle motion (Hill 1969; Metaxas and Meredith 1983; Von

Hippel 1954). The magnitude of heat generation is directly correlative to the degree of absorption of the incident wave where high wave absorption corresponds to high heat generation (Davletbaev et al. 2014; Sahni et al. 2000; Sresty et al. 1986). This wave absorption in the reservoir is described by the material property of complex permittivity, consisting of both a real and imaginary component (Clarke et al. 2003; Gross 1941; Von Hippel 1954). Heterogeneity in the reservoir results in constant changes in the constituent material of the composite reservoir which manifest as changes in the complex permittivity of the reservoir (Dinčov et al. 2004; Sun 2014). Therefore, microwave absorption characteristics change as a function of time and space in the reservoir owing to spatial heterogeneity and production of fluids. Understanding how changes in rock mineralogy and fluid saturations affect the overall dielectric response is vital to accurately predicting the heat gain associated with any microwave process.

Candidacy of reservoirs for EM wave introduction is determined by the complex permittivity of the system. The ability to estimate complex permittivity at any time-step or location in the reservoir is integral to any microwave propagation model (Abernethy 1976; Campanone and Zaritzky 2005). Both analytic and numerical models require this parameter as an input as absorption is greatly sensitive to variation in the dielectric properties of the material (Dinčov et al. 2004; Morte et al. 2018; Niu and Prasad 2016; Sun 2014). Conventionally, numerical models are performed on the basis of constant dielectric parameters (Carrizales 2010). Initial experimental results are considered representative of the sample as a whole where the complex permittivity is thought not to vary significantly. However, loss index is greatly sensitive to even slight variation in the

rock mineralogy or the fluid saturation which can have vast implications in the reservoir (Freedman and Vogiatzis 1979; Niu and Prasad 2016; Snyder and Fleming 1985). Underestimating the loss index will make the penetration depth seem larger while overestimation of the loss index will directly correspond to seemingly greater wave absorption (Metaxas and Meredith 1983). Therefore, the ability to accurately predict the dielectric behavior in the reservoir is of great interest to the industry.

Simplistic predicting models founded on volumetric contribution to the overall sample behavior, called mixing rules, are routinely implemented to estimate reservoir complex permittivity. Mutual exclusivity is necessary to utilize mixing rules where interaction between the individual components is minimal (Centeno et al. 2011; Punase and Hascakir 2016). Any interaction will render the model inaccurate and misleading as the response of the bulk mixture is considered to be only a function of additive contributions from each part (Hu et al. 2018b; Morte and Hascakir 2019). However, primary assumptions made to create these models are poorly supported by the experimental data (Feng and Sen 1985; Mathias et al. 1991; Seleznev et al. 2004). Therefore, they can introduce significant uncertainties into the quantitative definition of the complex permittivity of the mixture. Variability in the properties of the reservoir such as rock mineralogy or fluid saturation equate to changes in the overall complex permittivity of the composite material.

Primarily, the microwave absorption is realized in the pore space where the fluids are more capable of dipole rotation (Josh et al. 2015; Meador and Cox 1975; Myers 1991; Wharton et al. 1980). As a result, the contribution of the skeletal frame or rock matrix is

often ignored. The reservoir is often delineated by treating the rock matrix and the pore space as separate but they are coupled in terms of the dielectric properties (Abraham et al. 2016; Chute et al. 1979). A more holistic approach capturing the contribution of both is more representative of the true relationship (Martinez and Byrnes 2001; Sen et al. 1984). Current models employed to characterize the complex permittivity response fall short upon closer inspection of the loss index. Therefore, a more unique solution specific to components of the reservoir provides the necessary bridge to estimate the entirety of the complex permittivity response. Dielectric properties are vital to the effective representation of flow in the reservoir and accordingly are an integral modeling parameter in any simulation (Singh and Heldman 2001). The magnitude of temperature rise when utilizing microwaves is a function of the degree of wave content absorbed; so proper estimation of the absorptive capacity of the material is vital to correctly modeling temperature rise.

Interactions between the pore space and the rock matrix create a complex and dynamic environment where mixing rules are no longer valid (Feng and Sen 1985; Josh and Clennell 2015). The imaginary nature of the loss index, the governing parameter in heat generation, results in volumetric predictors being grossly inadequate in capturing the complexity that is inherent to the imaginary nature of the loss index (Morte and Hascakir 2019). Furthermore, current models employed falter in the presence of significant clays and also when the pore space is saturated with more than one fluid. Clays present a challenge stemming from their surface charge and great surface area. The clays attract a bound water layer followed by a diffuse layer, denoted the Stern double-layer (Bjorndalen

and Islam 2004; Chilingar et al. 1970; Garrouch and Sharma 1994; Josh et al. 2015; Li et al. 2006; Niu and Prasad 2016). The double-layer increases the separation of charges in the reservoir and therefore increases the polarity. Polarization effects are very important at higher frequencies and so clay content with varying water saturation is of particular interest (Garrouch and Sharma 1994).

Defining the interaction of the materials in the reservoir with the microwave is a challenge that requires the isolation of each contributing component. More sophisticated and targeted estimation techniques are therefore required to provide for realistic estimation of the overall dielectric response. The ability to ascertain the contribution of each constituent component of a mixture is a valuable tool necessary to adequately characterize a sample. By changing the volumetric proportionality of the pore space relative to the sample as a whole, the complex permittivity will accordingly change. The experimental data collected by varying the identified parameters will enable the development of a multivariable regression to produce an estimation of dielectric properties that accounts for mutual interactions. A multivariable regression offers the unique ability to express the intrinsic relationship experienced under the influence of reservoir properties. Therefore, a new estimation equation will be experimentally derived which is capable of predicting the real and imaginary components of complex permittivity.

The intricacies within both the skeletal frame and pore space are described in this study as relationships between rock mineralogy, fluid saturations, pressure, temperature, porosity, oil permittivity, and frequency. Consolidating all of the experimental results into a systematic and inclusive data set allows for the integration of the contribution of all

components of the reservoir to the dielectric response. A large number of experiments will result in a more universal relationship that can be implemented to estimate dielectric properties at any position or time-step in the reservoir. Establishing universality enables the curve to be implemented for any reservoir to provide a realistic estimation anywhere in a reservoir. The multivariable regression results in a more holistic understanding of absorption mechanics and enables a more accurate estimation of complex permittivity in the reservoir.

Experimental Procedure

Complex permittivity of synthesized rock samples was recorded by means of a vector network analyzer as the source and a dielectric probe kit as the transmitter. The microwave signal is generated by the network analyzer and then emanated out of the dielectric probe through a coaxial cable connection. The probe is positioned at the interface of the material under test so the incident wave is directed into the sample. The incident wave will be either reflected or transmitted at the surface of the material. This interaction of the incident wave with the material is directly dependent upon the complex permittivity of the system; so, the proportionality of transmitted and reflected wave is an indicator of the complex permittivity of the system. The dielectric probe behaves simultaneously as both the transmitter and receiver by measuring the proportion of reflected wave. The output of the vector network analyzer is both the dielectric constant, defined to be the real portion complex permittivity, and the loss index, defined to be the

imaginary portion. The raw experimental data was input into the multivariable regression, resulting in a predicting equation for both the dielectric constant and the loss index.

Confidence in the regressed model is derived from significant variability in the isolated parameters and a multitude of observations. To regress a more unique and intrinsic model which is better suited to capturing the true dielectric response, numerous experiments were performed on unconsolidated cores. Experimentally defining and systematically varying all parameters provides the means for isolating the contribution of each parameter to the overall response. The rock matrix is constituted of a systematic and stepwise variability of quartz sand, limestone sand, and kaolinite or bentonite clay. Weights of each of the added components of the synthetic cores were recorded to allow for the calculation of the pore volume. Measuring the bulk volume of the dry core enabled the definition of the porosity based on the known weights and density. Simple calculation produced a known rock matrix volume and, subsequently, the pore volume was taken to be the difference between bulk volume and rock matrix volume.

The dependence upon fluid saturations is once again reliant upon experimental manipulation of the saturation fluids. Filling the pore space with more lossy substances illuminates the contribution of the porosity component of the rock to the overall response. By varying fluid in the pore space, and therefore the complex permittivity of the pore space, the regression has enough data points to elucidate the relationship between the bulk rock response and that of the individual components. Control of the water saturation of the formulated core allowed for discrete quantities to be attained where the remainder of the pore space was filled with oil. Cores were constructed with water saturation values of

0, 20, 40, 60, 80, and 100 percent. The fabricated cores were ensured to be entirely filled with either the water or oil by inputting the exact volume of fluid equal to the calculated pore volume. The oil utilized for the mixtures had a dielectric constant of 2.69 with a loss tangent of .0192 to go along with a viscosity of 10,130 cP at room temperature. The mixing process is visualized in Figure 5.1 where all constituent components were combined to form the reservoir material.



Figure 5.1 - Picture of the before and after of the mixing of the unconsolidated core material including the rock mineralogy and the fluids

The first batch of cores consisted of a total of seventy-five samples with the volume of quartz arranged to be 0, 20, 40, 60, 80, and 100 percent with the remainder consisting of limestone. Subsequently, another twenty samples were constructed which focused on the isolation of the clay contribution where the volume of clay was varied with the blueprint of 4, 8, 12, 16, and 20 percent by volume. For those specific twenty experiments, the quartz volume was defined and controlled to be 75% with the remainder of the matrix volume being limestone and the aforementioned clays. Half of the clay experiments

utilized 100% bentonite clay while the other half was a mixture of 90% kaolinite and 10% illite. Utilization of the different clays encompassed different mechanisms and interactions with water and extended the domain of the regression model. The bentonite clay swells when in contact with the water, the illite is associated with pore bridging, and the kaolinite is considered pore filling. Repeatability analysis was performed where all of the above experiments were recreated and performed again to provide confidence in the data. All of the repeatability results were input into the regression so the model is the result of one hundred and ninety unconsolidated core measurements with a total of over 15,000 observation points.

The blending and compacting of the cores were attained by hand with the sample being forced into the core-holder that was built specifically for the regression experiments. The design of the core-holder is such that the structural integrity of the cores is maintained while allowing the probe and pressure system to access the material as depicted in Figure 5.2. Utilizing unconsolidated cores prevents the direct coaxial compression of the framework of the sample as there is no cementation among the grains to oppose the force. The sample is incapable of preserving the original shape and will be deformed. Packing the mixture into the core-holder serves to provide the structural support necessary to prevent a misshapen sample while avoiding any influence on the measurements themselves.

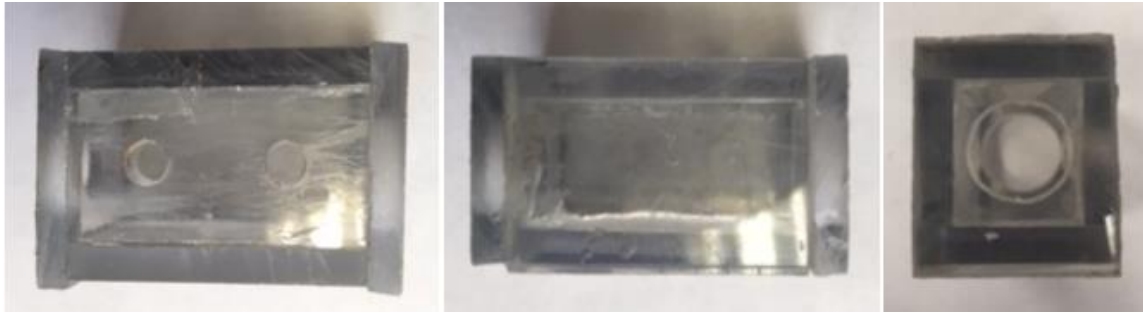


Figure 5.2 - Pictorial description of all three planes of the core-holders utilized to maintain structural integrity

The complex permittivity of the sample was investigated both in terms of the contribution of the constituent components of rock matrix and porosity, but also in the presence of pressure and temperature. Minimizing the pore space reduces the impact of the saturating fluid on the volumetric average of the sample and therefore minimizes the contribution of the pore space. The pressurized samples will undergo slight compaction as the fluids in the pore space are slightly compressible. However, the presence of the core-holder ensures that the bulk volume of the sample is consistent. Dielectric properties are volume-dependent measurements so maintaining volumetric consistency is vital. All constructed cores will be inundated with coaxial compression representing the pressure experienced by all reservoirs due to overburden. The pressure state imposed was varied with the step-size being 15 psi from 15 psig to 90 psig. Temperature was manipulated by means of a heating plate and measured by thermocouples introduced into the synthesized cores. Complex permittivity was measured every 10 °F from 95°F to 155 °F.

An extension of the pressure component throughout the rock matrix is the ability to trigger piezoelectricity resulting from the presence of the quartz crystals (Morte et al.

2019). Inherent piezoelectricity enables a dynamic polarization of the quartz crystal with the resulting change in the polarization vector manifesting itself through variation of the complex permittivity. The ability to experimentally define and vary properties of the unconsolidated cores in a stepwise fashion provides the opportunity to investigate the magnitude of the change in complex permittivity on both variable quartz volume and pressure. Change in complex permittivity will be captured and presented as overall change in the penetration depth as calculated by Equation 2.4 with d_p representing the penetration depth. Attenuation is defined as energy loss relative to the wave and is captured in Equation 2.3 with α being defined as the attenuation constant and f being the frequency. As is mathematically evident, wave absorption is inversely related to penetration depth and is governed by the material property of complex permittivity; so, manipulation of the complex permittivity will manifest as a change in the penetration depth.

Finally, the last independent and predictor variable in the regression is the frequency of the EM wave. Both the real and imaginary components of complex permittivity are sensitive to frequency, with the real component to a much lesser degree. A strong dependency of loss index on frequency warrants investigation into the response under the influence of simultaneous variability in reservoir composition. Complex permittivity is measured for all created cores in the frequency range of .5 GHz to 4 GHz. The ANOVA data analysis tool in Microsoft Excel was utilized to perform the regressions.

Experimental Results and Discussion

Applicability of the multivariable regression implemented is reliant upon established linearity in the dependence on all parameters. Deviance from a first order

relationship introduces additional uncertainty and minimizes the impact and confidence in the mathematical model. Extrapolation and estimation of parameters of higher order parameters create the potential to mask true relationships by forced curve fitting. Sensitivity to the parameters is best evidenced by linearity where the magnitude of the governing mechanism is easily seen and analyzed. Therefore, the isolated contribution of each parameter must be investigated first to validate the usage of the regression model.

As the most polar material in the typical reservoir, the water saturation is a parameter of particular interest. A majority of the wave absorption occurs as a result of the water in the pore space and the large dielectric constant and loss tangent of the water serves as a driver of the regression model. Dependence of the isolated water saturation is seen in Figure 5.3 where definitive linearity is evidenced between water saturation and overall dielectric constant and loss tangent. Establishing linearity provides confidence in the ability to implement a multivariable linear regression as the relationships between the predictor variables and the outcome are first order. Isolating the contribution of the water saturation to the overall response by controlling all other parameters allows for the governing relationship of the predictor variable to be revealed. All parameters other than water saturation remain consistent so all variability in the dielectric response can be attributed to the manipulation of the water saturation.

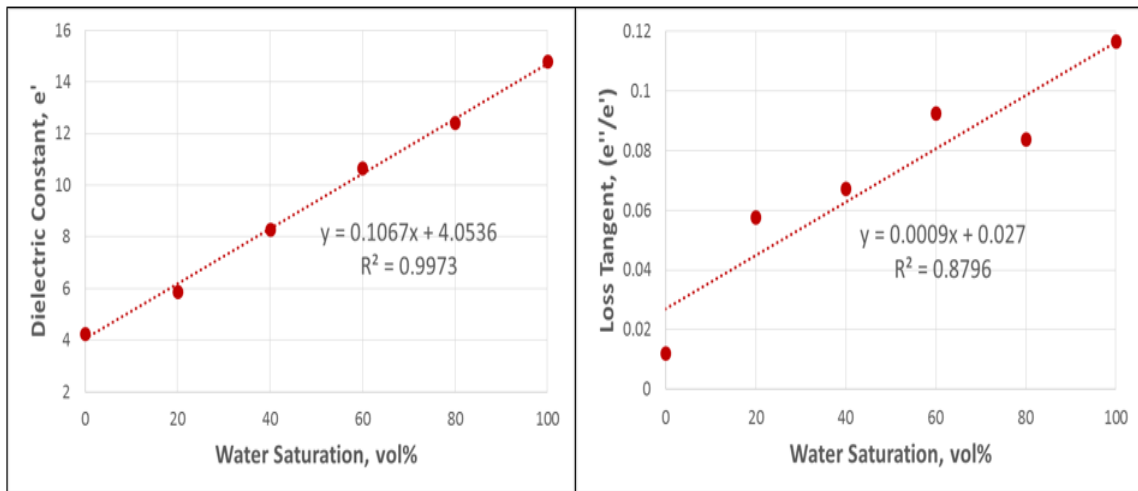


Figure 5.3 - Isolated dependency of complex permittivity on variable water saturation of the reservoir rock

The magnitude of change represented by the slope of the curve is quite large which reflects a high degree of sensitivity to the volume of water. Large disparity between the constituent volume dielectric properties of the water and the overall mixture dielectric properties results in great sensitivity to the changing volumetric proportionality of water. The increase in the dielectric constant is expected and intuitive as you are increasing the component which displays the highest individual dielectric properties. Water is much more polar than the oil and therefore will preferentially absorb a large amount of microwave energy. By increasing the volumetric proportionality of water, the volume of pore space with a high proclivity for absorption is increased. Greater magnitude of wave absorption corresponds to less remaining wave energy to continue propagation, resulting in poorer penetration depth. Absorption and penetration are inversely related so increasing water saturation necessitates lower penetration depth.

The applicability of the regression model as linear is further expounded by the dependency of the dielectric response on variable quartz content as seen in Figure 5.4. Sensitivity to variable quartz content is much less dramatic as is evidenced by comparison with the slope of the water saturation curve in Figure 5.3. However, the degree of linearity along with the minimal deviance from the line of best fit is still indicative of a strong dependency. Both parameters are integral components to the dielectric response in the reservoir. Complex permittivity is a material property that describes the ability to absorb microwave energy. Therefore, variation of the mineralogy will affect the penetration depth as the material in the rock matrix changes. Calcite has higher dielectric properties than quartz and will absorb more wave energy. For Figure 5.4, the sample is comprised of an unconsolidated mixture of only quartz and limestone sand so the lower quartz percentage corresponds to a higher calcite percentage.

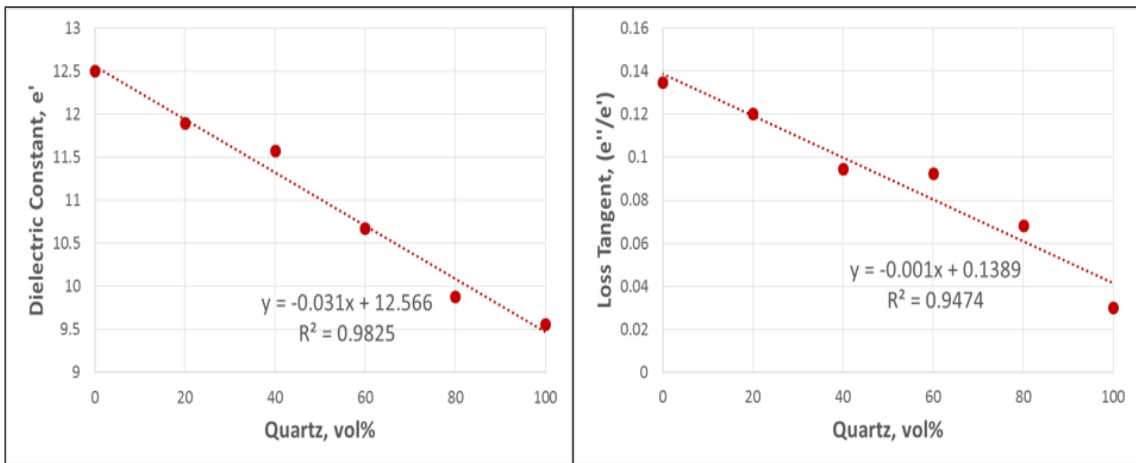


Figure 5.4 - Isolated dependency of complex permittivity on variable quartz volume of the reservoir rock

Predominately, the absorbance of microwave energy occurs in the pore space where the fluid resides. Delineation of the dielectric response to the pore space is achieved by manipulation of the porosity parameter. Investigation into the dielectric constant after isolation of all other parameters besides pore volume is evidenced in Table 5.1. The porosity was experimentally manipulated by utilizing sand grains of variable size. A mixture of grain sizes creates a non-uniform distribution inside the rock matrix with smaller grains filling the pore space of the larger grains of sand. Comparison between the two different porosity values for each of the water-saturated cores clearly shows an increase in dielectric constant with increase in pore volume. This behavior adheres to what is expected as a greater volume of fluid, especially water, corresponds to a greater volume of relatively high polarity substances. The trend is consistent for all analyzed data points where an increase in porosity corresponds to an increase in the dielectric constant value, providing confidence in the experimental results.

Table 5.1 - Comparative investigation into the isolated dependency of the dielectric constant (ϵ') on pore volume

Quartz, vol%	Water Sat, vol%	Porosity	Dielectric Constant, (ϵ')
60	20	0.28	4.93
60	20	0.35	5.97
60	40	0.28	6.06
60	40	0.35	8.35
60	60	0.28	8.17
60	60	0.35	10.71
60	80	0.28	11.01
60	80	0.35	12.49
60	100	0.28	13.19
60	100	0.35	15.01

Inspection of the unconsolidated cores with the addition of the kaolinite clay further displays the dependency on the porosity. With the addition of clay, the uniformity of the grain structure is disrupted so the porosity is decreased. The small size of the clay enables it to reside inside of the established pore between the grains of the quartz sand. Kaolinite clays are considered to be pore filling and therefore, with increasing clay content, the porosity is dramatically decreased. This relationship is easily evident in Figure 5.5. Both the dielectric constant and loss tangent decrease with increasing kaolinite clay content as a systematic result of the decreasing pore space. The byproduct of the pore filling clays is a decrease in the relative fluid volume and the overall dielectric response necessarily becomes more similar to the rock matrix. The dielectric constant response is an extension of the reduction in pore space with increasing clay content. Smaller pore volume equates to lesser fluid volume and therefore lower overall dielectric constant.

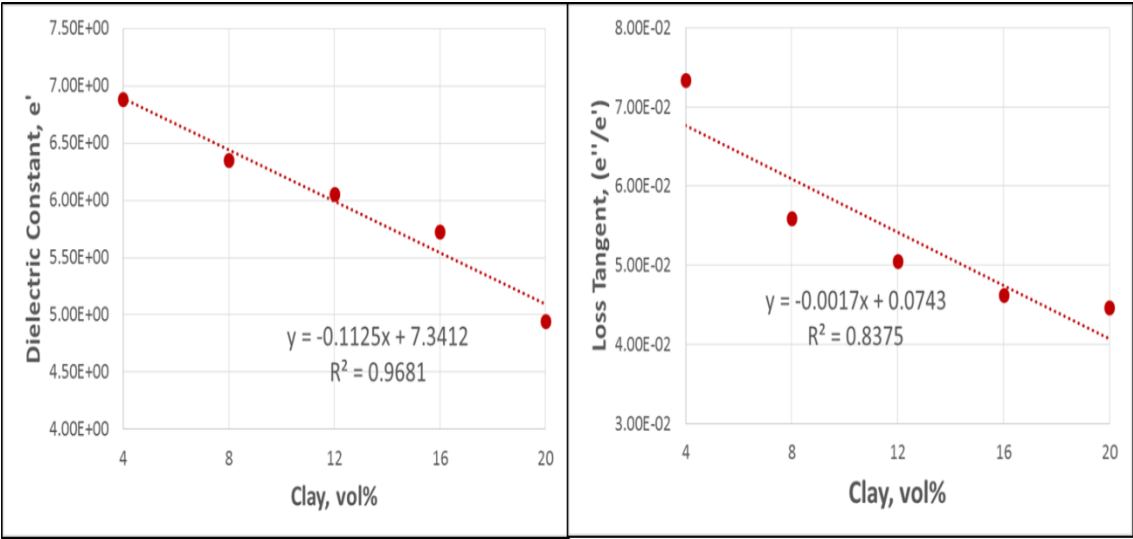


Figure 5.5 - Isolated dependency of complex permittivity on variable kaolinite clay volume of the reservoir rock

As opposed to the kaolinite clay, bentonite clay is considered to be clay swelling. The relationships achieved by the bentonite clay unconsolidated cores experience nuances that extend beyond a porosity dependency. The bentonite interacts with the water present in the reservoir to create a complex dielectric environment. Clays have a very large surface area and a negative surface charge. The charge on the clay surface is well documented in literature as is the propensity of the clay to interact with the water that is present in the pore space. The surface charge of the clay attracts water molecules and creates a bound water layer followed by a diffuse layer. Together they form the Stern double-layer which is itself polarizable.

The polarizable clay layer is evidenced upon comparison of the dielectric constant response in juxtaposition to the loss index as is seen in Figure 5.6. The dielectric constant experiences similar behavior to the kaolinite clay and is dominated by reduction in pore volume. The identified relationship would be expected to remain valid when investigating the loss index; however, the opposite is achieved. Increasing clay content results in increasing loss index where the counterintuitive relationship is attributed to the polarizability of the clay layer. The decrease in the pore space as a function of the increase in clay volume is overcome by the addition of the double-layer. This phenomenon manifests itself in the loss tangent as a result of the greater sensitivity of the imaginary component of complex permittivity to the reservoir environment. The presence of the double-layer is masked upon investigation of the dielectric constant by the presence of the decrease in water volume with increasing clay volume. The overwhelming driver of the dielectric constant parameter is the water saturation and this decrease overshadows the

contribution of the double-layer. Therefore, the driver of the dielectric constant response for the bentonite clay isolation is the reduction in pore space while the polarizable double-layer dominates the loss tangent behavior.

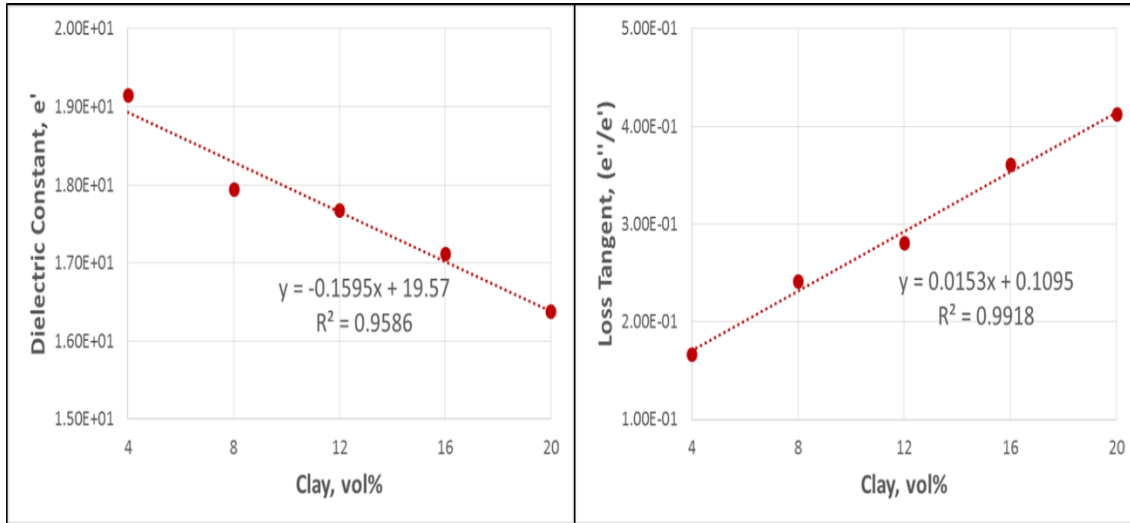


Figure 5.6 - Isolated dependency of complex permittivity on variable bentonite clay volume of the reservoir rock

Isolation of the temperature dependency is depicted in Figure 5.7 where a fully oil-saturated core is measured with temperature manipulation. The core in the figure is constituted of a rock matrix with 60% by volume quartz with the remainder being calcite. To allow for the heating of the core, the unconsolidated core was placed on a heating plate and therefore was not introduced to the pressure vessel. The temperature dependency was therefore performed at atmospheric pressure. All parameters besides the temperature are kept constant and the increase in both the real and imaginary component of complex permittivity is easily evident. A temperature dependency is primarily a function of the fluid that is in the pore space. The complex permittivity of heavy oil has been shown to

increase with temperature rise; so, the achieved response adheres to a fluid dominated dependency (Liao et al. 2018).

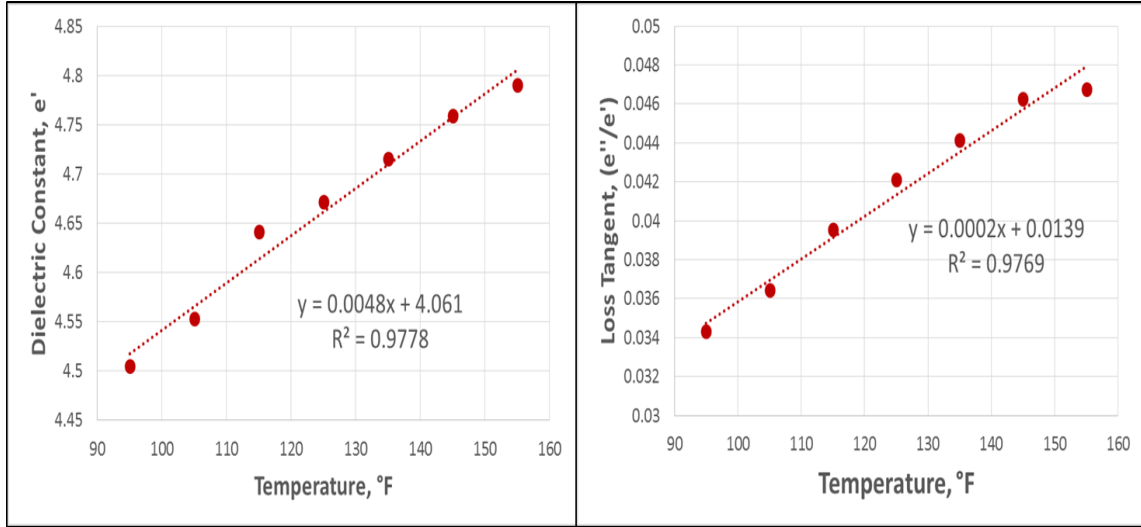


Figure 5.7 - Isolated dependency of complex permittivity on variable temperature of the reservoir rock

Complex permittivity is a volumetric measurement and accordingly is very sensitive to change in material volume. This is apparent from the depicted reaction of complex permittivity to variable pressure seen in Figure 5.8. No visible dependency is achieved with both dielectric constant and loss tangent being relatively insensitive to changing pressure. Lack of a discernible change is attributed to the inability of the pressure to compress the volume of the sample. Samples consist of a rock matrix along with a system of interconnected pore space which is where the saturating fluid resides. Water and oil are significantly less compressible than air and are therefore capable of opposing the stress or pressure applied to the core. The pressure does not affect the volume of the sample

so there is no change in the complex permittivity. Accordingly, there is no change in the penetration depth of the microwave as a function of solely varying pressure.

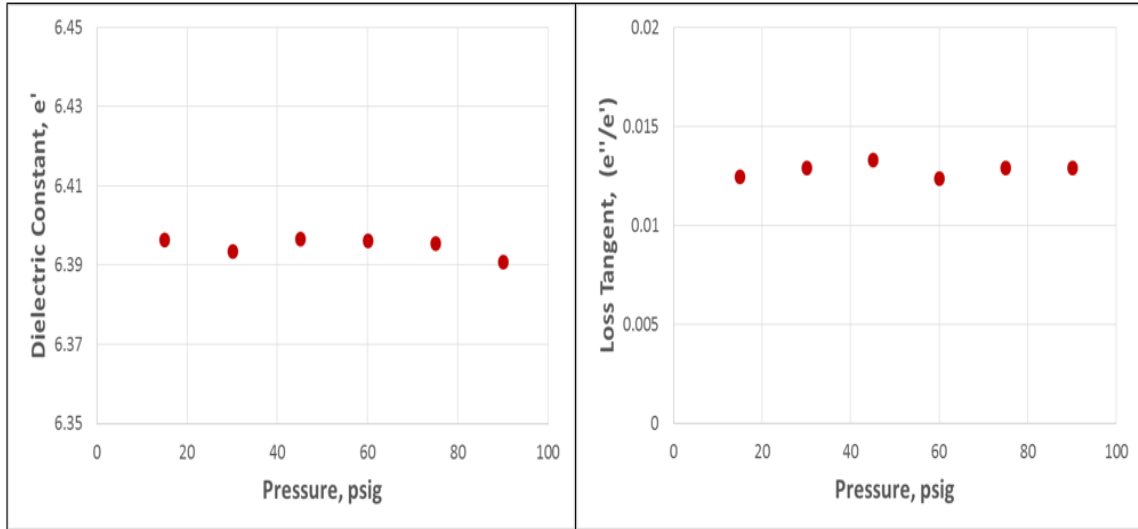


Figure 5.8 - Isolated dependency of complex permittivity on variable pressure of the reservoir rock

However, the breadth in the effects of the pressure component extend well beyond the above relationship and materialize when investigating penetration depth as a function of quartz content. Analyzing the change in the penetration depth under the presence of a coaxial mechanical stress coupled with the quartz content reveals a dependency on the pressure. Increasing the static loading of the rock matrix corresponds to an increase in the dynamic polarization of the quartz crystal. Figure 5.9 is evidence of the concept where the percent increase of penetration depth as a function of increasing quartz content is displayed. The established relationship substantiates the fact that the degree of dynamic polarization in the sandstone rock is dependent upon the volumetric proportion of piezoelectric material. Incorporating variable quartz content into a direct comparison of

the stressed and unstressed states clearly shows additive penetration depth with greater volume of quartz. Change in the complex permittivity of the system derived from the direct piezoelectric effect is a function of the magnitude of both the quartz content and the mechanical stress through the element.

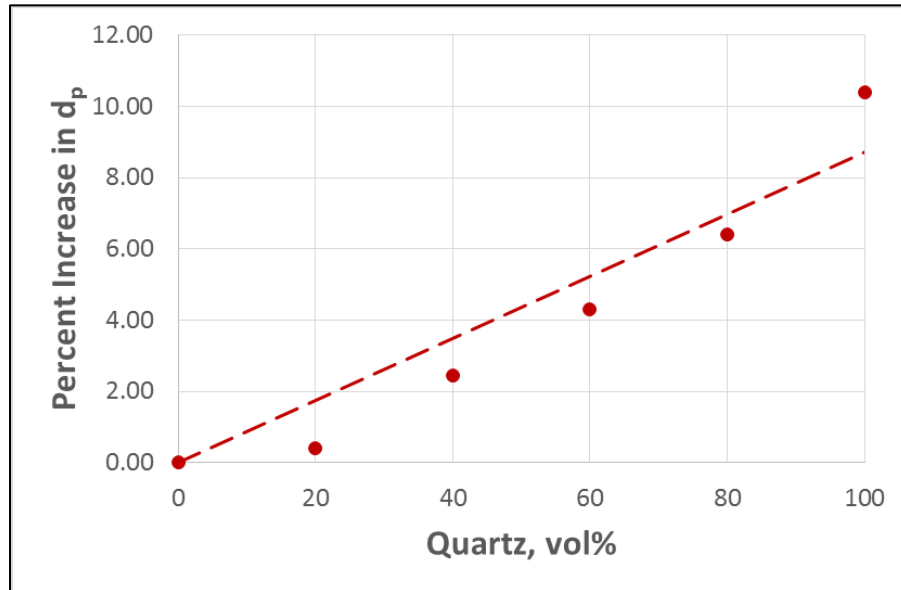


Figure 5.9 – Magnitude of microwave penetration depth increase between the stressed and unstressed state as a function of variable quartz content

A regression was performed separately for the dielectric constant as well as the loss index as a function of water volume (S_w), oil volume (S_o), quartz volume (V_q), limestone volume (V_L), kaolinite clay volume (V_{kao}), bentonite clay volume (V_{bent}), pressure in psig (p), frequency in Hz (f), and temperature in °F (T). Flexibility of the model is ensured by assigning the predictor variables of (S_w) and (S_o) to be the volume multiplied by the complex permittivity of the respective fluid. Therefore, all variation in oil as a function of unique regional oil properties are accounted for in the model itself,

resulting in universality. The predicting equations can be confidently applied to any oil sample stemming from the capability of the model to account for the specific complex permittivity of the fluid. Also, there is flexibility in the salt concentration of the brine as the complex permittivity of the water is a direct indicator of the salinity. The model is relaxed by the addition of the complex permittivity multiplier to both the saturating fluids, extending the applicability to all brines and oils.

As discussed, the regression is linear so each predictor will have the associated variable along with the magnitude. Greater sensitivity to the parameter results in a greater modifier. Statistical regression provides the ability not only to define the isolated contribution of each predictor but also tests the null hypothesis, ensuring sensitivity of the equation to every predictor variable. The null hypothesis is defined by the p-value quantity which tests the level of marginal significance within a statistical data set. The p-value for each parameter is within the threshold to justify the presence of the predictor in the regressed equation. The regressed form for the real component is seen in Eq 5.1 and achieved a R^2 value of .963, providing great confidence in the ability of the model to accurately estimate the dielectric constant. The imaginary nature of the loss index results in greater complexity relative to the real counterpart resulting in a slightly poorer match in terms of the R^2 value. The model can be seen in Eq 5.2 with a value of .84 for the R^2 .

$$\begin{aligned} \varepsilon' = &.4913(S_w) - .2782(S_o) - 7.22(V_q) - 4.05(V_L) - 11.32(V_{Kao}) - 19.768(V_{Bent}) - \\ &.000541(p) + .0197(T) + 1.276 * 10^{-10}(f) + 5.601 \end{aligned} \quad \text{Eq 5.1}$$

$$\left(\frac{\varepsilon''}{\varepsilon'}\right) = 3.02(S_w) + .102(S_o) + .508(V_q) - .221(V_L) - 4.87(V_{Kao}) + 1.93(V_{Bent}) + 1.914 * 10^{-5}(p) + 6.311 * 10^{-3}(T) + 1.407 * 10^{-11}(f) + .031 \quad \text{Eq 5.2}$$

Validation of the regressed model was performed to allow for confidence in the implementation. Usefulness of the regressed model hinges on the ability to accurately predict the dielectric response of reservoir rocks so both unconsolidated and consolidated cores were tested. The match of the unconsolidated cores are illustrated in Fig 5.10 which definitively depicts sound agreement between the predicted and measured values. The red curves consisted of a rock with pore space filled with 25% by volume water with the rest of the pore space being filled with oil. The rock matrix was constituted of 25% by volume quartz with the remainder being limestone. Figure 5.10 (A) shows the validation of the dielectric constant model while figure 5.10 (C) illustrates the match of the loss tangent model. The pore space of the black curves was saturated with 50% by volume oil with the remainder being water. Likewise, the rock matrix is a mixture of 50% by volume quartz with the remainder being limestone. The dielectric constant for the second unconsolidated core that was tested is seen in Figure 5.10 (B) and the match of the loss tangent is depicted in Figure 5.10 (D). As is evidenced in the figure, the regressed models are very capable of predicting the response of the unconsolidated cores. The agreement between the predicted and measured values is good with the match being indicative of a sound model.

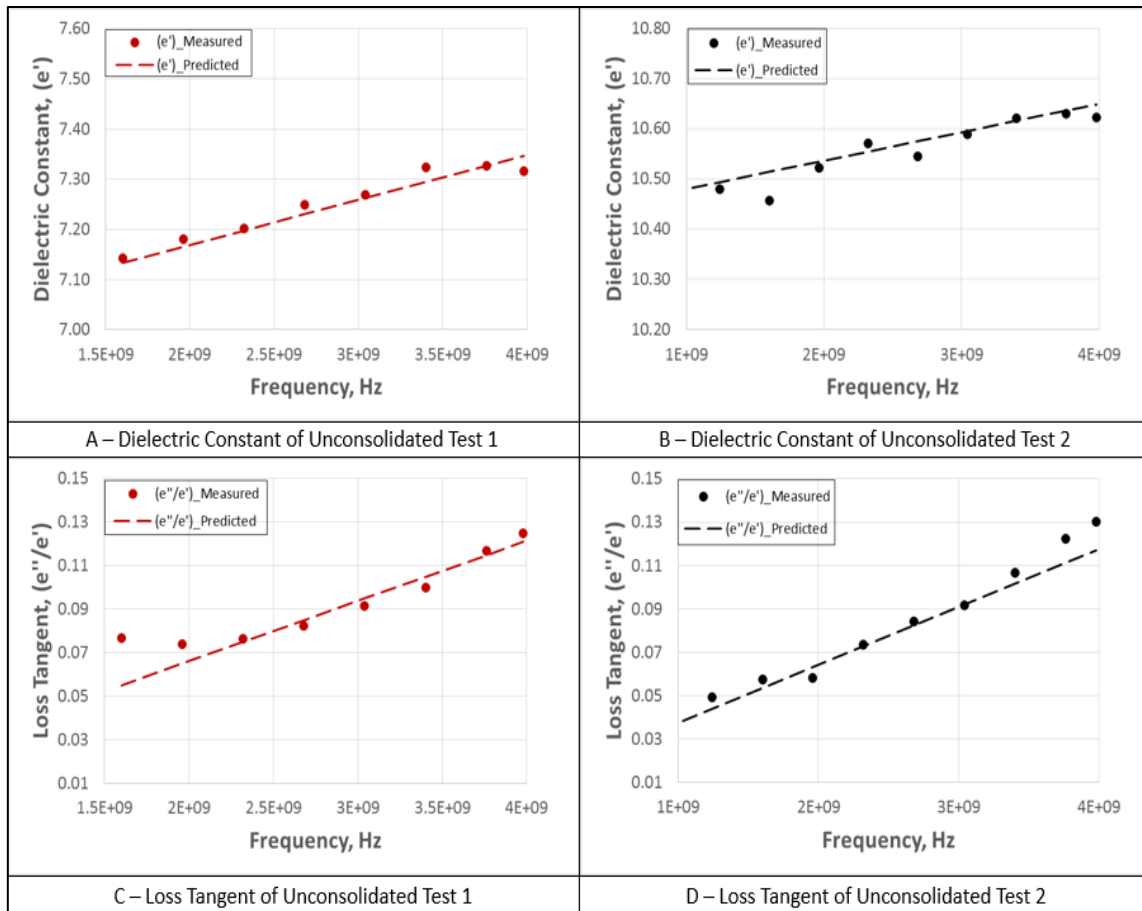


Figure 5.10 – Predicted and Measured Components of Complex Permittivity for the Unconsolidated Core Samples Test 1 and Test 2

The validation was expanded to include consolidated cores by testing the applicability and accuracy of the model with a known consolidated core saturated with a known crude oil. The core consisted of a rock mineralogy of 77.1 % quartz, 2.3% dolomite, 5.1% kaolinite, 2.8% illite, and 12.7% albite. The crude oil with a bulk dielectric constant of 2.69 and a loss tangent of .0192 fully saturated the pore space of 21%. The crude oil was categorized as heavy with a viscosity of 10,139 cP at room temperature and an API gravity of 12.09. Consolidated cores present a much more realistic material to test

the models as all reservoir rocks are consolidated to some extent. Extending the validation to encompass consolidated samples is vital for the application of the predictor models. The agreement of the predicted and measured dielectric response for the oil-saturated sample 1 is shown in Figure 5.11 (A) for the dielectric constant and Figure 5.11 (B) for the loss tangent. Once again the regressed model is very capable of predicting the complex permittivity as expounded by the good agreement with the measured values.

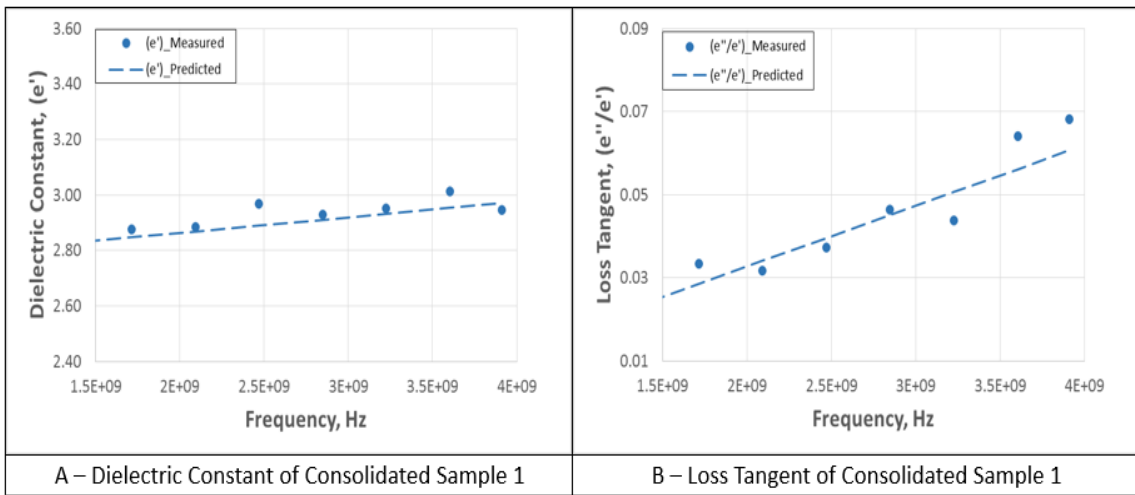


Figure 5.11 – Predicted and Measured Components of Complex Permittivity for the Consolidated Core Sample 1

Establishing universality of the predictor model required that the equations be tested on more than just the oil implemented in the study. Therefore, new unconsolidated cores were formulated and saturated fully with a new crude oil with bulk dielectric constant of 3.84 and a loss tangent of .0295. Similarly to the first and second unconsolidated tests, the porosity was experimentally defined to be 35%. The crude oil for unconsolidated test 3 was heavier than the oil used in the regression experiments with a viscosity of 53,146 cP at room temperature and an API gravity of 8.19. Utilization of the

new bulk crude oil enabled the extension of the estimation models beyond merely the scope of one specific oil, encompassing any oil with known dielectric properties. Sound fit between the measured and predicted values for the new unconsolidated mixture suggests that direct application to the petroleum industry is valid. The conducted experiments that govern the regression were not performed on the new oil but, as is clearly shown in Figure 5.12 the model is able to account for the change in oil properties. The predictor variable (S_o) is defined as the volume of oil occupying the pore space multiplied by the complex permittivity of that specific oil sample. Arising from the sound agreement illustrated, the regressed model can be confidently applied to all oil reservoirs with proven flexibility.

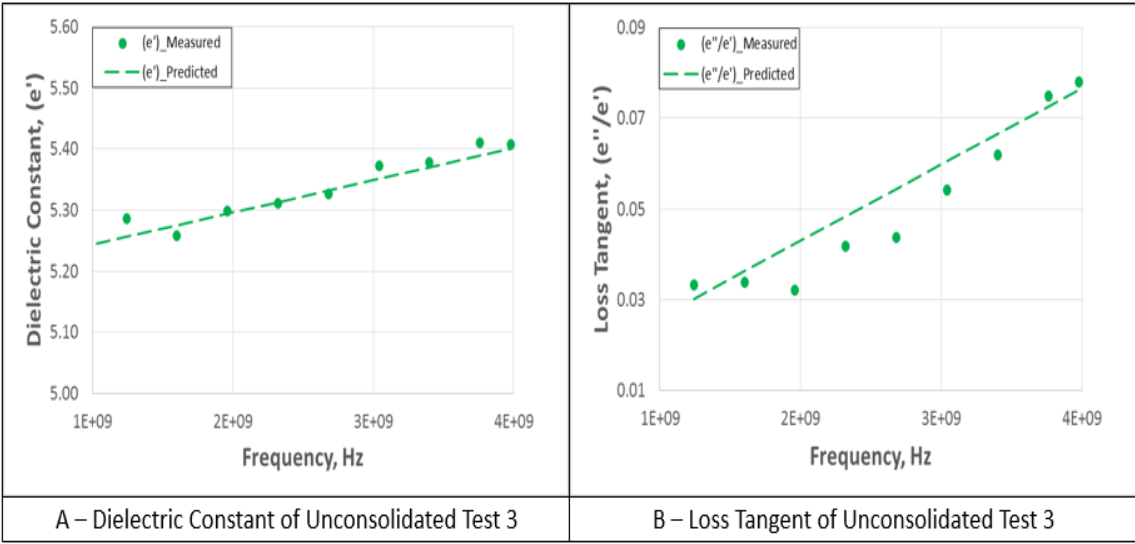


Figure 5.12 – Predicted and Measured Components of Complex Permittivity for the Unconsolidated Core Samples Test 3

Conclusions

Sensitivity of any numeric or analytic model to dielectric properties including both the real and imaginary components warrants proper mathematic description. Characterizing microwave absorption dynamics in the reservoir is vital to estimating both temperature increase as well as the distance the wave travels. However, dielectric properties vary as a function of the reservoir environment and estimation techniques currently employed are inadequate to effectively capture the relationships in the reservoir. Simplistic mixing rule models implemented fall short in capturing the complexity of heavy oil reservoirs. A unique and intrinsic model is developed which is better suited to specifically capturing the response in terms of the dielectric constant and loss index.

A multivariable regression offers the unique ability to express the intrinsic relationship experienced under the influence of reservoir properties and addresses the shortcomings of mixing rules. Mutual interactions experienced in the reservoir between the skeletal frame and the pore space as the microwave propagates are accounted for by the volumetric nature of the dielectric probe measurements. Unconsolidated cores allow for the experimental manipulation of the makeup of each of the core samples so that identified parameters can be isolated. The culmination of all individual experiments captures the natural interactions and relationships that are realized in any reservoir. The regressed relationship is specifically designed to describe the behavior of the combination of the pore space, rock matrix, temperature, pressure, and frequency.

Linearity is established for the contribution of each of the identified parameters to the overall response so a multivariable regression is applicable and valid. The sensitivity

of the regression to the water saturation is the driving factor which stems from the very polar nature of the water. The magnitude of the dependency is large as seen by the slope of the isolated relationship with the bulk dielectric constant. On the other hand, the complex permittivity of the sample decreases with increasing quartz content. Increasing quartz content corresponds to decreasing limestone content where the limestone experiences a higher individual dielectric constant. The decrease in limestone must equate to decrease in the volume of the higher dielectric constant volume relative to that of quartz.

The complex permittivity response to the presence of clays was captured where the polarizability of the clay surface was seen through comparative analysis of the dielectric constant and loss index. The presence of the double-layer results in an increase in loss index with increasing clay volume owing to the creation of the bound water layer and the diffuse layer. The presence of the double-layer is overshadowed for the dielectric constant response by the decrease in water volume. The magnitude of the sensitivity of the dielectric constant to the water volume is expansive and the polarizability of the double-layer is accordingly masked. The clays are primarily located in the pore space established by the grain boundaries of the quartz and limestone sand. The disparity between the particle sizes of the sands and the clays is quite large and the non-uniform distribution enables the clogging of the pore space by the clays. Decrease in the pore volume results in a decrease in the bulk dielectric constant owing to the relative decrease in the fluid volume of the reservoir.

Temperature-dependent behavior was also realized in the bulk complex permittivity response with an increase in both components of complex permittivity with

increasing heat. Absorption mechanics are an extension of the fluid-filled pore space so the rise in dielectric behavior with temperature is derived mainly from the pore space. Sensitivity to change in temperature is accordingly a function of the respective fluid saturations with the dielectric constant of water known to decrease with additive heat. Complex permittivity of heavy increases with temperature and the results in this study adhere to this behavior.

Variable pressure was likewise investigated both in terms of the manipulation in volume of the sample as well as for the ability to trigger the direct piezoelectric effect. No discernible impact on complex permittivity was achieved as a result of changing the pressure state. This behavior is attributable to the inability of the imposed stress to compress the measurably compress the sample. No change in volume was achieved and accordingly no change in the complex permittivity was measured. However, a systematic result of the pressure manifests itself through the triggering of the direct piezoelectric effect in high quartz volume samples. Introducing a pressure component in the presence of high quartz content enables the dynamic polarization of the sample. The magnitude of the change in the polarization vector was found to be a direct function of the volume of piezoelectric elements (quartz) in the sample.

The multivariable regression is sensitive to all identified parameters and provides for a more accurate and realistic interpretation of complex permittivity in the reservoir. Inadequacies in estimation of this vital parameter by simplistic mixing rules are addressed by capturing the response of the entire reservoir volume. Mixing rules require that the isolated response of the constituent components be pieced together and therefore are inept

at describing the inherent interactions that occur. Establishing linearity provides confidence in the ability to implement a multivariable linear regression as the relationships between the predictor variables and the outcome are first order. The regression in this study achieves an estimation model that inherently is representative of all interactions and contributions as the measurements are conducted on the bulk volume. The models can be implemented into any estimation model to characterize the absorption and penetration dynamics in the reservoir. Implications for reservoir simulation are vast as the regressed models can be directly introduced to bridge the gap between numerical simulation and experimentally obtained relationships.

References

- Abernethy, E. 1976. Production Increase of Heavy Oils by Electromagnetic Heating. *Journal of Canadian Petroleum Technology* **15** (03).
- Abraham, T., Afacan, A., Dhandharia, P. et al. 2016. Conduction and Dielectric Relaxation Mechanisms in Athabasca Oil Sands with Application to Electrical Heating. *Energy & Fuels* **30** (7): 5630-5642.
- Bjorndalen, N. and Islam, M. 2004. The Effect of Microwave and Ultrasonic Irradiation on Crude Oil During Production with a Horizontal Well. *Journal of petroleum Science and Engineering* **43** (3-4): 139-150.
- Campanone, L. and Zaritzky, N. 2005. Mathematical Analysis of Microwave Heating Process. *Journal of Food Engineering* **69** (3): 359-368.
- Carrizales, M.A. 2010. Recovery of Stranded Heavy Oil by Electromagnetic Heating.
- Centeno, G., Sánchez-Reyna, G., Ancheyta, J. et al. 2011. Testing Various Mixing Rules for Calculation of Viscosity of Petroleum Blends. *Fuel* **90** (12): 3561-3570.
- Chilingar, G.V., El-Nassir, A., and Stevens, R.G. 1970. Effect of Direct Electrical Current on Permeability of Sandstone Cores. *Journal of Petroleum Technology* **22** (07): 830-836.
- Chute, F., Vermeulen, F., Cervenán, M. et al. 1979. Electrical Properties of Athabasca Oil Sands. *Canadian Journal of Earth Sciences* **16** (10): 2009-2021.
- Clarke, R., Gregory, A., Cannell, D. et al. 2003. A Guide to the Characterisation of Dielectric Materials at Rf and Microwave Frequencies. *Institute of Measurement and Control/National Physical Laboratory*.

- Davletbaev, A., Kovaleva, L., and Babadagli, T. 2014. Heavy Oil Production by Electromagnetic Heating in Hydraulically Fractured Wells. *Energy & Fuels* **28** (9): 5737-5744.
- Dinčov, D., Parrott, K.A., and Pericleous, K. 2004. Heat and Mass Transfer in Two-Phase Porous Materials under Intensive Microwave Heating. *Journal of Food Engineering* **65** (3): 403-412.
- Feng, S. and Sen, P. 1985. Geometrical Model of Conductive and Dielectric Properties of Partially Saturated Rocks. *Journal of Applied Physics* **58** (8): 3236-3243.
- Freedman, R. and Vogiatzis, J.P. 1979. Theory of Microwave Dielectric Constant Logging Using the Electromagnetic Wave Propagation Method. *Geophysics* **44** (5): 969-986.
- Garrouch, A.A. and Sharma, M.M. 1994. The Influence of Clay Content, Salinity, Stress, and Wettability on the Dielectric Properties of Brine-Saturated Rocks: 10 Hz to 10 Mhz. *Geophysics* **59** (6): 909-917.
- Gross, B. 1941. On the Theory of Dielectric Loss. *Physical Review* **59** (9): 748.
- Hill, N.E. 1969. *Dielectric Properties and Molecular Behaviour*: Van Nostrand Reinhold. Original edition. ISBN.
- Hu, L., Li, H.A., and Ahmadloo, M. 2018. Determination of the Permittivity of N-Hexane/Oil Sands Mixtures over the Frequency Range of 200 Mhz to 10 Ghz. *The Canadian Journal of Chemical Engineering* **96** (12): 2650-2660.
- Josh, M. and Clennell, B. 2015. Broadband Electrical Properties of Clays and Shales: Comparative Investigations of Remolded and Preserved Samples broadband Electrical Properties of Clay. *Geophysics* **80** (2): D129-D143.
- Josh, M., Clennell, M.B., Raven, M.D. et al. 2015. Factors Controlling Dielectric Response of Clays and Shales. In *Seg Technical Program Expanded Abstracts 2015*: Society of Exploration Geophysicists.
- Li, G., Meng, Y., and Tang, H. 2006. Clean up Water Blocking in Gas Reservoirs by Microwave Heating: Laboratory Studies. In *International Oil & Gas Conference and Exhibition in China*: Society of Petroleum Engineers. ISBN 1555631835.
- Liao, H., Morte, M., Bloom, E. et al. 2018. Controlling Microwave Penetration and Absorption in Heavy Oil Reservoirs. Paper presented at the SPE Western Regional Meeting, Garden Grove, California, USA. 13. Society of Petroleum Engineers. DOI: 10.2118/190089-MS.
- Martinez, A. and Byrnes, A.P. 2001. *Modeling Dielectric-Constant Values of Geologic Materials: An Aid to Ground-Penetrating Radar Data Collection and Interpretation*: Kansas Geological Survey Lawrence, Kansas. Original edition. ISBN.
- Mathias, P.M., Klotz, H.C., and Prausnitz, J.M. 1991. Equation-of-State Mixing Rules for Multicomponent Mixtures: The Problem of Invariance. *Fluid Phase Equilibria* **67**: 31-44.
- Meador, R.A. and Cox, P. 1975. Dielectric Constant Logging, a Salinity Independent Estimation of Formation Water Volume. In *Fall Meeting of the Society of Petroleum Engineers of AIME*: Society of Petroleum Engineers. ISBN 1555637531.

- Metaxas, A.a. and Meredith, R.J. 1983. *Industrial Microwave Heating*: IET. Original edition. ISBN 0906048893.
- Morte, M., Bloom, E., Huff, G. et al. 2018. Factors Affecting Electromagnetic Wave Penetration in Heavy Oil Reservoirs. Paper presented at the SPE Canada Heavy Oil Technical Conference, Calgary, Alberta, Canada. 12. Society of Petroleum Engineers. DOI: 10.2118/189746-MS.
- Morte, M., Dean, J., Kitajima, H. et al. 2019. Increasing the Penetration Depth of Microwave Radiation Using Acoustic Stress to Trigger Piezoelectricity. *Energy & Fuels* **33** (7): 6327-6334.
- Morte, M. and Hascakir, B. 2019. Characterization of Complex Permittivity for Consolidated Core Samples by Utilization of Mixing Rules. *Journal of Petroleum Science and Engineering* **181**. DOI: <https://doi.org/10.1016/j.petrol.2019.06.042>
- Myers, M. 1991. A Saturation Interpretation Model for the Dielectric Constant of Shaly Sands. In *SCA International Symposium, San Antonio, Texas, Aug:21-22*.
- Niu, Q. and Prasad, M. 2016. Measurement of Dielectric Properties (Mhz–Mhz) of Sedimentary Rocks. In *Seg Technical Program Expanded Abstracts 2016*: Society of Exploration Geophysicists.
- Punase, A. and Hascakir, B. 2016. Stability Determination of Asphaltenes through Dielectric Constant Measurements of Polar Oil Fractions. *Energy & Fuels* **31** (1): 65-72.
- Sahni, A., Kumar, M., and Knapp, R.B. 2000. Electromagnetic Heating Methods for Heavy Oil Reservoirs. In *SPE/AAPG Western Regional Meeting*: Society of Petroleum Engineers. ISBN 1555633455.
- Seleznev, N., Boyd, A., Habashy, T. et al. 2004. Dielectric Mixing Laws for Fully and Partially Saturated Carbonate Rocks. In *SPWLA 45th Annual logging symposium*: Society of Petrophysicists and Well-Log Analysts.
- Sen, P.N., Chew, W., and Wilkinson, D. 1984. Dielectric Enhancement Due to Geometrical and Electrochemical Effects. In *AIP Conf. Proc.:(United States)*: Schlumberger-Doll Research, Ridgefield, CT.
- Singh, R.P. and Heldman, D.R. 2001. *Introduction to Food Engineering*: Gulf Professional Publishing. Original edition. ISBN 0080574491.
- Snyder, D.D. and Fleming, D.B. 1985. Well Logging—a 25-Year Perspective. *Geophysics* **50** (12): 2504-2529.
- Sresty, G.C., Dev, H., Snow, R.H. et al. 1986. Recovery of Bitumen from Tar Sand Deposits with the Radio Frequency Process. *SPE Reservoir Engineering* **1** (01): 85-94.
- Sun, D.-W. 2014. *Emerging Technologies for Food Processing*: Elsevier. Original edition. ISBN 0124104819.
- Von Hippel, A.R. 1954. *Dielectric Materials and Applications*: Artech House on Demand. Original edition. ISBN 0890068054.
- Wharton, R.P., Rau, R.N., and Best, D.L. 1980. Electromagnetic Propagation Logging: Advances in Technique and Interpretation. In *SPE Annual Technical Conference and Exhibition*: Society of Petroleum Engineers. ISBN 1555636934.

6. CONCLUSIONS

Microwave technology is a technically feasible tool that has the potential to greatly increase both the efficiency and volume of production of heavy oil and bitumen. These resources are expansive worldwide and the current trajectory of energy utilization requires that we access the virtually untapped reserves. Demand increases every year and is projected to continue to increase so implementation of microwave irradiation to heat the reservoir is a tool that will be integral to supply of hydrocarbons in the future.

However, poor penetration depth of the wave creates an economic environment which can't be sustained. Minimal heated oil prevents production levels to justify the large capital expenditure of the project. Accordingly, investigating ways to increase the penetration depth of the wave while maintaining the same absorption mechanisms in the reservoir is very important. Piezoelectricity inherent to quartz crystals provides the means to remain in the dielectric heating frequency range while increasing the distance the wave travels into the reservoir. Control experiments were performed on a pure quartz crystal to establish a proof of concept and expound the viability of the phenomenon. Large increase in penetration achieved by the stressed crystal is attributed to the polarization of the crystal stemming from the applied mechanical stress. The data that was collected on the quartz crystal provides confidence in the experimental procedure and the equipment as the identified behavior expected of the quartz crystal was attained.

Subsequently, a static mechanical load was placed across consolidated cores to extend the domain of the concept to envelope reservoir rock. Quartz is abundant in sandstone reservoirs, therefore, heavy oil/bitumen sands have the potential to display

piezoelectricity in the reservoir. Analysis of the three cores selected definitively shows that a static load provides the necessary stress to the element to trigger the benefit of the direct piezoelectric effect. Polarization of the quartz crystal is realized with the coaxial compression investigated where the absorptive capacity of the reservoir rock is manipulated. This allows for the wave to sustain penetration for larger distances and propagate further into the formation, heating greater volumes of oil.

Identifying the prospective capability of increasing the economics of the project warrants investigation into analogous mechanisms for the field-scale. Static loading of the reservoir is already in place for every petroleum system owing to the overburden present, prohibiting any differential compression to be applied. Applicability of the piezoelectric phenomenon for the field hinged upon the ability to introduce an additive mechanical stress to the reservoir. Acoustic waves travel through the material and bypass any issues with the presence of overburden. The acoustic wave is a mechanical wave that vibrates the particles in the medium to propagate; so a small additive stress is applied to the reservoir rock matrix. Once again, the magnitude of the introduced stress component to the skeletal frame of the rock was above the required threshold to trigger the benefit of the direct piezoelectric effect. Additive penetration was achieved as a result of the propagation of the acoustic wave. Core sample 2 has a greater volume of quartz comparatively to that of sample 1 and would accordingly be expected to realize greater benefit of piezoelectricity. A qualitative analysis corroborates this expectation as sample 2 achieves a greater differential penetration than sample 1.

However, addressing the issue of poor penetration depth is a solution to only part of the problem. Optimization of any process requires simulation where fluid flow over the course of years is easily attainable on a much more manageable timescale. Complex permittivity is the parameter that directly describes the ability of the material to absorb microwave energy and is accordingly an integral input into any model. Therefore, candidacy and effectiveness of the material as a microwave absorber is predicated upon correctly identifying the parameter of permittivity. Both the real and imaginary components of complex permittivity are material properties which are sensitive to the environment. Complex and dynamic interactions that occur in the reservoir make characterization of these parameters very difficult. Simplistic mixing rules operate on the governing mechanics of solely volumetric proportionality. Derivation of volumetric mixing rules requires assumptions which run directly counter to what is known to occur in the reservoir. Both the skeletal frame and the pore space interact through the presence of clays, temperature, precipitation, etc. and mutual exclusivity cannot be achieved.

Multivariable regression innately accounts for all manner of microscopic and macroscopic interactions as a function of the governing volumetric nature of the dielectric probe method. Adaptation of the model stems from the isolation of individual parameters contained in the regression where the contribution of each constituent part is inherently captured as the electromagnetic wave propagates. Insight into the behavior of the reservoir under the interaction of microwaves provides the ability to estimate the absorptive capacity of the material at any position or time-step. Unconsolidated core samples were experimentally defined which allowed for the direct variation of the identified parameters.

Isolation of each predictor variable resulted in a linear dependency on the overall response so a first order regression model was applicable. Elucidation of each predictor was achieved for both the dielectric constant and the loss tangent. The established equations are better able to estimate the complex permittivity as they inherently capture all complexity within the reservoir itself. Numerical simulation and analytical modeling rely on an accurate description of all parameters with high sensitivity to the overall response. The regressed equations are the means for increasing both the accuracy and the applicability of any estimation model that inputs complex permittivity.

The new regression models formulated in conjunction with the implementation of the direct piezoelectric effect are steps in the right direction for the economic utilization of microwave technology. Enhanced understanding of the nuances in the reservoir considering the absorptive and penetration dynamics leads to greater evolution of the technology. The novel concepts investigated are the exploitation of piezoelectricity in the context of electromagnetic wave introduction for petroleum reservoirs as well as the means for characterizing absorption in the complex reservoir environment. The potential benefit achieved has vast economic implications and helps to alleviate some of the concerns of poor economic return on investment with microwave technology.